HEAT AND MASS TRANSFER. VOLUME 7, 1968

A. V. Lykova, et al

Foreign Technology Division
Wright-Patterson Air Force Base, Ohio

20 August 1969

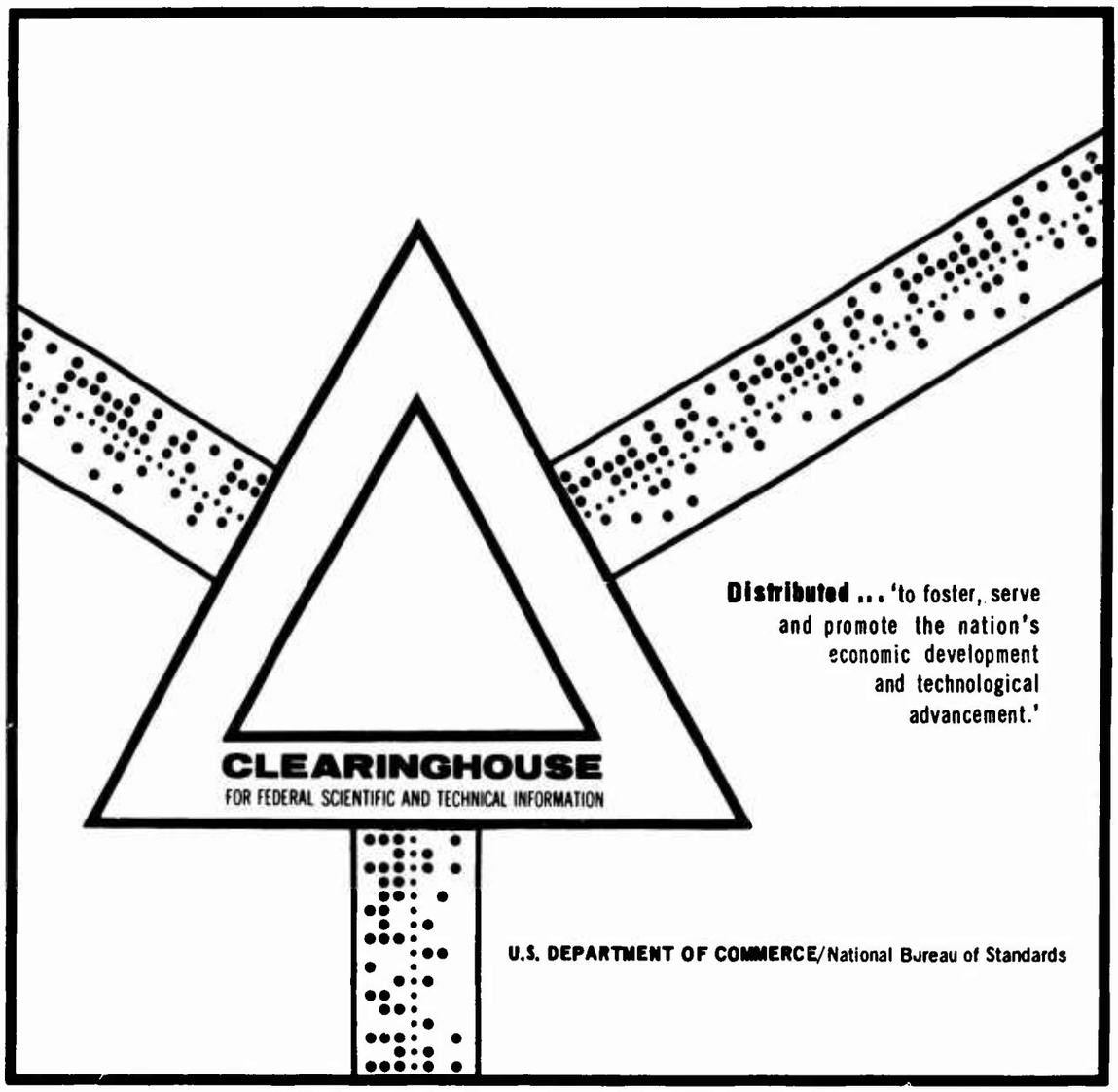

FTD-HT-23-820-68 Part 2 of 3

FOREIGN TECHNOLOGY DIVISION

HEAT AND MASS TRANSFER

By

A. V. Lykova, B. M. Smol'kogo

FTD-HT- 23-820-68
Part 2 of 3

EDITED TRANSLATION

HEAT AND MASS TRANSFER

By: A. V. Lykova, B. M. Smol'kogo

Source: Teplo-I Massoperenos, (Heat and Mass Transfer) 1968, Vol. 7, pp. 1-609

English Pages: 244 - 462

Translated Under: F33657-68-D-1287

PREPARED BY:

TRANSLATION DIVISION
FOREIGN TECHNOLOGY DIVISION
WP-AFB, OHIO.

PART TWO

METHODS AND INSTRUMENTS FOR DETERMINING PARAMETERS OF HEAT AND MASS TRANSFER

THERMOPHYSICAL METHODS IN DETERMINING COMPOSITION OF ABSORBED DOSES OF IONIZING RADIATION

B. A. Briskman, V. D. Bondarev, Yu. V. Matveyev
and N. D. Stepanov

When sources of mixed radiation are used (mainly, nuclear reactors), the task of determining the composition of absorbed doses of ionizing radiation cropped up, since in this case the absorbed energy is caused by different kinds of radiation. Existing methods are highly approximational.

When radiation interacts with a compound, a gradient of energy release is induced, corresponding in direction with the gradient of radiation flux. The value of this gradient depends on the kind of radiation and its energy.

In the case of uniformly distributed sources of heat and symmetrical boundary conditions, steady-state temperature distribution symmetrically relative to the mean plane of the specimen irradiated or its axis (depending on the geometry of the system) a maximum is produced at the center of the specimen. When there is a gradient of heat release, the symmetry of temperature distribution is violated in the direction of the gradient, and this violation is the stronger, the greater the gradient of heat released. Harmonizing the type of temperature distribution and the size of the heat release gradient, we could from the nature of temperature distribution estimate the kind of radiation interacting with the given system. It is first necessary to establish a relationship between the gradient of absorbed radiation doses and the kind of irradiation at a specific energy.

With the above considerations allowed for, a method has been developed for determining the composition of absorbed doses applied to nuclear reactors, where polyethylene was used as the specimen material. In this case in practical terms the contribution to the absorbed dose was made by two kinds of radiation -- fast neutrons and γ-quanta of the reactor spectrum.

Experimental results of authors show that distribution of energy releases (absorbed doses) in a polyethylene specimen having the geometry under study can be described both for γ-radiation as well as for the fast neutron flux by an exponential relationship of the type $\bar{q}_V = \exp(-kx)$. The density of the sources is practically constant in the direction of the transverse axis y. The exponent k is taken as equal to 7.0 m^{-1} for the γ-radiation of the reactor spectrum, and k = (18.0-20.2) m^{-1} for the neutron irradiation of the corresponding spectrum.

Choice of polyethylene was determined by the following considerations: 1) low specific weight -- weak attenuation of γ-radiation; 2) high content of hydrogen -- great attenuation of neutron radiation, that is, we had a sharp difference in attenuation of two types of radiation examined; 3) relatively low coefficient of thermal conductivity ($\lambda \approx 0.35$ w/m °C) -- high temperature gradients at relatively low intensity of heat release sources.

For the given geometry of the transducer and the energy release distributions obtained, the two-dimensional steady-state task of thermal conductivity was solved for the case λ = const and $\bar{q}_V = \exp(-kx)$. In view of the cumbersomeness, results of the analytical solution are not given here. Solution of the problem was undertaken in parallel on the MSM-1 analog network machine. Analysis of temperature distributions showed that the following relationships can serve as criteria that are most sensitive to the energy release gradient:

$$c = (t_н - t_н)/(t_ц - t_{ср}),$$

$$\beta = (t_н - t_н)/(t_ц - t_н)$$

and

$$\alpha = \beta c = (t_н - t_н)^2/(t_{ц} - t_{ср})(t_ц - t_н).$$

Experimental results demonstrate that for several reasons it is most convenient to use the criterion c = f(h, k), where $h = \alpha/\lambda$. Based on the exponential

form of the attenuation curves, the function k = f(m) was obtained for each of the two kinds of radiation. From the relationships c = f(h, k) and k = f(m) the following functions were obtained as working curves, c = f(h, m, k_n), which are shown in Figure 1. Here, k_n = exponent for the neutron component taking on values from k = 18.0 to k = 20.0 m^{-1} depending on the distance to the center of the active zone.

The transducer design is shown in Figure 2. Thirteen copper-constantan thermocouples in quartz capillaries were encapsulated in a polyethylene block. Distances between the thermocouples were measured by means of X-ray spectroscopy. Previously, the unknown ratio h was determined with the aid of a Fourier equation by graphic differentiation of the curve of temperature distribution or with the aid of the approximational equality,

$$h \approx (t_2 - 5_1)/t\delta_{1-2}.$$

Thermocouples (12) and (13), shown in Figure 2, were used in arranging the transducer in such a way that the plane of the thermocouple embedding coincided with the radiation flux gradient.

The evaluation made of the effect of intrinsic absorption of radiation by thermocouples on measurement precision showed that this factor is substantially important only in the nonsteady state regime. The effect of intrinsic absorption is negligible for the steady state when it is taken into account that temperature quantities enter into the dimensionless criteria.

The maximum error in the method is 6-9 percent and the reproducibility of the method is 4-5 percent. This error is considerably less than the maximum error of existing methods (20-25 percent), which is very essential for several practical applications. The range of applicability of the method lies in two-component radiations given symmetry of the radiation flux.

Symbols

q_v = relative intensity of internal heat-release sources; α = coefficient of heat release; λ = thermal conductivity coefficient; δ_{1-2} = distance between heated arms of thermocouples (1) and (2) (cf. Figure 2); k = exponent of the

curve of heat-release attenuation; m = relative value of the neutron component; x = variable thickness; t_H, t_K, t_{cen} and t_{med} = temperatures on the transducer wall facing the radiation source, on the opposite wall, in the transducer center and in the ambient environment, respectively.

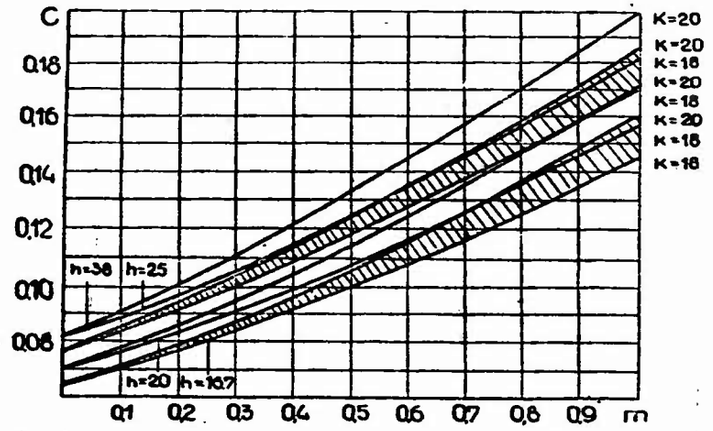

Figure 1. Temperature criterion c as a function of the value of the neutron component in the overall absorbed dose in polyethylene, $h = \alpha/\lambda$, m^{-1}; λ = const.

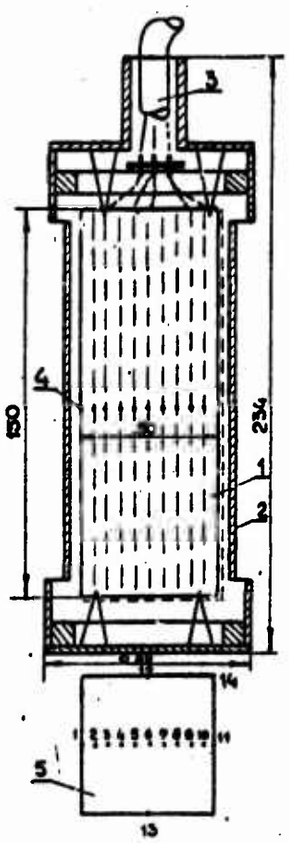

Figure 2. Sketch of transducer used in measuring composition of absorbed dose of mixed ionizing radiation: 1, Polyethylene block; 2, Aluminum sleeve; 3, Thermocouple cable; 4, Heated arm of thermocouple; 5, Cross section of transducer.

ERRORS IN DETERMINING THERMOPHYSICAL COEFFICIENTS OF A BODY

L. A. Brovkin

Errors in determining thermophysical coefficients are caused by errors in measuring temperature at a given point of the body. With the nonsteady-state method, distortion of transducer readings occur owing to the difference of its heat capacity C_T from the heat capacity of the body being tested C_M. In the quasi-steady state regime (or the regime approximating it) in which the specimen is heated at the rate U deg/sec, the region of ΔV occupied by the transducer can be considered as a region in which there exists a fictitious heat source of intensity $\Delta Q = \Delta V(c_M - c_T)U$ joules/sec. Errors in measuring temperature are determined after superimposing on the main temperature field of the body the source field under the condition that the mean temperature value of the field of the fictitious source is equal to zero. Thus, for a transducer -- a wire of diameter d, lying along the axis of a cylindrical specimen of diameter D, we get

$$\delta T = \frac{(c_M - c_T)d^2U}{8\lambda_n}\left(\ln\frac{D}{d} - \frac{3}{4}\right) \qquad (1)$$

As another possible cause of error in temperature measurements, we will consider nonequilibrium thermal state of a body arising in the course of thermal conductivity, when the energy in degrees of freedom of a molecule in the gaseous body is distributed with a deviation from the laws of its distribution under the conditions of thermal equilibrium [1-3]. We distinguish the temperature of a gas calculated on the presumption of local thermal equilibria with respect to the energy of the external degrees of freedom T_{ext}, and the temperature corresponding to the energy of vibrational degrees of freedom T_{int}. The temperature corresponding to the overall energy reserve of thermal movement on the assumption of its equilibrium distribution

over degrees of freedom, T_{eq}, is determined by the formula

$$T_{равн} = \frac{C_{внешн} T_{внешн} + C_{внутр} T_{внутр}}{C_{внешн} + C_{внутр}} . \qquad (2)$$

If in the thermal conductivity process measurement of the temperature T_{meas} is carried out by some ideal instrument so that $T_{meas} = T_{eq}$, then it is possible that the nonequilibrium thermal state of the compound has not been given attention. Actual methods of measuring temperature are accompanied by the error $\delta T = T_{meas} - T_{eq}$. In particular, measurement of the gas temperature from its density gives $T_{meas} \approx T_{ext}$, since the pressure and the specific volume of the gas is determined by parameters of translational degrees of freedom. Then

$$\delta T_1 = \frac{C_{внутр}}{C_{внешн} + C_{внутр}} (T_{внешн} - T_{внутр}) \qquad (3)$$

Measurement of a gas temperature by its emission gives $T_{meas} \approx T_{int}$, since radiation of the gas is caused mainly by parameters of its vibrational degrees of freedom. Then

$$\delta T_2 = \frac{C_{внешн}}{C_{внеш} + C_{внутр}} (T_{внутр} - T_{внешн}) \qquad (4)$$

Let us evaluate numerical values of δT. For simplification, let us assume that in the collision of molecules only the energy of the external degrees of freedom is transmitted and specifically by way of transport in space of this energy from molecule to molecule and that a given flux $\lambda \cdot \nabla T$. The rate of energy transport is evaluated by the quantity $W = \sqrt{a/\tau_{relax}}$ [3]. For monoatomic gases, τ_{relax} is defined as the time of relaxation of energy of translational degrees of freedom, for diatomic gases (especially at low temperatures) -- as the time of rotational relaxation, and for polyatomic gases at high temperatures -- as the time of vibrational relaxation.

At a given moment in time, $\frac{\lambda \cdot \nabla T}{w}$ of the "transit" energy of external degrees of freedom is enclosed per unit volume of the body. At this energy the processes of its transport cannot be redistributed in the equilibrium ratio between external and internal degrees of freedom, since the characteristic time of the process $\tau_{proc} = \nu/w$ sec (where ν = length of the free path of particle that serves as energy carrier) is considerably less than the time of vibrational relaxation τ_{relax}. Since for N_2 and CO_2 under normal conditions, the time of vibrational relaxation is evaluated (by extrapolation of data) [2] as $\tau_{relax} = 3 \cdot 10^{-2}$ sec and $\tau_{relax} = 4 \cdot 10^{-6}$ sec and the ratio τ_{relax}/τ_{proc}, respectively, is $7.5 \cdot 10^{7}$ and 180. The presence of the "transit" energy is caused by the drop $T_{ext} - T_{int} = \frac{\lambda \cdot \nabla T}{w \cdot c_{ext}}$. The additional drop $T_{ext} - T_{int}$ arises when there is some heating rate at a given point of the body. If the energy of internal degrees of freedom is supplemented only by way of energy of external degrees in the relaxation process, then $T_{ext} - T_{int} - \tau_{relax,vib} \cdot u$. As a whole, in the thermal conductivity process we have

$$T_{внешн} - T_{внутр} = \frac{\lambda \cdot \nabla T}{w c_{внешн}} + \tau_{рел,кол} \cdot \frac{\partial T}{\partial \tau} . \qquad (5)$$

For CO_2 at 700°C, we have $c_{int} = 0.45/c_{int} + c_{ext}$ and $\tau_{relax,vib} = 10^{-6}$ sec [2]. Then when $dT/d\tau = 0$ and $\nabla T = 10^{5}$ deg/m, from formulas (3) and (4) we find $\delta T_1 = +0.89°K$ and $\delta T_2 = -1.09°K$. Different methods of measuring the temperature of a gas in our example give errors in the limits $+0.89°K > \delta T > -1.09°K$.

For any method of measuring temperature, some error δT, caused by deviation of the actual law of distribution of molecules by velocities from the equilibrium Maxwellian distribution. On the basis of dynamic equilibrium when there is steady-state thermal conductivity of the molecular diffusion process responsible for the deviation, and of the relaxation process leading to its elimination, we derive the formula

$$\delta T' = -\frac{b(\nu \cdot \nabla T)^2 M}{2(1+2bT)} \qquad (6)$$

The values of $\delta T'$ from formula (6) are small and can be taken into account only for polyatomic gases at high rarefaction. As we know, in a rough approximation formulas describing thermal conductivity in gases extend also to solids. Interesting results have been obtained calculating $\delta T'$ from formulas (3, 4, 6) for polymers of the rubber type that are of high molecular weight. (The number of molecules forming the lattice of a body is small per unit volume of the body.) It can be assumed that thermal resistance of a body is mainly determined by resistance at the molecular faces and that the main role in the thermal conductivity process is played by phonons having a wavelength that exceeds intermolecular distances. Then, by determining the heat capacity of external degrees of freedom of the lattice by the Dulong-Petit law, we find the length of the free path of the lattice phonon from the formula $\nu = \frac{3\lambda}{c_{ext} \cdot \omega}$. Small values of c_{ext} (fraction of a percent of the heat capacity of intramolecular degrees of freedom) and the low velocity of sound ω (for rubber, two orders of magnitude lower than for glass) give upon calculation high values of ν and values of $\delta T'$ estimated by order of magnitude of degrees even for relatively small temperature gradients ($\sim$ 8000 deg/m). If for gases the error δT is small, and upon experimental determination of coefficients can scarcely be detected, then for some solids, as it appears to us, this possibility is not precluded.

Symbols

c_{ext} and c_{int} = contribution to the heat capacity of the body of the external and internal degrees of freedom, respectively; λ = coefficient of thermal conductivity; ∇T = temperature gradient; M = number of collisions of molecules leading to establishment of thermal equilibrium; b = rate of rise in heat capacity of gas with temperature rise; a = temperature coefficient of thermal conductivity.

References

1. Hirschfelder,J.; Curtis, C. and Byrd, R. , *Molekulyarnaya Teoriya Gazov i Zhidkostey, (Molecular Theory of Gases and Liquids)*, IL Press, Moscow, 1961.

2. *Sb. Gazodinamika i Teploobmen pri Nalichii Khimicheskikh Reaktsii, (Collection: Gas Dynamics and Heat Transfer with Chemical Reactions)*, IL Press, Moscow, 1962.

3. Lykov, A. V., *IFZh*, Vol. 9, No. 3, 1965.

METHODS OF INVESTIGATING THERMOPHYSICAL PROPERTIES OF SOLID MATERIALS IN A REGIME OF MONOTONIC TEMPERATURE CHANGE

S. Ye. Buravoy, Ye. S. Platunov and Yu. P. Shramko

In recent years great interest has been shown in research on modern heat-resistant materials: oxides, carbides, nitrides, silicides, borides and their compounds. The efficiency of these materials to a large extent is determined by their thermophysical properties. However, investigation of these properties involves serious methodological difficulties, especially in the temperature range above 500°C, where tests as a rule are conducted on large-size specimens and are prolonged and expensive.

The present study considers two methods affording investigation in a comprehensive way in a single experiment of the temperature dependence of heat capacity and the temperature dependence of thermal diffusivity of the above-indicated materials practically up to the melting points. The methods mutually supplement each other, having different zones of working temperatures. Their basis is general regularities intrinsic to methods of monotonic temperature change [1, 2]. For testing, rod-shaped specimens are used. Earlier, methods analogous to the experimental regime were advanced applicable to long rods with $L/D > 10$ [3, 4]. The methods examined here are the generalization of these earlier methods for the case of short rods ($L/D \geq 1$). The methods are suitable in studying not only the above-indicated, but also any other isotropic materials with thermal conductivity of (5-40) w/m·deg.

The first method is intended for research in the temperature range (50-900)°C for specimens of (20-30) mm diameter. A schematic is shown in Figure 1. The main elements of the device consist of a low-inertial tubular heater, a system of lateral and end-face screens, a radiation calorimeter, and three thermocouples. The thermocouples were mounted in hypodermic needles, which were subsequently securely attached to the base of a

massive hermetic chamber. The tests were conducted in an inert medium. The specimen was mounted on the thermocouples and placed inside the heater (its length coincided with the specimen height). Later the specimen was monotonically heated with an electric heater. Screens reduced the heat losses from the ends of the sample and the external surface of the heater, and the heater losses were directly measured by the radiation calorimeter. The operating principle and the design features of the calorimeter have been described in detail in [5].

The mean-bulk temperature $t_v(\tau)$ was measured along with the radiation drop $\theta_{or}(\tau)$ in the specimen, the electrical intensity of the heater $W(\tau)$ and the calorimeter readings $Q_p(\tau)$. The heater was supplied with alternating current of industrial frequency. Its supply conditions were chosen in such a way that the temperature drop in the specimen was 10-30 degrees. This corresponds to usual heating up at rates of (1-3) deg/sec. All electrical signals were recorded by the EPI-09 type electronic potentiometer. Thermal converters of the same type as in [6] were installed to record the current and voltage in the heater circuit.

Calculation of heat capacity $c(t_v)$ was carried out by means of the formula

$$c(t_v) = \frac{W - Q_p}{m \cdot \beta_v} (1 - \Delta\sigma_0 - \Delta\sigma_T). \qquad (1)$$

which derived from analysis of the heat balance of the measuring device, if it is taken into account that the total thermal flux of the heater W is expended mainly in heating up the specimen and in the losses Q_p in the surrounding medium. Heat losses in warming up the heater proper, screens and leaks from specimen faces were small and were taken into account in formula (1) by the analytical corrections $\Delta\sigma_c$ and $\Delta\sigma_T$. The correction $\Delta\sigma_c$ was calculated by means of the relationship

$$\Delta\sigma_0 = \frac{c_H \cdot \beta_H + c_2 \cdot \beta_2}{c_0 \cdot \beta_v} \qquad (2)$$

The structure of the correction $\Delta\sigma_T$ is determined by the system of end-face screens and by the properties of the gaseous medium. It is advisable to include in it also heat leaks from thermocouples and from the mounting reinforcements of the specimen. In the optimally corrected calorimetric device, both corrections in the total can be reduced to the values 0.03-0.1, commensurable with the permissible error of the method, therefore their analytical estimation is wholly justified.

In calculating the coefficient of thermal diffusivity $a(t_v)$, we used the formula

$$a(t_v) = \frac{B_v \cdot R^2}{4 \cdot \vartheta_{0R}} \cdot (1 + \Delta\sigma_h - \Delta\sigma_a) \qquad (3)$$

where $\Delta\sigma_h$ and $\Delta\sigma_a$ = corrections allowing for end-face heat transfer of the specimen and the temperature dependence of thermophysical coefficients

$$\Delta\sigma_h = \frac{1}{2} \frac{q_h}{q_R} \cdot \frac{R}{h} \qquad (4)$$

$$\Delta\sigma_a = \frac{1}{4} \cdot (K_\lambda - 2K_a + K_{\beta,\sigma}) \cdot \vartheta_{0R} \qquad (5)$$

Formula (3) with the correction (4) and (5) were obtained on the basis of solution of the nonlinear equation of thermal conductivity

$$\frac{\partial^2 \vartheta}{\partial \tau^2} + \frac{1}{\tau} \frac{\partial \vartheta}{\partial \tau} + \frac{\partial^2 \vartheta}{\partial x^2} = \frac{B_0}{a_0} - \left[\frac{B_0}{a_0} \cdot (K_a - K_{\beta,\sigma}) \cdot \vartheta + K_\lambda \cdot \left(\frac{\partial \vartheta}{\partial \tau} \right)^2 \right] \qquad (6)$$

at the boundary conditions

$$\left| \lambda \frac{\partial \vartheta}{\partial \tau} - q_R \right|_{\tau = R} = 0 \qquad (7)$$

$$\left|\lambda\frac{\partial\vartheta}{\partial x}+q_h\right|_{x=h}=0 \qquad (8)$$

In deriving the system of equations (6)-(8), specific simplifying presuppositions and assumptions were brought into the picture. In particular, interrelated restrictions on permissible ratios between specific fluxes q_h and q_R and temperature drops θ_{or} and θ_{oh} in the specimen were adopted

$$q_h<0{,}2\cdot q_R;\ |\vartheta_{oh}|<0{,}2\cdot|\vartheta_{oR}| \qquad (9)$$

A restriction on the permissible value of the radial drop θ_{or} in the specimen was introduced, as a consequence of which it served as the presupposition on the linear nature of change in $\lambda(t)$, $a(t)$ and $b(t)$ in the limits θ_{or} used in solving (6)-(8):

$$\lambda=\lambda_0(1+K_\lambda\cdot\vartheta_z);\ a=a_0(1+K_a\cdot\vartheta_z)\ \text{и}\ b=b_0(1+K_{b,z}\cdot\vartheta_z) \qquad (10)$$

The specific value of the permissible quantity θ_{or} was selected from the condition

$$|K_\lambda\cdot\vartheta_{oR}|<0{,}1;\ |K_a\cdot\vartheta_{oR}|<0{,}1\ \text{и}\ |K_{b,z}\cdot\vartheta_{oR}|<0{,}1 \qquad (11)$$

which must be fulfilled jointly.

The combined solution of equations (6)-(8) were made by the method of successive approximations ("small-diamteter" method) [1-4]. In the problem under consideration, the first approximation is an analytical expression for the temperature field of the specimen $\theta(x, r, \tau)$ with a precision not poorer than ±1 percent. From practical considerations in going from $\theta(x, r, \tau)$ to formula (3), a shift in the base temperature $t_o(\tau)$ was made from the central point of the specimen to the point having a mean-bulk temperature $t_v(\tau)$. This shift allows us to decrease the size of the corrections $\Delta\sigma_h$ and $\Delta\sigma_a$.

Equation (6) has in explicit form the coefficients $k_{b,r}$, characterizing change in heating rate at specimen points differing in coordinates r at a specific moment of time. However, the correction $\Delta\sigma_a$ in (5) includes the

coefficient $k_{b,\tau}$ in place of $k_{b,r}$, the former coefficient [$k_{b,\tau}$] nonlinearity of specimen heating with time. The substitution was made with account taken of the relationship [1]

$$K_{\delta,\tau} = K_{\delta,\omega} - K_a \qquad (12)$$

and was justified by the fact that experimental determination of $k_{b,\tau}$ is more preferable than for $k_{b,r}$.

The second method was intended for research at temperatures higher than 900°C. The specimen can be rectilinearly prismatic in form (long rod of square cross section) and round-shaped rod-like in form with L/D = 1, or cubic. The smallest dimension of the specimen, depending on the value of its thermal conductivity, can be 10-20 mm. The experiment was conducted in a regime of free cooling of a preheated specimen in a vacuum medium at room temperature. A description of a similar method developed for investigating specimens in the form of a square-ended prism is found in adequate detail in [7, 9], therefore here it is convenient to note only its distinguishing features, paying attention to additional factors that become manifest when we pass on to investigating small-size specimens (cylinder of finite length and cube).

Figure 2 presents a diagram of the experimental layout of the method. Its main assemblies include a vacuum chamber with a tubular electric heater, a luminosity photographic pyrometer, and a radiation calorimeter with the EPP-09 type electronic potentiometer. Supplementary equipment of the layout includes a vacuum unit, a heater power supply system, and a system for water cooling of the chamber.

The tested specimen was secured in the working zone of the chamber by means of thin tungsten or molybdenum tension wires. The heater was made from a graphite tube 24 mm in diameter with 2-mm-thick walls. The tube was cleaved in the vertical plane into two halves. After the specimen was heated (Figure 2, b), both halves of the heater were shifted by means of a driving gear (shown in Figure 2, c by arrows), turning toward the specimen with its external water-cooled screens, owing to which the specimen is able to be subject to free cooling in the working zone of the chamber.

The radiation calorimeter, as in the previous method, measured the thermal scattering flux. In this diagram, this flux is emitted directly by the specimen surface and completely determines the heat balance of the latter from the medium.

When the specimen is freely cooled over its surface, as well as through its entire bulk, a nonuniform temperature field is induced. The photographic pyrometer used in the diagram affords recording with time of the temperature field over the lateral surface of the specimen. The presence of a dead-end opening with L/D = 4 affords measurement of the true temperature in the central portion of the specimen. The pyrometer was put together based on the Zenit series-produced camera, in which the shudder was replaced by a synchronously rotating disk with a slit, the frame was reduced down to 4 mm with respect to film length, and the film itself is advanced discretely by means of an electromagnet operating synchronously with the disk. A detailed description of the pyrometer can be found in [8, 9].

The calculation formula for the coefficient of thermal diffusivity is of the form

$$a(t) = \frac{\beta_0 \cdot l^2}{k \cdot \vartheta_c} \cdot (1 - \Delta\sigma_a) \tag{13}$$

Here k = shape factor (for the square-end prism k = 4, for the cube and cylinder with L/D = 1, k = 6). The corrections entering into (3) allow for the effective temperature dependences for $\lambda(t)$, a(t), $\varepsilon(t)$ and b(t), usually do not exceed 0.2 in value, and can be estimated by means of approximational relationships.

For the cube with 2h × 2h × 2h:

$$\Delta\sigma_a = \left[K_{\beta,\sigma} \frac{3l^4 - 7h^2l^2 - 8h^4}{2l^2(h^2+l^2)} + K_a \cdot \left(1 - 2\frac{h^2}{l^2}\right) + \right.$$
$$\left. + K_\lambda \frac{13h^2 - 7l^2 + 18(h^4/l^2)}{3(h^2+l^2)} + K_\varepsilon \frac{2l^2 - 4h^2 - 6(h^4/l^2)}{h^2+l^2} \right] |\vartheta_c| \tag{14}$$

For the bounded cylinder with L/D = 1

$$\Delta\sigma_a = Bi\,\frac{9\ell^4 - 77R^4 - 53\ell^2R^2 - 15(R^6/\ell^2)}{144(\ell^2+R^2)} - \frac{9(\ell^4/R^2) - R^2 + 11\ell^2 - 3(R^4/\ell^2)}{(\ell^2+R^2)} \times (K_{\Phi,t} - 2K_a - \tfrac{2}{3}K_\lambda)\,|v_\ell| \qquad (15)$$

The calculation formula (13) with the corrections (14) and (15) was obtained just as formula (3) of the preceding method. The procedure in solving the problem and the prerequisites used agree with those for the square-end prism [4].

In calculating the mean-bulk heat capacity of specimens (cube and cylinder with L/D = 1), the following general formula is valid

$$c(t_v) = \frac{3Q_p}{|B_v| \cdot \gamma \cdot h} \qquad (16)$$

Formulas (13) and (16) are fundamental and do not reflect practical features of the measuring layout in the method. In particular, the ratio (b/θ) in (13) when a photographic pyrometer is present is replaced by the ratio of the corresponding drops in photographic densities in the film [7]. The photographic pyrometer and the radiation calorimeter afford direct measurement of the luminosity and radiation temperatures on the surface of the specimen. When we move on to the true temperature, we must know the spectral $\varepsilon_\Lambda(t)$ or the overall $\varepsilon(t)$ blackness coefficients. The coefficient $\varepsilon_\Lambda(t)$ is determined by comparing emission of the dead-end opening and that from the specimen surface, and the coefficient $\varepsilon(t)$ -- from readings of the radiation calorimeter. However, in several cases, in view of the instability of the values $\varepsilon\Delta(t)$ and $\varepsilon(t)$, it is advisable to repeat the experiment with a specimen whose surface is artificially coated with graphite or other coating, whose blackness coefficient is known.

Radiation calorimeters in both methods consist of multi-arm thermopiles. Their calibration was carried out in the fully assembled experimental layout

for the power consumed by the heater in the steady-state operating regime.

Both methods considered have been actually tested in the form of laboratory type experimental layouts (Figure 3). In the course of their development the devices were used to study several materials, including armco-iron, heat-resistant steels, titanium alloys, zirconium carbide, α-corundum and magnesite. By way of example, Figure 4 presents experimental data for armco-iron and this data is compared with the most reliable literature data.

Symbols

$D = 2R$ = specimen diameter; $L = 2h$ = height; r and x = running coordinates; ℓ = distance of fixed point on specimen face relative to its center; τ = time; $t(x, r, \tau)$ = temperature; $b = \delta t/\delta\tau$; $t_o(\tau)$, $t_v(\tau)$ and $t_n(\tau)$ = central mean-bulk and mean-surface temperatures; $b_v = \delta t_v/\delta\tau$; $b_o = \delta t_o/\delta\tau$; $\theta(r, x, \tau) = t(r, x, \tau) - t(0,0\tau)$;

$$\vartheta_{oR} = t(R,0,\tau) - t(0,0\tau); \quad \vartheta_{oh} = t(0,h,\tau) - t(0,0,\tau); \quad \vartheta_{\ell} = t(\ell,h,\tau) - t(0,h,\tau)$$

q_R and q_h = specific thermal fluxes at the lateral and end-face surfaces; m = mass specimen; $\lambda(t)$, $a(t)$, $c(t)$, $\varepsilon(t)$ and $\varepsilon_\Lambda(t)$ = coefficients fo thermal conductivity, thermal diffusivity, heat capacity, overall and spectral blackness of the specimen; k_λ, k_a and k_ε = relative temperature coefficients of λ, a and ε; ($k_i = 1/i_o\ di/dt$); $k_{b,\tau} = 1/b_o\ db/dt$ = coefficient characterizing change of rate in time; $k_{b,r} = 1/b_o\ db/d\theta$ = coefficient characterizing change of rate with respect to coordinate r; W = total power of heater; Q_p = radiation flux from heater (or from specimen) into the surrounding environment.

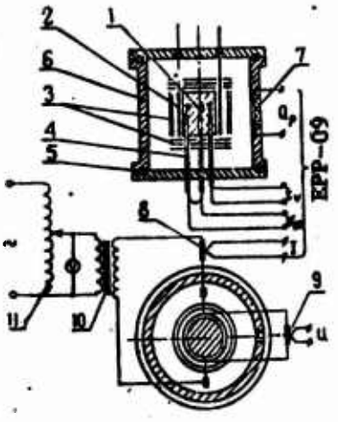

Figure 1. Diagram of measurements in the temperature range (50--900)°C: 1, Specimen tested; 2, Heater; 3, Metal screens; 4, Thermocouples; 5, Vacuum gasket; 6, Water-cooled housing; 7, Radiation calorimeter; 8, Thermal converter of current; 9, Thermal converter of voltage; 10, Step down transformer; 11, Automatic transformer.

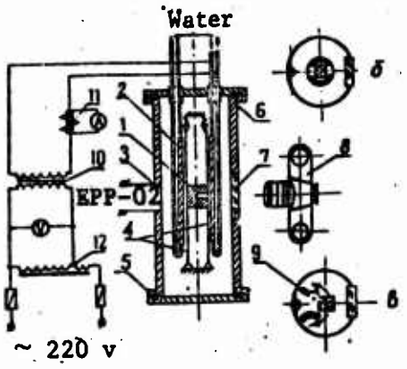

Figure 2. Diagram of measurements in the temperature range above 900°C: 1, Specimen tested; 2, Graphite heater; 3, Radiation calorimeter; 4, Tension wires; 5, Vacuum gasket; 6, Shifting vacuum gasket; 7, Peephole; 8, Photographic pyrometer; 9, Water-cooled heater screen; 10, OSU-40 step down transformer; 11, Current transformer; 12, AOSK-25 automatic transformer.

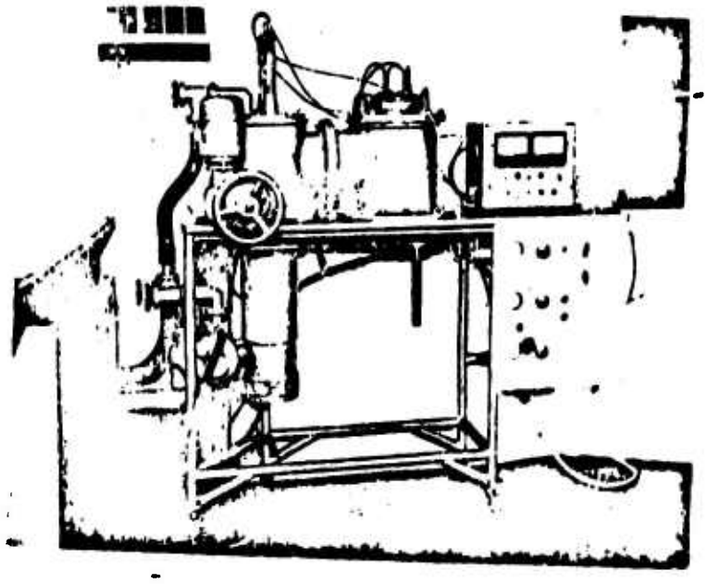

Figure 3. External appearance of experimental device for temperatures (50-900)°C

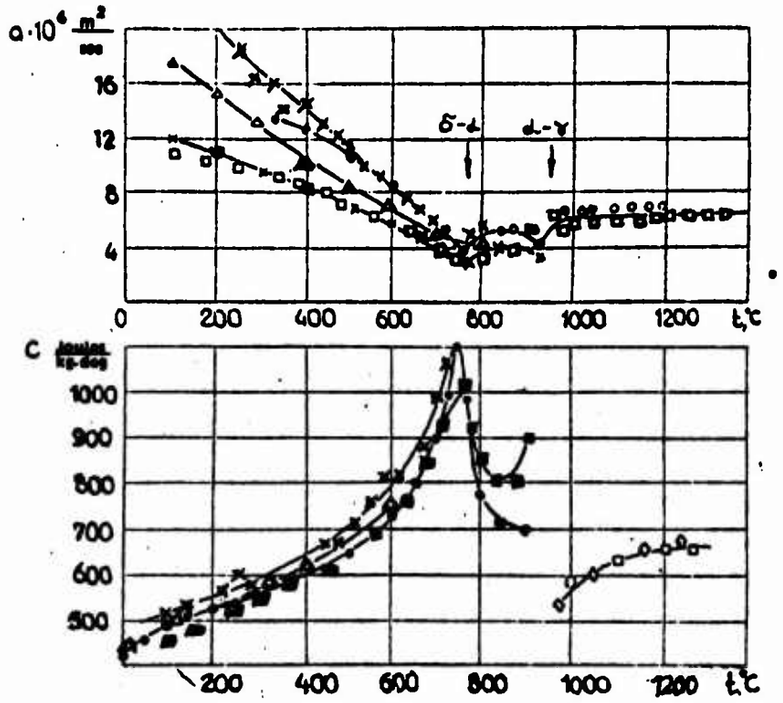

Figure 4. Experimental data on thermal diffusivity and heat capacity of armco-iron: ○, [11], initial heating heating in vacuum; ×, [11], after repeated heatings and coolings in vacuum; △, [10]; ×, our data, first heating in argon; □, our data, second heating in argon; ○, [12]; ○, [13]; ◇, [14]; ⌂, [15].

References

1. Platunov, Ye. S., *Teplo- i Massoperenos, (Heat and Mass Transfer),* ITIMO Press of the Academy of Sciences Belorussian SSR, Vol. 7, 1968.
2. Platunov, Ye, S., *IZV, Vuzov. Priborostroyeniye,* Vol. 7, No. 5, 1964.
3. Dul'nev, G. N., Ye. S. Platunov, V. V. Kurepin, and S. Ye. Buravoy, *Teplo-i Massoperenos, (Heat and Mass Transfer),* Nauka i Tekhnika Press, Minsk, Vol. 7, 1966.
4. Platunov, Ye. S., et al., *TVT,* No. 6, 1965; No. 1, 1966; No. 1, 1967.
5. Buravoy, S. Ye., *IZV, Vuzov. Priborostroyeniye,* No. 2, 1967.
6. Buravoy, S. Ye, G. N. Dul'nev, V. V. Kurepin, and Ye. S. Platunov, *GOSINTI,* PNTO Press, No. 18-66-989/72, 1966.
7. Platunov, Ye. S. and Yu. P. Shramko, *TVT,* No. 1, 1967.
8. Platunov, Ye. S. and Yu. P. Shramko, *Izv. Vuzov. Priborostroyeniye,* Vol. 9, No. 6, 1966.
9. Shramko, Yu. O., S. Ye, Buravoy, and Ye. S. Platunov, *GOSINTI,* PNTO Press, No. 18-67-197/19, 1967.
10. *Spravochnik po Teplofizicheskim Svoystvam Veshchestv, (Handbook on Thermophysical Properties of Compounds),* ed. N. B. Vargaftik, Fizmatgiz Press, Moscow, 1956.
11. Osipova, V. A. and M. I. Pak, *Teploenergetika,* No. 6, 1967.
12. Abeles, *J. Appl. Phys.,* Vol. 31, No. 9, 1960.
13. Parker, Et al., *Pribory dlya Nauchnykh Issledovaniy,* No.1, 1962.
14. Palister, P. P., *J. Iron and Steel Inst.,* Vol. 161, p. 87, 1949.
15. Wallace, D. C., P. H. Sidles, and G. S. Danielson, *J. Appl. Phys.,* Vol. 31, No. 1, 1960.

SUBSTANTIATION OF SEVERAL METHODS OF DETERMINING THERMOPHYSICAL CHARACTERISTICS BASED ON ANALYSIS OF TWO-DIMENSIONAL TEMPERATURE FIELDS

G. M. Volokhov

Temperature fields induced in bodies of various forms when they are heated or cooled in a constant temperature environment have been most fully investigated [1-3]. Analysis of these fields served as the theoretical basis for regular regime methods [2]. However, most of the known methods of investigating thermophysical properties derived from one-dimensional solutions of the equation of thermal conductivity with constant coefficients. Use of these solutions as a rule involves additional, more painstaking investigations, the purpose of which is to substantiate use of idealized models or to introduce corrections reflecting actual experimental conditions. Often these corrections are formulated on purely empirical material, which hampers their application in studying such phenomena. The lack of a unified approach in allowing for the effective actual experimental conditions on formation of temperature fields makes impossible an objective evaluation of the investigational methods themselves, above all, from the viewpoint of their precision.

Studies in the literature dealing with investigation of two- and three-dimensional temperature fields are purely either theoretical [3] or else are used to validate particular methods of determining thermophysical characteristics [1, 5, 6].

An attempt is made in the present study founded on analysis of corresponding three-dimensional and one-dimensional temperature fields to substantiate use of one-dimensional solutions in realizing first-order boundary conditions for some surfaces of the bodies tested and the presence of heat transfer from other surfaces.

We also take up certain general regularities in the development of two-dimensional temperature fields and their application in determining the Bi criterion. The two-dimensional problem presented below reflect the most typical cases of interaction of object with ambient environment.

1. A cylinder of 2h in height and 2R diameter (origin of coordinates in the center) initially is at the temperature of the ambient environment t_c. At some moment in time its bases acquire the constant temperature $t_o \neq t_c$, and the lateral surface exchanges heat with the ambient environment according to Newton's law. It is required to find an expression for the temperature field of the cylinder, that is, it is necessary to solve the differential equation of thermal conductivity

$$\frac{\partial t}{\partial \tau} = a\left(\frac{\partial^2 t}{\partial r^2} + \frac{1}{r}\frac{\partial t}{\partial r} + \frac{\partial^2 t}{\partial z^2}\right)$$

under the following initial and boundary conditions

$$t(r,z,0)=t_c=\text{const};\quad t(r,h,\tau)=t_o=\text{const};$$
$$\frac{\partial t(r,0,\tau)}{\partial z}=0;\quad \frac{\partial t(0,z,\tau)}{\partial r}=0;\quad \frac{\partial t(R,z,\tau)}{\partial r}=-\frac{\alpha}{\lambda}\left[t(R,z,\tau)-t_c\right]$$

Solution of this problem can be presented in the form

$$\Theta=\frac{t-t_c}{t_o-t_c}=\sum_{n=1}^{\infty}\frac{A_n J_0(\mu_n\frac{r}{R})\operatorname{ch}\mu_n\frac{z}{R}}{\operatorname{ch}\mu_n K}+$$
$$+2\sum_{n=1}^{\infty}\sum_{m=1}^{\infty}(-1)^m\frac{A_n\lambda_m J_0(\mu_n\frac{r}{R})\cos\lambda_m\frac{z}{h}}{(\mu_n^2K^2+\lambda_m^2)}\exp\left[-(\mu_n^2K^2+\lambda_m^2)\right]Fo, \qquad (1)$$

where μ_n = roots of the equation

$$\frac{J_0(\mu)}{J_1(\mu)}=\frac{\mu}{Bi} \qquad (2)$$

$$Fo=\frac{a\tau}{h^2};\quad \lambda_m=(2m-1)\frac{\pi}{2};\quad Bi=\frac{\alpha R}{\lambda};\quad A_n=\frac{2J_1(\mu_n)}{\mu_n\left[J_0^2(\mu_n)+J_1^2(\mu_n)\right]}$$

The parameter k = h/R characterizes the relationship between linear dimensions of the cylinder.

Detailed tables of the values A_n and μ_n are presented in [1].

2. A bounded cylinder with constant temperature of the lateral surface and in heat exchange at the end faces

$$\Theta = \frac{t-t_0}{t_c-t_0} = 2\sum_{m=1}^{\infty} \frac{J_0(\delta_m \frac{r}{R}) ch \frac{\delta_m}{R} z}{\delta_m J_1(\delta_m)(ch\delta_m K + \frac{\delta_m K}{Bi} ch\delta_m K)} + \tag{3}$$

$$+2\sum_{m=1}^{\infty}\sum_{n=1}^{\infty} \frac{A_n J_0(\delta_m \frac{r}{R})\delta_m \cos\frac{\mu_n z}{h}}{J_1(\delta_m)(\frac{\mu_n^2}{K^2}+\delta_m^2)} \exp\left[-(\frac{\mu_n^2}{K^2}+\delta_m^2)Fo\right]$$

where μ_n = roots of characteristic equation cot $\mu = \mu/Bi$ [1], δ_m = roots of the equation $i_0(\delta) = 0$, $Bi = \alpha n/\lambda$, $Fo = a\tau/R^2$.

It follows from solutions of (1) and (3) that

$$\Theta = f(\frac{r}{R}, \frac{z}{h}, Bi, Fo)$$

when Fo → ∞ (steady-state)

$$\Theta = \varphi(\frac{r}{R}, \frac{z}{h}, Bi)$$

Temperature fields calculated from solutions of (1) and (3) were compared, respectively, with the temperature fields of an unbounded sheet (when k < 1, the cylinder can be regarded as a disk), on the basis of which the identical temperature is maintained, and an unbounded cylinder, whose lateral surface temperature is constant [1].

Two-dimensional temperature fields in the center of the disk (k = 1/3) and in the center of the bounded cylinder (k = 3) are shown in Figure 1. Independently of the heat exchange intensity when the ratio of disk height to disk diameter is 1/3, the temperature in the disk center with variation in Fourier's criterion in the limits 0 < Fo < 0.6 rises as if the disk were unbounded (curve 1). Later, the temperature in the disk center deviates from the corresponding one-dimensional value, and the magnitude of this deviation

is determined by the Bi and Fo criteria. Maximum deviations (approximately 6 percent) are observed when Fo → ∞ and the criterion Bi = ∞ (curve 4), that is, under the most unfavorable heat exchange conditions. At low and moderate values of the Bi criterion, these deviations vary within the limits of 2 percent. Thus, when specimens in the form of disks or square sheets are used, conditions of single-dimensionality are satisfied with a high degree of precision, if $k \leq 1/3$, and nonsteady-state methods of investigation have clearcut advantages, since in this case heat exchange from the lateral surface does not at all distort the temperature field in the central areas of the bodies indicated.

The zone of field uniformity is retained in the neighborhood $r/R \leq 0.1$ for any values of the heat exchange coefficient, expanding as one approaches the plane $z = h$. At low and moderate values of Bi, the field is practically uniform in the region $r/R < 0.4$. When cylindrical specimens are used ($k \geq 3$), the temperature in the central areas of the cylinder satisfies the one-dimensional solution (curve 7) with a precision of up to 0.2 percent. Even when the ratio of height to diameter is equal to two, and Bi = ∞, the maximum deviation from one-dimensionality does not exceed 2.5 percent.

Let us examine several aspects of the expansion of two-dimensional temperature fields. It follows from solutions of (1) and (3) that in the steady-state the relative dimensionless temperature does not equal zero. Therefore at the regularization stage, which we take to mean the possibility of describing the temperature field by a simple exponential, it is best to introduce the cooling rate in the following form

$$m = \frac{\ln(\theta_1 - \theta_{cr}) - \ln(\theta_2 - \theta_{cr})}{\tau_2 - \tau_1} = \frac{\ln b_1 - \ln b_2}{\tau_2 - \tau_1} = \text{const} \qquad (4)$$

Similar expressions for the cooling rate are valid also when there exists within the body internal heat sources [1]. Based on (1) and (3)

$$m = \frac{a}{h^2}\left(\mu_1^2 K^2 + \lambda_1^2\right); \quad m = \frac{a}{R^2}\left(\frac{\mu_1^2}{k^2} + \delta_1^2\right) \qquad (5)$$

When $k \to 0$ for the disk and $k \to \infty$ for the cylinder, the relationships (5) are identical to the cooling rates of unbounded sheet and unbounded cylinder. Analysis of solutions of (1) and (3) shows that the cooling rate or heating rate of bounded bodies when combined boundary conditions are realized is represented by a broken line, consisting of two sections: the first of which has a slope that is the same as if the body were unbounded, and the slope of the second branch is determined by the heat exchange intensity. The angle between the broken line depends both on the Bi criterion as well as on the ratio between the linear dimensions of the specimen.

Thus, variation of the cooling rate can be a characteristic indicating that moment of time, beginning from which heat exchange will increasingly distort the temperature field in the range of measurements. In determining thermophysical characteristics, the heat exchange factor is practically precluded if in the experiments we use specimens with parameters $k \leq 1/3$ for sheets and $k \geq 3$ for the cylinder.

It is altogether obvious that temperature as a functional relationship of the Bi criterion can be used in determining the latter. For this purpose it is necessary to provide for experimental conditions under which the previously undesirable heat exchange would have a substantial effect on formation of the temperature field (cf., for example, curves 5 and 6). In the regular regime stage $\ln \theta - \theta_{st}) = f(\tau)$ or $\ln b = f(\tau)$ in semilogarithmic coordinates equals a straight line from whose slope the cooling rate is determined. From the relationship (5)

$$\mu_1 = \frac{\sqrt{\frac{mh^2}{a} - \lambda_1^2}}{\kappa} \tag{6}$$

Substituting (6) in (2) we find that

$$Bi = \frac{J_1 \mu_1}{J_0(\mu_1)} \frac{\sqrt{\frac{mh^2}{a} - \lambda_1^2}}{\kappa} \tag{7}$$

Experimental layouts for the determination of the coefficient of thermal diffusivity and the Bi criterion are extremely simple: the required boundary condition is provided for at the bases of the disk or the lateral surface of the cylinder (when friable materials are tested) [7], technically more convenient than immersing the specimen in the thermostat bath (cf., for example, the diagram for the α-calorimeter).

Knowing the thermal flux allows us to make a comprehensive determination of thermophysical characteristics. Theoretical evaluation of the one-dimensionality of heat fluxes in multilayer systems involves great difficulties. However, there are grounds to assume that the conclusions drawn will be valid also for the systems.

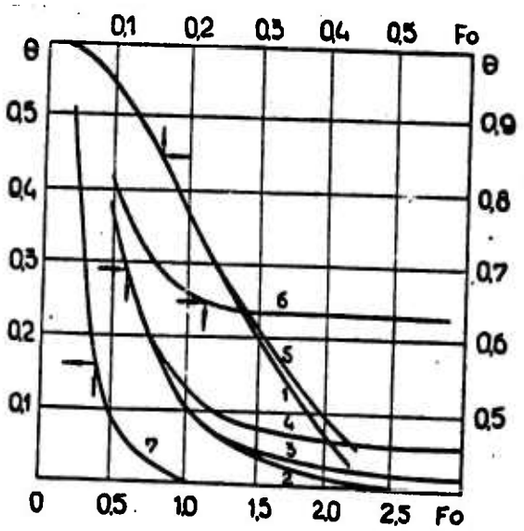

Figure 1. Two-dimensional temperature fields: 1, k = 0 (unbounded sheet), and also for $k \leq 1/3$, $0 < Bi \leq \infty$; 2, k = 0, and also for $k \leq 1/3$, $0 < Bi \leq 0.1$; 3, k = 1/3, Bi = 1.0; 4, k = 1/3, Bi = ∞; 5, k = 1/2, Bi = ∞; 6, k = 1/2, Bi = ∞; 7, k = ∞ (unbounded cylinder), and also for $k \geq 3$, and $0 < Bi \leq \infty$.

References

1. Lykov, A. V., *Teoriya Teploprovodnosti, (Theory of Thermal Conductivity)*, Vysshaya Shkola Press, Moscow, 1967.

2. Kondrat'yev, G. M., *Regulyarnyy Teplovoy Rezhim, (Regular Thermal Regime)*, GITTL Press, Moscow, 1952.

3. Karslou, G. and D. Yeger, *Teploprovodnost' Tverdykh Tel, (Thermal Conductivity of Solids)*, Nauka Press, Moscow, 1964.

4. Kirichenko, Yu. A., *Trudy VNIIM*, No. 51, 1961.

5. Frayman, Yu. Ye. and G. A. Surkov, *IFZh*, No. 5, 1965.

6. Slobodyanyuk, L. I. and A. A. Sendetskiy, *IFZh*, No. 10, 1961.

7. Volokhov, G. M., *IFZh*, No. 5, 1966.

DETERMINATION OF THERMAL CONDUCTIVITY OF EXTREMELY THIN LAYERS OF VARIOUS MATERIALS

V. S. Vol'kenshteyn and N. N. Medvedev

In the first method of two temperature-time intervals [1], the relative temperature θ at the boundary of the sheet studied and the heat receiver was determined by the equation:

$$\theta = t/t_n = (1+\alpha)(\operatorname{erfc} y - \alpha \operatorname{erfc} 3y + \alpha^2 \operatorname{erfc} 5y - \ldots) = f(\alpha, y) \qquad (1)$$

where

$$y = \frac{h}{2\sqrt{a\tau}}, \quad \alpha = \frac{\varepsilon - 1}{\varepsilon + 1}, \quad \varepsilon = \frac{\lambda}{b\sqrt{a}}. \qquad (2)$$

This equation allows us to compile a table of functions $\varepsilon/y = f(\varepsilon)$ for various values of θ. Figure 1 gives the graphs of this function for several values of θ and for $\varepsilon < 1$. It is clear from these graphs that for large values of θ and small values of ε, the ratio ε/y does not depend on ε, that is, the value $(\varepsilon/y)_{max} = M$ will be constant for a given value of θ.

The value of $(\varepsilon/y)_{max} = M$ will differ for different θ.

Figure 2 gives the function $(\varepsilon/y)_{max} = M = f(\theta)$. From the expressions (2), it follows that:

$$\lambda = b\varepsilon\sqrt{a} = be\frac{h}{2y\sqrt{\tau}} = \frac{bh}{2\sqrt{\tau}} \cdot M \qquad (3)$$

Determination of the thermal conductivity coefficient boils down to measuring the interval of time counted from the beginning of contact of the free surface of the material under study with the heater until some moment of

time corresponding to a value of $\Theta = 1 - N/N_0$ that is convenient for measurements, where N and N_0 = readings of the galvanometer connected to the circuit of a differential thermocouple and corresponding to the temperatures t and t_{htr}. One of the thermocouple arms is placed between the material studied and the heat receiver, and the other in the constant-temperature heater.

We find from the graph $M = f(\Theta)$ the corresponding value $M = (\varepsilon/y)_{max}$. Substituting this value M into formula (3), we find λ. In order to obtain a small value of the parameter $\varepsilon = \lambda/b\sqrt{a}$, at which the condition $\varepsilon/y = const$ is valid in the experiment, it is necessary to use a heat receiver with a large value of the constant b.

Let us present an example in which we determine the coefficient of thermal conductivity of micaceous compounded insulation on the lacquer PE-935. The layer thickness $h = 0.15$ mm $= 1.5 \cdot 10^{-4}$ m. Let us take as the heat receiver marble, whose thermal activity is $b = 1750$ w·sec$^{1/2}$/m^2·deg. The period of movement of the light indicator of the galvanometer from N_0 to $N = 0.15\ N_0$ is obtained as equal to $\tau = 27.4$ sec. This division N corresponds to the relative temperature

$$\Theta = 1 - \frac{N}{N_0} = 1 - 0{,}15 = 0{,}85 = 85\%.$$

The graph shown in Figure 2 gives for this value of Θ the value of $M = 7.3$, consequently:

$$\lambda = \frac{b\,h}{2\sqrt{\tau}} \cdot M = \frac{1750 \cdot 1{,}5 \cdot 10^{-4}}{2 \cdot \sqrt{27{,}4}} \cdot 7{,}3 \frac{w}{m \cdot deg} = 0{,}183 \frac{w}{m \cdot deg}.$$

Instead of measuring the time τ counted from the beginning of contact, we can measure the interval of time $\Delta\tau$ corresponding to the difference $\Delta N = N_1 - N_2$, where

$$\frac{N_1}{N_0} = 1 - \Theta_1 \qquad \text{and} \qquad \frac{N_2}{N_0} = 1 - \Theta_2 .$$

The graph shown in Figure 2 gives values of M_1 and M_2 corresponding to the values of Θ_1 and Θ_2. In this case

$$\lambda = \frac{b\,h}{2\sqrt{\Delta\tau}} \cdot M', \qquad \text{where} \qquad M' = \sqrt{M_2^2 - M_1^2}\,.$$

Choice of the values Θ_1 and Θ_2 must satisfy the conditions:

$$M_1 = \varepsilon/y_1 = \text{const}_{\text{I}} \qquad \text{and} \qquad M_2 = \varepsilon/y_2 = \text{const}_{\text{II}}$$

(cf. Figure 1).

This method allows us to investigate materials with very low layer thickness h. Thus, for example, if the heat receiver is lead (b = = 6960 $w \cdot sec^{1/2}/m^2 \cdot deg$) and Θ = 90 percent M = 11.2), when τ = 16 sec and λ = 0.1 $w/m \cdot deg$, then we will have

$$h = \frac{2\sqrt{\tau}\,\lambda}{b\,M'} = \frac{2 \cdot 4 \cdot 0{,}1}{6960 \cdot 11{,}2}\ \text{м} \approx 0{,}01\ \text{мм}$$

Symbols

λ = coefficient of thermal conductivity; a = coefficient of thermal diffusivity; h = thickness of layer investigated; τ = time; b = thermal activity of the heat receiver; d_{htr} = temperature of heater; $\Theta = t/d_{htr}$ = = relative temperature.

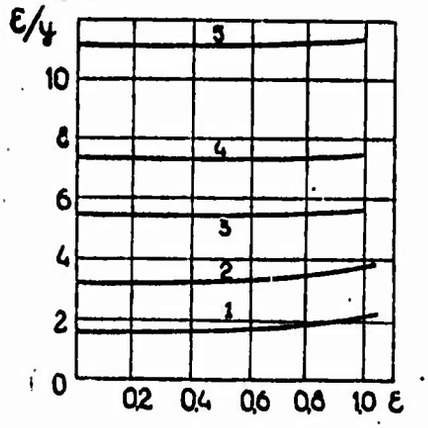

Figure 1. The function $\varepsilon/y = f(\varepsilon)$ for the series of values Θ: 1, 0.5; 2, 0.7; 3, 0.8; 4, 0.85; 5, 0.9.

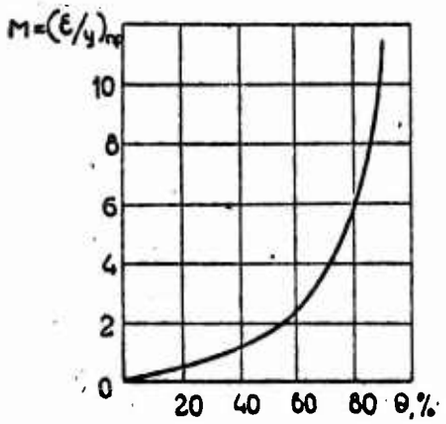

Figure 2. The function $M = (\varepsilon/y)_{max} = f(\Theta)$.

References

1. Vol'kenshteyn, V. S. and N. N. Medvedev, *IFZh*, Vol. 2, No. 10, 1959.

THERMOMETRIC DETERMINATION OF THERMOPHYSICAL CHARACTERISTICS

O. A. Gerashchenko, T. G. Grishchenko,
A. M. Pilipenko and V. G. Fedorov

By thermometrics we denote the section of heat physics that deals with methods of measuring, controlling and regulating heat fluxes. It has been markedly developed only in the last 10-15 years. Substantial results were obtained relatively rapidly. In particular, a series of sensitive elements embracing measurement of heat fluxes in the range from 10^{-2} to 10^{6} w/m^2 [1] has been developed in the Laboratory for Thermal Measurements Methods of the Institute of Technical Heat Physics of the Academy of Sciences, Ukrainian SSR.

Providing fuller quantitative information, the results of thermometric measurements are of interest in various fields of science. Available equipment allows us to make measurements in geophysical studies of geothermal heat fluxes, in physiological investigations of organisms as a whole and of particular organs, in an extremely wide range of technical measurements, and several other areas.

Indirect measurements are of interest per se, making it possible to obtain from primary thermometric information secondary information of a broader nature, in particular, determination of thermophysical characteristics of compounds and structures as a whole or by parts. A number of applications associated with determinations of such thermophysical characteristics as thermal conductivity and thermal diffusivity and integral heat capacity of structures and their parts are examined below.

The formal advantage of the thermometric approach is that in the right-hand side of the thermal conductivity equation, the first-order operator with respect to flux appears instead of the differential second-order operator with respect to temperature. Advantages posed by reducing the order of the

of the differential operator in the equation are self-evident, however the possibilities uncovered are still finding very restricted use.

Below we set forth only a few cases in which the thermometric approach was reduced or is being reduced to an instrumental stage making it possible to secure direct measurements of characteristics.

Instrument for Determining Thermal Conductivity Coefficients

The first and simplest application was an instrument developed and already approved for determining thermal conductivity by the flat-sheet method in conditions that are steady state with respect to time.

A key advantage of the instrument is that all the quantities needed in determining the thermal conductivity coefficient (heat flux, thickness of specimen and temperature difference in the specimen) are obtained by direct measurement.

The specimen, in the form of a disk or sheet, is squeezed between a heater and a refrigerator. The heat flux transducer lies in the center of the refrigerator and measures local specific flux. Peripheral regions fulfill functions of protective belts. External thermal perturbations in the disk squeezed between sheets with high thermal conductivity are propagated to a depth of the order of one disk thickness.

To determine the temperature difference, initially thermocouples are used whose arms lie on the surfaces of the heater and the refrigerator. At this point there is a substantial scatter (up to ±12 percent) of the results of measurement even for well prepared specimens. Later, the thermocouples are placed on backing made of thin elastic rubber. Here, the requirements for quality in treatment of results are reduced, and scatter of results of measurements made on standard specimens of fused quartz and and polymethyl methacrylate of various thicknesses does not exceed the limits ±5 percent.

Radiometric calibration of the transducer together with the refrigerator allows us to find the working coefficient of the transducer in the absolute system. Here the values of the thermal conductivity coefficients of the standard specimens are obtained as equal to the mean values from reliable tabulated data [2-4].

A substantial advantage of the instrument is the possibility of making measurements not only on solid specimens, but also on liquids and gases.

Table 1 presents the results of measurements of thermal conductivity of several new materials at temperatures 20-100°C for which no handbook data yet exists, in comparison with standard materials.

Table 1. Results of Testing Materials for Thermal Conductivity

Number	Material	Thermal conductivity, w/m · deg
1.	Terephthalate film	0.10
2.	Petryanov fabric	0.036
3.	Elektronit[1]	0.31
4.	FAED[1] + PEPA[1]	0.20
5.	FAED + PEPA ... + V[1]	0.27
6.	FAED + GMDA[1]	0.21
7.	FAED + FMDA + ... PZh[1]	0.65
8.	Glass-textolite [resin-impregnated laminated cloth]	0.32
9.	Glass-lacquer-linen	0.18
10.	Glass-linen, bakelized	0.21
11.	Polymethyl methacrylate	0.19
12.	Fused quartz	0.30

Determination of Effective Heat Capacity and Thermal Conductivity of Insulation Protection

The possibilities of local thermometry allow us to carry out the problem of determining thermophysical characteristics of heat-insulation materials under natural conditions. In some cases, determination of effective thermophysical characteristics by means of the below-described method seems to be the only possible approach, for example, when packing protective coverings with fibrous material. The density and structure of the material, and consequently, its thermophysical characteristics, cannot be previously determined unambiguously with adequate precision.

[1]See p. 293

To determine the effective heat capacity and thermal conductivity, a section of the enclosure must be selected in which the heat flux is normal to both surfaces of the enclosure. In this operation it is carried out by means of two heat flux transducers placed on the same normal to the wall from opposite sides. The absence of lateral heat loss is controlled by equating the specific heat fluxes at the inlet and outlet from the walls under conditions of steady-state thermal regime. To determine heat capacity it is necessary to measure the value of the energy accumulated or expended by a section of the enclosure of unit area during the period of the transient thermal regime between two steady-state regimes (one of them can be the zero regime, equilibrium), the increment in the temperature of the section during the transient process, and the thickness of the insulation. The effective bulk heat capacity is calculated from the equation

$$c'_{эфф} = \frac{Q}{\delta \cdot \Delta t} \qquad (1)$$

The quantity Q is determined based on readings taken during the period of heat fluxes through both enclosure surfaces in the transient regime:

$$Q = \int_{\tau_1}^{\tau_2} (q_1 - q_2)\, d\tau \qquad (2)$$

Here $(q_1 - q_2)$ = difference of heat fluxes at inlet and outlet from walls. In practical terms, the integral (2) is determined by planimetry of the area bounded by the following curves

$$q_1 = f_1(\tau) \qquad \text{and} \qquad q_2 = f_2(\tau)$$

The heat capacity value found must be related to the mean temperature of the enclosure section during the process. Usually it is sufficient to measure the temperatures of both insulation surfaces and in equation (1) to substitute the rise in mean section temperature. The entire device consists of two transducers for temperature and heat fluxes placed on the enclosure surfaces.

The thermal flux and temperature transducers must have inertia and intrinsic heat capacity two-three orders of magnitude less than the period of the transient process and the enclosure heat capacity.

The effective thermal conductivity coefficient is determined in the steady-state regime from the value of the thermal flux q, the temperature drop at the walls $\Delta t'$, and the enclosure thickness δ:

$$\lambda_{эфф.} = \frac{q \cdot \delta}{\Delta t'}$$

Thus, heat capacity at a single temperature and thermal conductivity at one (if one of the steady-state regimes is the equilibrium regime) or at two temperatures are determined in a single experiment. Measurement results are given in Figures 1-3 and in Table 2. Figure 1 shows variation in fluxes at inlet and outlet in a single-layer closed space made of PS-B styropore 0.07 m thick. The square pulse of the thermal flux was set by switching on a low-inertia electric heater. Figures 2 and 3 present data on the determination of effective thermophysical characteristics of a multi-layer enclosure -- the door of the domestic Smolensk refrigerator (SNP copolymer 0.003 m thick, PS-B styropor, 0.026 m thick, and steel sheet 0.001 m thick). Figure 2 corresponds to the transient regime from the equilibrium to the steady-state regime of refrigerator operation (with the switched off temperature control device); Figure 3 presents the transition to the equilibrium state from the steady-state regime via the sudden opening of the door. The change in sign of the derivative in Figure 2 is accounted for by the fact that the cold productivity of the compressor unit depends on the temperature in the refrigeration chamber and drops off as the temperature is reduced during the period of departure from the regime.

For comparison, the effective heat capacity of the multi-layer enclosure can be calculated from the formula

$$C'_{эфф.} = \frac{\sum_{i=1}^{n} c_i \rho_i \cdot \delta_i \cdot \Delta t_i}{\Delta t \cdot \delta}$$

Table 2. Comparison of Experimental and Calculated Thermophysical Characteristics of Multi-layer Enclosures

No.	Enclosure	°C of enclosure	Experimental data			Calculated data	
			kJ/m^2	c'_{eff} $kJ/m^3 \cdot deg$	λ_{eff}, $n/m \cdot deg$	$kJ/m^3 \cdot deg$	$w/m \cdot deg$
	Single-layer:						
1.	PS-B styropor, $\delta = 0.07$ m, $\rho = 45$ kg/m^3; (Figure 1)	35	77	107	0.056	60-95	0.04-0.06
	Two layer:						
2.	1. Copolymer SNP, $\delta = 0.003$ m 2. PS-B styropor, $\delta = 0.077$ m, $\rho = 35$ kg/m^3	10	175	148	0.042	120-145	0.04-0.05
	Three-layer						
3.	1. Copolymer SNP, $\delta = 0.002$ m 2. Glass wool, $\delta = 0.054$ m 3. Steel sheet $\delta = 0.001$ m	40	116	155	0.054	150-180	0.046-0.060
4.	Door of Smolensk refrigerator						
	1. Copolymer SNP, $\delta = 0.003$ m 2. Styropor PS-B, $\delta = 0.026$ m, $\rho = 35$ kg/m^3 3. Steel sheet $\delta = 0.001$ m (Figures 2 and 3)	12	182	356	0.042	290-350	0.04-0.05

It is interesting to note that for the arrangement of enclosure of components nonsymmetrical in the sense of sequence, the effective heat capacity depends substantially on what side heat action on insulation comes into play. In particular, for the refrigerator door heat capacity when there is heat action from the outside (change in room temperature) can prove to be 50 percent greater than for heat action from within (change in operating conditions of refrigerator unit).

Determination of Thermal Diffusivity and Thermal Conductivity of Rocks

Several methods of determining thermophysical properties have been based on consideration of problems of nonsteady-state thermal conductivity. Some of them [5] make it possible to carry out determination of thermophysical characteristics of rocks, construction materials and other materials in situ without resorting to removal of material and preparation of specimens.

Here the thermometric approach also provides some methodological conveniences.

The physical arrangement of the problem is carried out as follows. A certain bounded body exhibiting high thermal conductivity and thermal diffusivity with initial temperature u_o is brought in contact through a thermometric transducer with the rock mass being tested. The temperature $t(r, \tau)$ of the mass at the initial moment is presumed to be identical and naturally differs from the temperature of the test body. After contact, equalizing of temperatures takes place at an intensity that depends on thermophysical characteristics of the mass under testing. If we neglect heat exchange at the free uncontacting surfaces of the bodies, the differential equation of thermal conductivity for the case under consideration will be of the following form:

$$\frac{\partial t(r,\tau)}{\partial \tau} = a \cdot \left[\frac{\partial^2 t(r,\tau)}{\partial r^2} + \frac{2}{r} \cdot \frac{\partial t(r,\tau)}{\partial r} \right].$$

at the boundary conditions

$$t(R,\tau) = U(\tau)$$

$$\lambda \cdot F \frac{\partial t(R,\tau)}{\partial r} = C \frac{dU(\tau)}{d\tau}$$

The solution for the case under consideration is as follows:

$$\frac{t(R,\tau)}{U_0} = \frac{\beta}{\beta-\alpha}\cdot\exp(\beta^2 a\tau)\cdot\operatorname{erfc}(\beta\sqrt{a\tau}) -$$

$$-\frac{\alpha}{\beta-\alpha}\cdot\exp(\alpha^2 a\tau)\cdot\operatorname{erfc}(\alpha\sqrt{a\tau}),\quad -\frac{\partial t(R,\tau)}{\partial\tau}\cdot\frac{R}{U_0} =$$

$$=\frac{R}{\sqrt{\pi a\tau}} + \alpha(\alpha R-1)\exp(\alpha^2 a\tau)\operatorname{erfc}(\alpha\sqrt{a\tau}) -$$

$$-\beta(\beta R-1)\exp(\beta^2 a\tau)\cdot\operatorname{erfc}(\beta\sqrt{a\tau})$$

is difficult to subject to analysis. To simplify the analysis, it is convenient to use the asymptotic expansion in powers of dimensionless times:

$$\frac{t(R,\tau)}{U_0} = 1 + a_1\cdot Fo^{\frac{1}{2}} + a_2 Fo + a_3\cdot Fo^{\frac{3}{2}} + \ldots$$

$$-\frac{\partial t(R,\tau)}{\partial\tau}\cdot\frac{R}{U_0} = b_0 + b_1 Fo^{-\frac{1}{2}} + b_2 Fo^{\frac{1}{2}} + b_3 Fo + b_4 Fo^{\frac{3}{2}} + \ldots \qquad (3)$$

These are rapidly converging series for small times and for the ranges of thermophysical characteristics under consideration (for example, for rocks). The dimensionless coefficients a_i and b_i include the area of surface contact, the integral heat capacity of the test body and the thermophysical characteristics of the mass being tested. The functions

$$\frac{t(R,\tau)}{U_0} = f(Fo),\quad -\frac{\partial t(R,\tau)}{\partial\tau}\cdot\frac{R}{U_0} = g(Fo)$$

shown in Figure 4 were plotted for rocks.

The solution (3) derived, as in most cases, tends toward the regular regime. As a consequence, beginning with the value Fo = 1, the ratio of temperatures $t(R, \tau_1)/t(R, \tau_2)$ for a constant Fourier interval remains remains practically constant. Thus, if the temperature ratio is chosen

(according to the graph in Figure 4) in such a way that $\Delta Fo = 1$, the thermal diffusivity can be determined from the relationship

$$a = \frac{R^2}{\tau_2 - \tau_1}$$

Unfortunately, the solution with respect to thermal flux (4) does not approach a regularity; however, the possibility of directly measuring thermal fluxes allow us to use the graph of the function (4) in determining thermal conductivity, which can be calculated from well known values of dimensionless times using the formula:

$$\lambda = \frac{q(\tau'') - q(\tau')}{\left[-\frac{\partial t(R,\tau'')}{\partial \tau}\cdot\frac{R}{U_0}\right] - \left[-\frac{\partial t(R,\tau')}{\partial \tau}\cdot\frac{R}{U_0}\right]}\cdot\frac{R}{U_0}$$

It is desirable to make two separate measurements of the flux in order to avoid errors that can crop up owing to imprecision in fixing the onset of the process.

This method is proposed for practical application using an instrument in which the role of the test body will be played, for example, by a copper bar which can be kept in an ice-filled flask until it is brought into contact with the mass. A semispherical recess must be readied in the mass under testing. Signals from the quantities being measured (temperature and thermal flux) are suggested to be fed to self-recording instruments. The length of the experiment is not more than 15 min.

The applications considered do not exhaust the potentialities of thermometric methods. The authors are convinced in the significance of their advantages and are in hopes of their extensive development in the most varied realms of measurement practice, in particular, for determining thermophysical characteristics.

Symbols

a = thermal diffusivity, m^2/sec; c = integral heat capacity, joules/deg; c'_{eff} = effective bulk heat capacity, joules/m^3·deg; c = mass heat capacity, joules/kg·deg; F = surface of contact, m^2; Q = thermal energy, joules/m^2; q = thermal flux, w/m^2; R = radius of contact surface, m; r = radial spherical coordinate, m; $t(r, \tau)$ = temperature of mass, deg; $u(\tau)$ = temperature of test body, deg; u_o = initial temperature of test body, deg; θ = thickness, m; Δt = rise in temperature in the enclosure section, deg; $\Delta t'$ = temperature drop at walls, deg; λ = thermal conductivity, w/m·deg; ρ = density, kg/m^3; τ = time, sec; Fo = dimensionless time (Fourier coefficient).

GRAPHIC NOT REPRODUCIBLE

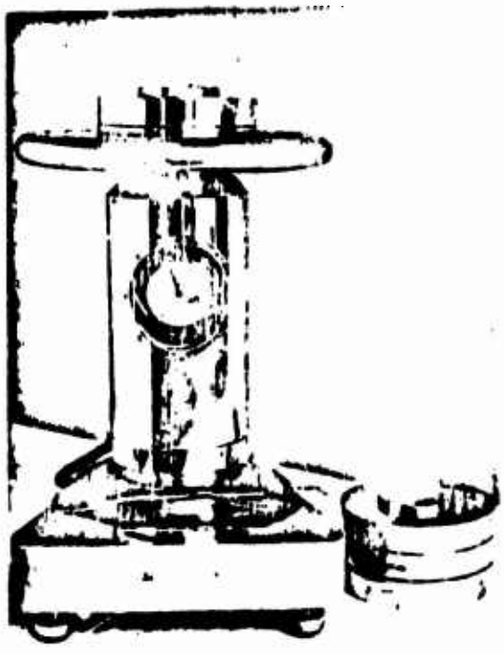

Figure 1. External appearance of instrument for determining thermal conductivity

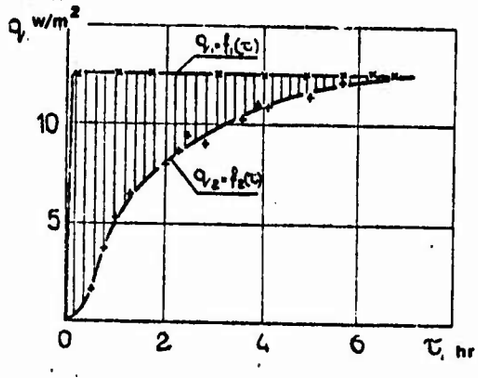

Figure 2. Transient process in the single-layer styropor enclosure, Q = 77 kilojoules/m^2

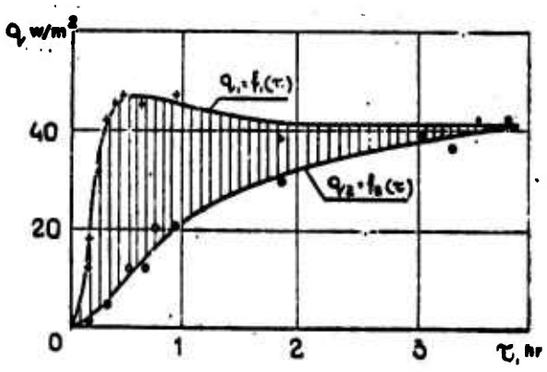

Figure 3. Transient process in the door of the Smolensk refrigerator upon plugging into electrical outlet, Q = 186.3 kilojoules/m^2

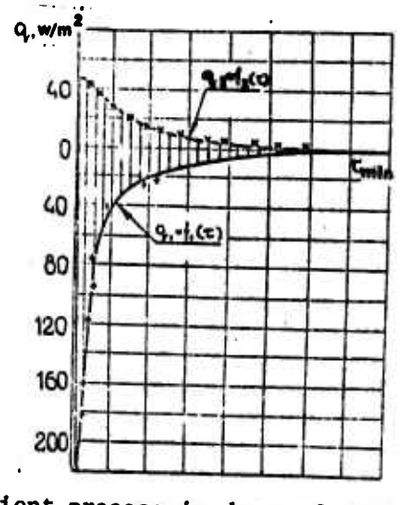

Figure 4. Transient process in door of Smolensk refrigerator when the door is opened suddenly

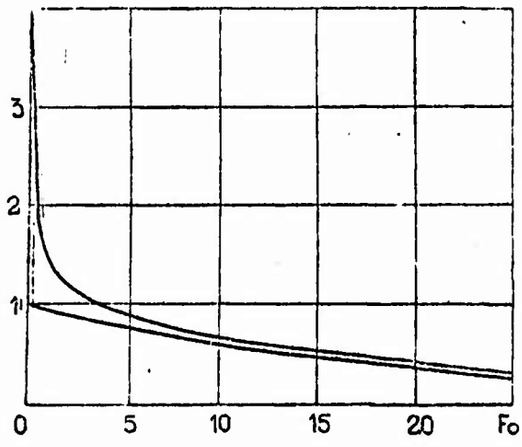

Figure 5. Graphs of $t(R, \tau)/u_o$ (1) and $\frac{\partial t(R, \tau)}{\partial r} \frac{R}{u_o}$ (2) as functions of Fo

Footnotes

1. To p.282 Transliterated from the Russian--Tr.

References

1. Gerashchenki, O. A. and V. G. Ferorov, *Teplovyye i Temperaturnyye Izmereniya, Spr. Ruk, (Heat and Temperature Measurements, Handbook)*, Naukova Dumka Press, Kiev, 1965.

2. Voronkova, Ye. M., B. N. Grechushnikov, G. I. Distler, and I. P. Petrov, *Opticheskiye Materialy dlya Infrakrasnoy Tekhniki, (Optical Materials for Infrared Equipment)*, Nauka Press, Moscow, 1965.

3. *Spravochnik Mashinostroitel'ya pod red., (Machine-builder's Handbook)*, Edited by N. S. Acherkana, Volume 2, Mashgiz Press, Moscow, 1960.

4. Devyatkova, Ye., A. V. Petrov, I. A. Smirnov, and B. Ya. Moyzhes, *Fizika Tverdogo Tela*, Vol. 2, No. 4, 1960.

5. Morachevskiy, I. I., B. V. Spektor, and V. I. Ryazantsev, *Sb. Teplo- i Massoobmen, (Collection: Heat and Mass Transfer)*, Academy of Sciences Belorussian SSR Press, Minsk, Vol. 1, 1962.

USE OF THERMAL FLUX TRANSDUCERS

O. A. Gerashchenko, V. G. Karpenko and Yu. M. Chimisov

In solving a multitude of problems both in propagation of heat within a solid, as well as problems on heat transfer on the surfaces of solids, we must know the amount of heat transmitted, that is, the value of the thermal flux.

Determination of thermal fluxes in solids by analytical methods is possible only in particular cases, usually for solids of the most simple configuration (sheet, cylinder, sphere) when we know the thermophysical properties and the boundary conditions [1]. As far as local heat transfer coefficients are concerned, their analytical determination also involves great difficulties. Here we must have information on a large number of factors. Therefore, as a rule, thermal fluxes have to be determined experimentally.

The Laboratory for Methods of Thermal Measurements of the Institute of Technical Heat Physics of the Academy of Sciences Ukrainian SSR has devised various thermal flux transducers that can be used in directly measuring overall and local thermal fluxes. The transducers developed can be divided into two main types -- isolated and battery.

The former is a distinctive oblate differential thermocouple , whose intermediate thermoelectrode serves as a supplementary wall [2].

The battery transducer consists of a large number of series-connected thermal elements. The role of the thermal elements in the transducer is played by coils in which one of the thermoelectrodes is a galvanically coated semicoil, and the second is an uncoated coil. The thermoelement packing density in this battery amounts to 2000 units per square centimeter, owing to which not only is high transducer sensitivity provided, but also its relatively low thermal resistance.

The main requirements which are governing in development of thermal flux transducers is their universality, the high precision and stability of readings, relatively low inertia and minimum distortion of the thermal flux field when the transducers are in use. The latter of course does not mean that no account need be taken of spherical thermal, hydrodynamic and temperature environments when thermal flux transducers are used under specific sets of conditions in order not to introduce appreciable distortions into the physical picture of the heat transfer process intrinsic to the transducer.

When the transducer is placed within a wall, such distortions are avoided if the thermal conductivity of the wall and the transducer is identical, that is, if the thermal resistance of the system is kept invariant.

Realizing this measurement layout as a rule is very laborious, and in most cases introduction of transducers inevitably distorts to a greater or lesser extent the thermal flux field, and the results of measurements are in need of appropriate correction.

When there is conductive heat transfer, the thermal flux transducer as a rule is placed in the bulk of the body being tested. The thermal conductivity of the transducer here can be higher or lower than the thermal conductivity of the wall. These cases have been investigated by the electrothermal analog method [2].

When investigating convective and radiative heat transfer, transducers are usually placed on the wall surface, bringing about local increase in thermal resistance and, consequently, distortion of the thermal flux.

In the general case, solution of the problem is taxing. However, for the case of measurements on metallic surfaces, it can be presupposed that the temperature at the heat-transfer surface with the placed transducer does not change, that is, the temperature under the transducer and in neighboring surface areas is the same. If in this case we can make the wholly realistic assumption that heat transfer coefficients at the external surface of the thermal flux transducer and on the surfaces not covered by it are the same, then we can obtain an expression that allows us to find the true value of the

thermal flux from transducer readings:

$$q_u = q\left(1 + \frac{q\,\varepsilon/\lambda}{t_n - t_{op} - q\,\delta/\lambda}\right) \qquad (1)$$

For experimental verification of expression (1), we used a copper block whose surface was kept at a specific temperature of t_{sur} by means of a heater and a temperature control device. The transducer swept by a current of air was embedded in the body of the block flush with the surface. By varying the air flow conditions the intensity of heat transfer from the surface was varied. A low-inertia radiator was positioned opposite from the transducer at a specific distance from the surface.

Measurement of fluxes emanating from the transducer surface did not present any difficulty, since the relationship between the transducer signal and the thermal flux penetrating it is known from calibration.

By taking account of the high thermal conductivity of copper, it can be calculated that the block temperatures at its surface and under the transducer are the same. This assumption was used in determining true fluxes and was attained by the following procedure. The flux from the transducer to air was determined in the steady-state regime. Then the radiator was switched on and a radiation regime was selected under which the transducer signal became zero. At this juncture the radiation energy penetrating the transducer surface was wholly swept off by the air current, that is, the true thermal flux equaled the density of the penetrating radiation.

Experimental data obtained finds good agreement with the expression (1).

In the general case, the effect of thermal resistance of the transducer on distortion of thermal flux can be allowed for if, in addition to transducer readings, we record the temperature drop between the heat transfer surface and the circumfluent medium. Here, the true thermal flux is associated with the recorded flux by the following simple relationship:

$$q_u = \frac{q}{1 - \frac{q\delta}{(t_{cp} - t_n)\lambda}} \qquad (2)$$

For complex heat transfer by radiation and convection, there is a possibility in principle of making separate measurements of the radiative and the convective components by using thermal flux transducers with different absorption coefficients.

By placing two transducers with different absorption coefficients on a high-thermal conductivity surface and measuring the temperature drop between the wall surface and that of the medium, we can determine the values of the radiative and convective components from the following system of equations:

$$\begin{cases} q_1 = q_{к1} + \varepsilon_1 q_л \\ q_2 = q_{к2} + \varepsilon_2 q_л \\ \dfrac{q_{к1}}{q_{к2}} = \dfrac{t_{ср} - t_п + q_1 r_1}{t_{ср} - t_п + q_2 r_2} \end{cases} \qquad (3)$$

In the case when the temperature drop between the medium and the heat-transfer surface in practical terms is not amenable to measurement, the individual determination of the radiative and convective components of the thermal flux can be obtained by using three thermal flux transducers with different absorption coefficients. The solution can be obtained from the following system of simple relationships:

$$\begin{cases} q_1 = q_{к1} + \varepsilon_1 q_л \\ q_2 = q_{к2} + \varepsilon_2 q_л \\ q_3 = q_{к3} + \varepsilon_3 q_л \\ \dfrac{q_1 r_1 - q_2 r_2}{q_2 r_2 - q_3 r_3} = \dfrac{q_{к2} - q_{к1}}{q_{к3} - q_{к2}} \end{cases} \qquad (4)$$

It is interesting to note that under conditions of complex heat transfer, use of thermal flux transducers having different absorption coefficients makes it possible to determine the heat transfer coefficient by convection even in those cases when it is impossible to measure the temperature of the ambient environment.

Actually, the heat transfer coefficient is easily calculated from the following simple relationship:

$$\alpha = \frac{q_{k_1} - q_{k_2}}{q_2 r_2 - q_1 r_1} . \qquad (5)$$

In conclusion, it must be stated that use of thermal flux transducers opens up sweeping vistas in the field of thermophysical measurements. These transducers can considerably simplify the technique of measuring heat transfer coefficients. Further, cumbersome and laborious measurements in compiling heat balances are obviated. The high sensitivity of battery transducers creates favorable conditions for development with the transducers as a basis of sensitive absolute instruments and devices for calorimetry, measurements of radiative energy, emission properties of surfaces, etc. The possibility of direct measurements with the aid of thermal flux transducers of local thermal fluxes does away with the need to install protective heaters when determining thermophysical properties of materials.

Symbols

q_{tr} = true value of thermal flux; q = thermal flux penetrating the transducer; q_k = convective component of thermal flux; q_Λ = density of impinging radiation; ε = absorption coefficient; α = heat transfer coefficient; λ = coefficient of transducer thermal conductivity; δ = thickness of transducer; t_{sur} = temperature of wall surface; t_{av} = ambient temperature; r = thermal resistance of transducer.

References

1. Mikheyev, M. A., *Osnovy Teploperedachi, (Fundamentals of Heat Transfer)*, GFI Press, Moscow-Lenigrad, 1956.

2. Gerashchenki, O. A. and V. G. Ferorov, *Tekhnika Teplotekhnicheskogo Eksperimenta, (Equipment in Heat Engineering Experiments)*, Naukova Dumka Press, Kiev, 1964.

METHODS OF STUDYING THERMOPHYSICAL CHARACTERISTICS OF HEAT CARRIERS AND CONSTF ;CTION MATERIALS AT HIGH TEMPERATURES

V. A. Gruzdev, O. A. Krayev and A. N. Solov'yev

Research on new materials in wide temperature ranges has required new methods. Several original methods developed in the Institute of Heat Physics of the Siberian Division of the Academy of Sciences USSR are presented in the present article.

γ-Method of measuring density (Figure 1). The method is based on exponential change in intensity of a monoenergetic parallel beam of γ-quanta in its passage through material. In the actual case it is necessary to take into account change in the geometry of the container and change in the "parasitic" absorption in the structural parts and in the gas with variation in temperature. Since it is impossible to calculate with adequate precision the coefficients of absorption, the γ-method is worthwhile using in investigating the temperature dependence, and the absolute values of density are determined from a reference density value. The calculated formula of the method is as follows:

$$\rho(T) = \rho(T_0)\frac{\ln J'/J}{\ln J_0'/J_0}\cdot\frac{1+\alpha T_0}{1+\alpha T}.$$

Use of an electronic timer and stabilized sources of current made it possible to boost measurement precision up to 0.1 percent.

Vibration method of measuring viscosity. Parameters of forced vibrations of a flat sheet (amplitude, frequency and phase shift) depend on viscosity of the ambient medium. For low-viscous liquids

$$\sqrt{\lambda\rho} = \frac{C_1}{A} - C_2.$$

Methods of Measuring Surface Tension

Automated vertical plate method (Figure 2). The force with which a flat plate, a thin-walled tube, or other body is drawn into liquid is determined. The working formula is

$$\sigma = \frac{P + P_{rup}}{\pi \cos\theta}.$$

Here P = force of attraction, P_{rup} = force of repulsion.

Key improvements are introduced in the present study: a reliable metal vapor condenser has been developed, a new technique of conducting the experiments has been formulated that makes it possible to vary the depth of immersion, artificially form the boundary angle $\theta = 0$, to allow for the weight of the condensed metal, and to make weighing automatic. Measurements of surface tension of alkali metals have been made up to 1200°K. The scatter of experimental values for most of the experiments was 0.5-0.8%.

The two-jump method (Figure 3). The method is designed to measure surface tension of aggressive liquids in an atmosphere of their own vapor. Liquid is slowly evacuated from a system of three capillaries connected in parallel, two of which abruptly intergrade into tubing of somewhat greater diameter. When the level of the liquid passes through the sites of transition, a jumplike redistribution of the heights of the capillary rise at three bends. The working formula is

$$\sigma = \frac{\gamma \Delta V}{2\pi} \frac{1}{(R_1^2 + r_2^2 + r_3^2)\left(\frac{1}{r_2} - \frac{1}{R_1}\right)} = C\gamma\Delta V.$$

In a comparison version of the method, determination can be made not of ΔV, but of a quantity proportional to it, for example, the number of pulses of an electromechanical counter proportional to the number of rotations of the drive shaft of an engine moving a piston.

Measurements of surface tension of alcohol-water mixtures and of molten sodium and potassium have been made. The scatter of experimental values is approximately 1.5 percent.

Method of measuring thermal diffusivity of metals (Figure 5). A specimen of metal in the form of a plate is placed in a vacuum and heated by electronic bombardment of one of its sides. The temperature wave is propagated deep within the plate, reaches the opposite face, and is recorded with the aid of a photocell. A phase shift ϕ exists between fluctuations in thermal flux and temperature at the opposite face, depending on thermal conductivity λ, thermal diffusivity a, frequency of temperature fluctuations ω, thickness of specimen δ, and heat transfer at the faces α. For $Bi = \alpha\theta/\lambda \geq 0.01$ and at $z = \delta\sqrt{\omega/a} \geq 1.6$, the phase shift is practically independent of the heat transfer condition at the faces, and for $z \geq 2$, the relationship of z and ϕ in approximate terms is described by the equation $z = 1.414\phi - 1.11$. The thermal diffusivity of several refractory metals was determined by this method: tungsten, tantalum, molybdenum, niobium and others up to 3300°K.

Pulse method of determining heat capacity of metals (Figure 5). A specimen of the material under study in the form of a thin wire is heated at a high rate (up to 10^5°C/sec) by an electric current passing through it. In this case heat losses in the ambient medium can be neglected, and the working formula takes on the form

$$C_p = \frac{\alpha^2 U(E-U)^3 R_0}{mER^2 dU/d\tau} \cdot$$

In the experiment measurement was made of the time interval $\Delta\tau$ during which the voltage in the specimen varied from the fixed value U_1 to U_2. Then $dU/d\tau = \frac{U_2 - U_1}{\Delta\tau}$ and $U = \frac{U_1 + U_2}{2}$. Threshold circuits were used in switching the meter on and off. The heat capacity of platinum was investigated. Scatter of experimental values was approximately 2 percent. In addition to the differential method described, a method of measuring heat capacity by means of measuring voltage, and consequently, of temperature in the specimen as a function of time was also formulated and tested. Here, $U_1 = 0$, and U_2 changes stepwise.

Phase method of measuring thermal diffusivity of gases (Figure 6). The gas studied was placed in a metal capillary heated by alternating current.

The temperature wave in the gas produced as a consequence led to the inception of pressure fluctuations in the gas. The amplitude of the pressure fluctuations is proportional to the mean gas temperature, and their phases coincide. Analysis of the solution of the corresponding differential equations shows that there is an unambiguous relationship of phase shift between the gas pressure fluctuations and the capillary wall temperature fluctuations, and that in the range of parameter $R\sqrt{\omega/a}$ change from one to three (which corresponds to the phase difference 7-35°) a good linear section exists. The tube containing the gas under study was heated by a generator current. The signal from the pressure transducer was amplified and fed to a phase meter. A reference signal was sent to the phase meter from the generator through a phase inverter. The latter was designed to compensate for phase shift in the amplifier. The phase shift between current and temperature owing to the presence of heat transfer can be made to closely approach 90° by selection of tubing diameters and generator frequency.

Bridge method of measuring heat capacity of gases (Figure 7). The gas under study was passed successively through two metallic capillaries heated by electric current. The capillaries were connected into a bridge which in the absence of the gas flow was in equilibrium. The gas passing through the tubings in opposite directions upset the symmetry of the temperature fields and varied the resistance of the bridge arms. For low amounts of gas passed, the unbalance of the bridge is proportional to heat capacity and to the weight consumption. This version of the flow calorimeter is free of difficulties in measuring low thermal fluxes and temperature differences and can be used in measuring heat capacity at high temperature. The outlay of gas through the calorimeter is provided by a water manostat and is measured by the pressure drop in a long thin capillary.

Controlled measurements have been made of the heat capacity of air and carbon dioxide up to 350°C. The scatter of experimental values does not exceed 0.2 percent. The calorimeter is of small size, simple design, and can be used in measuring heat capacity of gases at elevated temperatures.

Symbols

ρ = density; γ = bulk weight; T = temperature; I = intensity of radiation beam; α = coefficient of linear expansion; η = viscosity; Ai = amplitude of fluctuation; σ = surface tension; P = force; Θ = boundary angle; Π = wetting perimeter; r_i and R_i = radii of capillaries and tubings; ΔV = change in volume; C_i = instrument constants; ϕ_i = phase shift; λ = coefficient of thermal conductivity; a = coefficient of thermal diffusivity; α_i = coefficient of heat transfer; ω = frequency of fluctuation; δ = thickness of plate; c_p = heat capacity; U = voltage drop; E = electromotive force of power source; m = mass of specimen; τ = time; R = electrical resistance; κ = temperature coefficient of resistance.

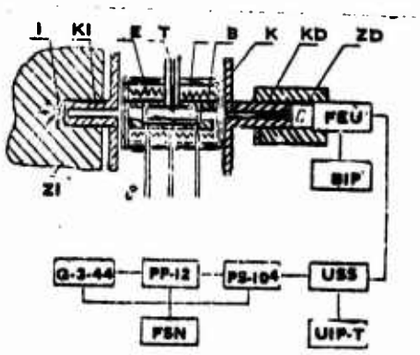

Figure 1. Diagram of device for determining density by the γ-method: I = source of radiation (Co^{60}); KI and KD = collimators at the source and at the detector; ZI and ZD = lead shielding at the source and the detector; T = crucible containing molten metal; B = thermostating block; P = furnace; E = shield; K = housing of furnace containing inert gas; C = scintillator crystal; FEU = photomultiplier; BIP = battery power source; USS = amplifier; UIP-1 = power source; PP-12 and PS-10,000 = scaling circuits; G-3-44 = precision deca-e generator.

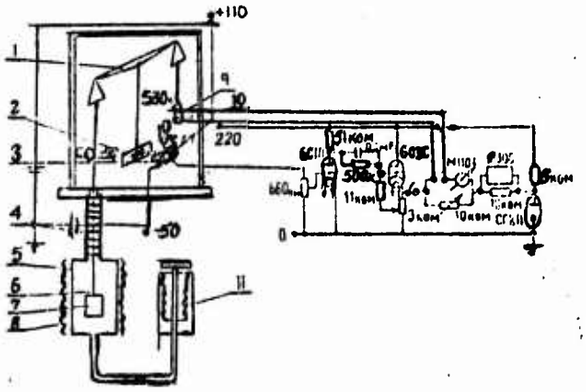

Figure 2. Circuit of experimental device for determining surface tension: 1, Scale; 2, Screen; 3, Photoconductive cell; 4, Condenser; 5, Crucible; 6, Filament; 7, Plate; 8, Furnace; 9, Coil; 10, Magnet; 11, Bellows dosimeter.

KOM = Kilo-ohms
MF = Millifarads

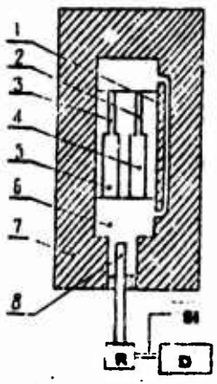

Figure 3. Diagram of the "two-step" method: 1, 2, 3, Capillaries; 4, 5, Tubings; 6, Lower chamber; 7, Thermostating block; 8, Rod; P, Reducing gear; SI, Pulse counter; D, Electric motor.

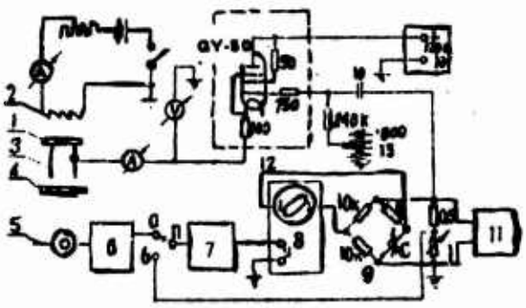

Figure 4. Diagram of experimental device for determination of thermal diffusivity: 1, Specimen (anode); 2, Cathode; 3, Tungsten reference tubing; 4, Photometric wedge; 5, Photoelectric cell; 6, Cathode follower; 7, Selective amplifier; 8, Oscillograph; 9, Phase inverter; 10, Current source; 11, Audio generator; 12, Modulator; 13, External power source.

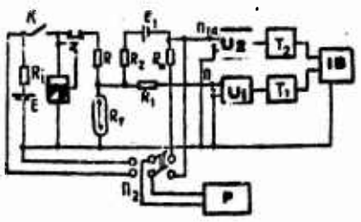

Figure 5. Diagram of device for determination of heat capacity of metals by fast heating methods: N, Key; RV, Time relay; U_1 and U_2, Amplifiers; T_1 and T_2, Flip-flops; IV, Time meter; P, Direct current potentiometer; P_1 and P_2, Switches; R_t, Specimen; R_2, R_N, R, Resistances of the compensation circuit; E_1 and E, Current sources.

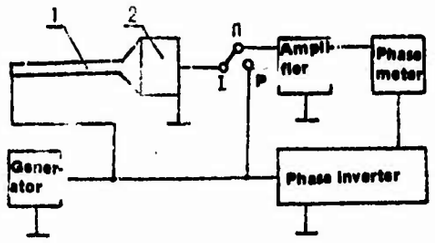

Figure 6. Circuit of experimental device for determining thermal conductivity of gases by the phase method: 1, Gas-containing capillary; 2, Pressure transducer.

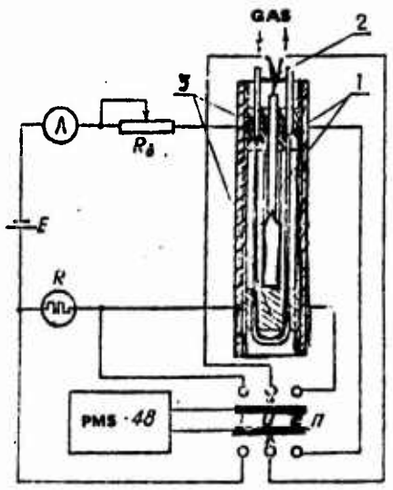

Figure 7. Circuit of experimental device for determining heat capacity of gases: 1, Capillary; 2, 3, Apexes of electrical bridge; R_θ, Regulating resistance; A, Ammeter; E, Current source; R_N, Normal resistance coil; P, Switch.

MEASUREMENT OF THE THERMAL CONDUCTIVITY OF GAS MIXTURES

K. M. Diykema and D. A. de Vriz

Precise values of thermal conductivity of gases are necessary in designing apparatus for investigating heat transfer in gases and in developing the kinetic theory of gases, in particular, the theory of gas mixtures.

There is extensive literature on this question cited in this present article [1-8].

Measurement of thermal conductivity we conducted in the laboratory involved studying physical properties of gas mixtures. Since we were interested in heat and moisture transfer in porous bodies we used mainly air (and its components, nitrogen and oxygen) and water vapor.

Additionally, thermal conductivity measurements can be used to determine the composition of a gas mixture.

In other words, thermal conductivity can be a measure of the absolute humidity of air. We made such humidity measurements.

The present article sets forth a description of two types of devices for measuring thermal conductivity: a device based on use of coaxial cylinders, and a device containing a bridge circuit with thermistors. The latter were especially designed to measure small changes in thermal conductivity and to determine the amount of water vapor in air under controlled conditions.

Cylindrical Cell

The space between two cylindrical cylinders was filled with gas having a thermal conductivity λ, and constant power Φ is fed to the inner cylinder. The outer cylinder is kept at a constant temperature. In the steady-state regime

$$\Phi = \frac{2\pi\lambda l(T_1 - T_2)}{\ln(r_2/r_1)} \qquad (1)$$

Here r_1 and r_2 = radii of inner and outer cylinders, T_1 and T_2 = their wall temperatures, l = length of cylinders. When all values in expression (1) are determined), we can calculate the thermal conductivity λ.

The inner cylinder consists of a platinum wire 25.4 μ in diameter and 169 mm in length. It is heated by electric current. The wire's electrical resistance is measured with the aid of a sensitive Wheatston bridge. Current 1 passing through the wire is determined by measuring the voltage across a standard resistance for 1 cm with a compensator.

The temperature of the wire is found from its resistance R, and the power equals $\Phi = I^2R$. The platinum wire is soldered to copper wires of 0.1 mm diameter.

The outer cylinder consists of a brass tube with 2.13 mm internal diameter and 200 mm long. It is placed in a thermostating device. The temperature on the surface of the cylinder is maintained with precision of 0.001°C.

Placement of the platinum wire in the center of the brass tubing presents a major problem. Copper wires inserted in a teflon stopper was used here. The wire was then fastened to two phosphorus bronze springs.

In deriving the equation (1) it was presupposed that heat is transferred in a radial direction only by thermal conductivity. It was necessary to introduce corrections for heat transfer by radiation and by convection and for the end-face effects, since at the ends the temperature varies along the wire and thermal flux is not wholly radial.

Measurements were made at pressures of 1 atm. When the mean free path was comparable to the wire radius, it was necessary to introduce a correction for the temperature jump.

From theoretical considerations and experiments at reduced pressures, we concluded that at room temperature the correction for radiation is 0.1 percent. This is also most valid for free convection. The effect of the

temperature jump can be neglected at atmospheric pressure.

The weightiest ccorrection was the correction for the end-face effects, 8 percent. Since it is difficult to obtain by a calculational method, we used a second cell containing a platinum wire 40 mm long. This cell was placed on an arm of the Wheatston bridge, the opposite arm of which contained the first cell (Figure 1). Both cells contained the same gas at the same temperature and pressure [8].

Since resistances R_2 and R_3 of the remaining arms of the bridge were equal, an equal current passed through both cells when the bridge was balanced.

The absolute precision of our measurements was limited by the precision with which the diameter and length of the wire were determined.

Thermal conductivity measurements of nitrogen at 20°C and atmospheric pressure gave the value of 24.85 ± 0.09 mw/m-°C; Barua (1959) found a value of 24.94 mw/m-°C; the relative error is 0.36 percent.

Below are given values of the thermal conductivity of clean gases at a temperature of 20.5°C and a pressure of 80 kN/m^2 (≈ 0.8 atm).

Gas	(mw/m-deg)
H_2	174.8
O_2	25.58
A	17.24

Thermistor-Containing Bridge

Thermal conductivity was measured with the aid of the katharometer method. Constant power was fed to a bead thermistor. Under steady-state conditions, this power was scattered by thermal conductivity or convection in the gas surrounding the thermistor, by thermal conductivity along the conducting wires, and by radiation. The equilibrium temperature which the thermistor attained depends, among other things, on the physical properties of the gas. Under appropriate conditions, this temperature is a measure of the thermal conductivity of the medium surrounding the thermistor. A temperature difference on the order of 10^{-4}°C can be detected by using a suitable device. A similar method was employed in [7].

A diagram of this device is given in Figure 2. The Wheatston bridge operates on alternating current of 5000 cps, which is supplied from a 0.6-w source. The ac arm contains the thermistor for measuring thermal conductivity T_m, together with a series-connected resistor. The AB arm contains the second thermistor T_c, together with a series-connected resistor. The CD arm contains a specified resistor, and the BD arm a specified resistor series-connected with a variable resistor. The power is fed to the thermistor from a 4.5-w direct current source. The direct current cannot pass from A along B and D owing to the presence of two condensers C_1 and C_2.

The variable signal is amplified by a 3000 gain amplifier. Both thermistors are shown in Figure 3. The thermistors with series-connected resistors were selected in such a way that during operation the bridge equilibrium is not disturbed by varying the temperature of the medium surrounding the thermistors.

This means that the AB and AC arms must have an identical relationship between resistance and temperature, while at the same time T_m is heated by direct current, and T_c is not.

The thermistors were beadlike, 1 mm in diameter. Their resistance at room temperature was 2500 ohms; the power supply to T_m is 2 mw; it produced an approximately 5°C rise in air temperature. Below are given the values of the resistances comprising the bridge.

R_1 = 1412 ohms, R_2 = 50 ohms, R_3 = 659 ohms, R_4 = 588 ohms, R_5 = = 1312-1500 ohms with a 47-ohm step change. $C_1 = C_2$ = 100 microfarads.

The measuring head containing the thermistors was placed in a measuring chamber containing the gas or a gas mixture. The temperature of this chamber was kept constant with a precision of 0.001°C.

In order to obtain the desired reproducibility and precision of results, it is necessary to maintain the tubing temperature with a precision of ±0.5°C.

A more detailed description of the instrument together with theoretical analysis of various factors influencing its performance will be published later. Precision of thermal conductivity measurements was 0.1 percent of the absolute value.

Results of measuring the thermal conductivity of the O_2-N_2 mixture at atmospheric pressure and 26.5°C are given in Figures 4 and 5. Figure 4 shows the thermal conductivity of this mixture as a function of composition. Figure 5 presents a graph of the function $\lambda_m - [(1 - x)\lambda_{N_2} + x\lambda_{O_2}]$, where λ_m = experimental thermal conductivity value of the mixture, x = mole fraction of oxygen, $[(1 - x)\lambda_{N_2} + x\lambda_{O_2}]$ = thermal conductivity of the mixture governed by a linear law.

The sensitivity of the instrument for measuring thermal conductivity of the mixture is characterized by how the experimental points fit a smooth curve.

Measurements of thermal conductivity of the mixtures nitrogen-water vapor, oxygen-water vapor, and air-water vapor will be published later.

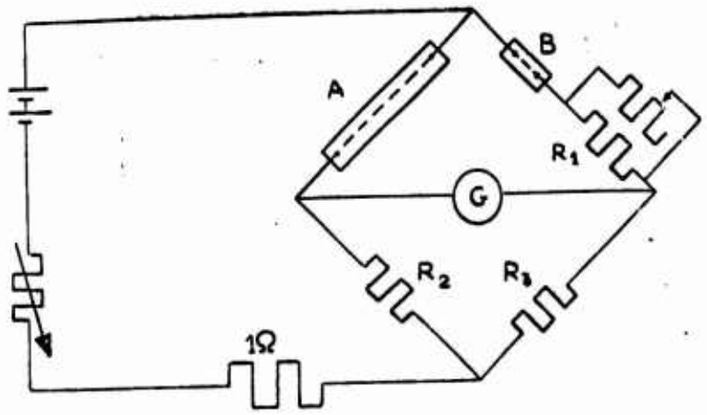

Figure 1. Diagram of device for measuring thermal conductivity. A, Measurement cell; B, Cell containing a short platinum wire to compensate the end-face effects; G, Galvanometer.

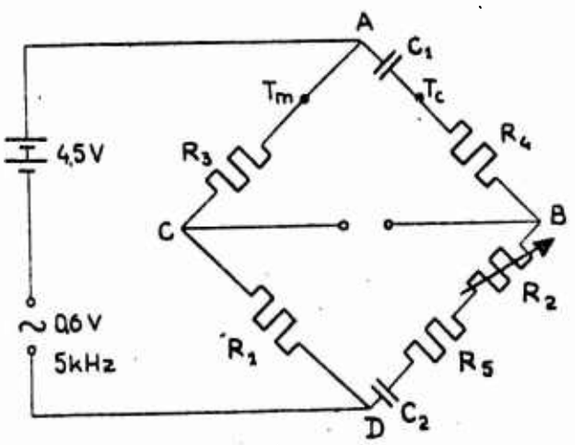

Figure 2. Bridge circuit with thermistor

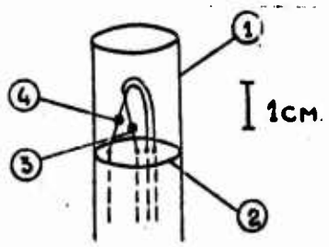

Figure 3. Measurement head of bridge-containing thermistor: 1, Brass screen; 2, Teflon stopper; 3, Measurement thermistor T_m; 4, Compensation thermistor T_c.

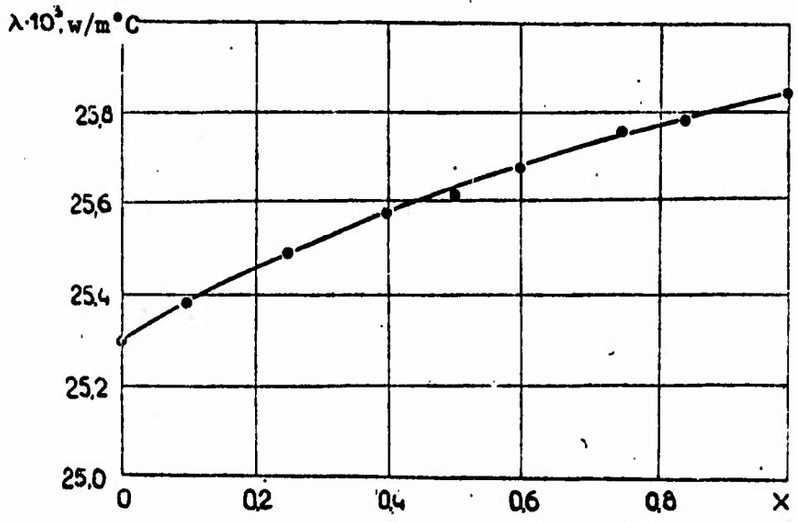

Figure 4. Thermal conductivity of the O_2-N_2 mixture

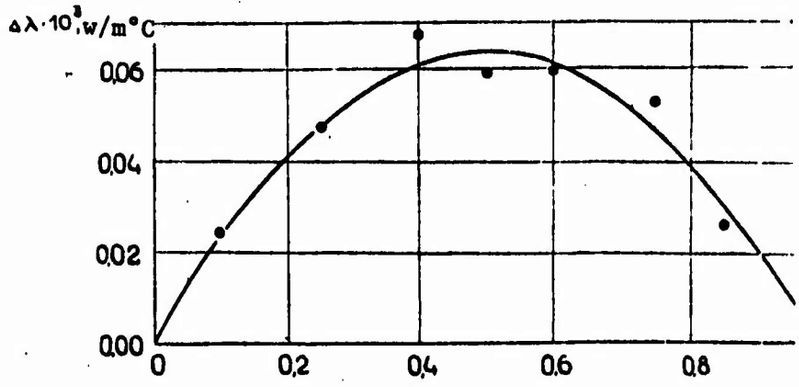

Figure 5. Deviation from linearity [Δλ) of data given in Figure 4

References

1. Barua, A. K., *Physica*, Vo.. 25, p. 1275, 1959.

2. Brokaw, R. S., *J. Chem. Phys.*, Vol. 42, p. 1140, 1965.

3. Meisenard, A., *Conductivite thermique des solides, liquides, et de leurs melanges*, Eds. Eyrolles, Paris, 1965.

4. Monchick, L, A. N. G. Pereira, and E. A. Mason, *J. Chem. Phys.*, Vol. 42, p. 3241, 1965.

5. Saxena, S. C., M. P. Saxena, R. S. Gambhir, and J. M. Gandhi, *Physica*, Vol. 31, p. 333, 1965.

6. Tsederberg, N. V., *Thermal conductivity of gases and liquids*, Scripta Technica, MIT Press, Cambridge, (Mass.), 1965.

7. Walker, R. E and A. A. Westenberg, *Rev. Sci. Instr.*, Vol. 28, p. 789, 1957.

8. Weber, S, *Ann. der Physik*, Vol. 54, p. 325, 1917; Vol. 82, p. 479, 1927.

LATERAL HEAT TRANSFER IN TESTING SPECIMENS IN THE FORM OF A BOUNDED CYLINDER

V. V. Kurepin

A layout for measuring thermal diffusivity coefficients under quasi-steady-state or monotonic heating conditions, shown in Figure 1 [1-5], has found wide acceptance.

The test specimen is placed in contact with two metal sheets and is symmetrically heated by them. The lateral surface of the specimen is surrounded by an air collar, acting as heat insulation. The flux scatter from the lateral surface amounts to 5-10 percent of the flux absorbed by the specimen, which makes it possible to take the temperature field of the specimen as one-dimensional, axial. It is described by a second-order parabola with adequate precision. The thermal diffusivity coefficient is calculated from the formula

$$a = \frac{bh^2}{2v_0} \cdot \qquad (1)$$

Distortion of the temperature field of the specimen owing to the presence of lateral heat transfer has not been allowed for by most researchers. Choice of specimen dimensions was also made without any substantiation.

The present article sets forth results of an analysis of the temperature field in the air collar layer surrounding the lateral surface of the specimen. The effect of lateral heat transfer on the temperature field of the specimen is investigated.

It is assumed that heat transfer within the closed collar layer is mainly by thermal conductivity.

Since the rate of rearrangement of the temperature field in the air layer is considerably higher than the heating rate employed in a = calorimeters, the

temperature field in the layer can be considered as steady-state at each moment in time. With allowance for the assumptions made, let us examine a hollow bounded cylinder $R_1 < r < R_2$, and of height $0 < z < H$ (Figure 1, a). The thermal conductivity equation

$$\frac{\partial^2 t(r,z)}{\partial r^2} + \frac{1}{r}\frac{\partial t(r,z)}{\partial r} + \frac{\partial^2 t(r,z)}{\partial z} = 0 \qquad (2)$$

boundary conditions

$$t(r,0) = t(r,H) = t(R_2, z) = 0, \qquad (3)$$

$$t(R_1, z) = p(z^2 - zH). \qquad (4)$$

Solution of (2) under conditions (3) and (4), obtained by the method of separating variables, is of the form

$$t(r,z) = \frac{4pH^2}{\pi^3}\sum_{n=1}^{\infty}\frac{[(-1)^n - 1]}{n^3}\cdot\frac{I_0(\psi_n R_2)K_0(\psi_n r) - K_0(\psi_n R_2)I_0(\psi_n r)}{I_0(\psi_n R_2)K_0(\psi_n R_1) - I_0(\psi_n R_1)K_0(\psi_n R_2)}\sin(\psi_n z) \qquad (5)$$

The total thermal fluxes $Q_{1,2}$ and $Q_{1,3}$ are found by integrating over the appropriate surfaces

$$Q_{1,2} = Q_{1,4} = -2\pi\lambda\int_{R_1}^{R_2}\left|\frac{\partial t(r,z)}{\partial z}\right|_{z=0}\cdot r\,dr;$$

$$Q_{1,3} = -2\pi R_2\lambda\int_0^H\left|\frac{\partial t(r,z)}{\partial r}\right|_{r=R_2}\cdot dz.$$

The mean temperature of the specimen surface is

$$\bar{t}(R_1, z) = \frac{1}{H}\int_0^H p(z^2 - zH)dz = -\frac{pH^2}{6}.$$

and the mean temperature drop between different surfaces is

$$\bar{\vartheta} = \bar{\vartheta}_{1,2} = \bar{\vartheta}_{1,3} = \bar{\vartheta}_{1,4} = -\frac{pH^2}{6}.$$

Thermal conductivities between the surfaces of interest to us can be determined as the ratio of thermal flux in a given direction to the difference in mean surface temperatures, that is,

$$\sigma_T = \sigma_{1,2} = \sigma_{1,4} = \frac{Q_{1,2}}{\bar{\vartheta}} = \frac{96\lambda R_1}{\pi^2} \sum_{m=1}^{\infty} \frac{1}{(2m-1)^5} \times$$

$$\times \frac{I_0(\psi_m R_2)[R_2 K_1(\psi_m R_2) - K_1(\psi_m R_1)] - K_0(\psi_m R_2)[R_2 I_1(\psi_m R_2) - I_1(\psi_m R_1)]}{I_0(\psi_m R_2) K_0(\psi_m R_1) - I_0(\psi_m R_1) K_0(\psi_m R_2)}, \quad (6)$$

$$\sigma_\delta = \sigma_{1,3} = \frac{Q_{1,3}}{\bar{\vartheta}} = \frac{192\lambda R_2}{\pi^2} \sum_{m=1}^{\infty} \frac{1}{(2m-1)^5} \times$$

$$\times \frac{I_0(\psi_m R_2) K_1(\psi_m R_1) + K_0(\psi_m R_2) I_1(\psi_m R_1)}{I_0(\psi_m R_2) K_0(\psi_m R_1) - I_0(\psi_m R_1) K_0(\psi_m R_2)}. \quad (7)$$

For several values of $\bar{H}$ and $\bar{R}_2$, the conductivities σ_T and σ_δ were calculated on the Minsk-2 electronic digital computer and are shown in Figures 2 and 3 in the form of graphs of dimensionless complexes

$$\frac{\sigma_T}{\lambda_b R_1} = f(\bar{H}, \bar{R}_2), \quad \frac{\sigma_\delta}{\lambda_b R_1} = f(\bar{H}, \bar{R}_2) \quad (8)$$

The graphs allow us to determine the flux scattered from the lateral surface of the specimen at given values of $\bar{H}$ and $\bar{R}_2$ from the formula

$$Q_{рас} = (\sigma_\delta + 2\sigma_T)\bar{\vartheta}. \quad (9)$$

Under conditions when the main role in heat transfer is played by thermal conductivity, the distribution of flux over the lateral surface of the specimen is governed by the law $\sin(\psi_{sur} z)$. To the first approximation it

can be represented by a parabola of the form (4). Here the specific thermal flux on the surface proves to be linearly related to the temperature drop

$$\lambda \frac{\partial t}{\partial r} + \alpha(t - t_{cp}) = 0 . \qquad (10)$$

The heat transfer coefficient on the lateral surface of the specimen is determined from the expression

$$\alpha = \frac{Q_{pac}}{\vartheta \cdot F_1} . \qquad (11)$$

Use of the relationship (10) allows us to relatively simply take into account in the working formula (1) the effect of the scattering flux on the lateral surface. The correction coefficient is found as the result of integrating the equation (Figure 1, b)

$$\frac{\partial^2 t(r,z,\tau)}{\partial z^2} + \frac{\partial^2 t(r,z,\tau)}{\partial r^2} + \frac{1}{r}\frac{\partial t(r,z,\tau)}{\partial z} = \frac{b}{a} , \qquad (12)$$

under linear boundary conditions

$$\lambda \frac{\partial t(R_1,z,\tau)}{\partial r} + \alpha\left[t(R_1,z,\tau) - t(R_1,h,\tau)\right] = 0 , \qquad (13)$$

$$\frac{\partial t(0,z,\tau)}{\partial r} = 0, \qquad \frac{\partial t(r,0,\tau)}{\partial z} = 0 . \qquad (14)$$

Solution for the bounded cylinder is put together in the form of a product of solutions for an infinite cylinder and an unbounded sheet under the appropriate boundary conditions [6]

$$t(r,z,\tau) - t(h,0,\tau) = \vartheta_0\left(1 - \frac{z^2}{h^2}\right)\left(1 - Kr\frac{r^2}{R_1^2}\right). \qquad (15)$$

Solution of (15) for the entire range of values considered ($0 < r < R_1$ and $-h < z < h$) is approximational; however, for the points (0,0) and ($\pm h$,0) used in the measurements, it satisfies the thermal conductivity equation (12) and the boundary conditions (13) and (14). Based on (12) and (13), we find

$$\vartheta_0 = \frac{\delta h^2}{2a} \frac{1}{1 + 2Kr\, h^2/R_1^2}, \tag{16}$$

$$Kr = \frac{Bi}{2 + Bi}. \tag{17}$$

The working formula we are seeking for the thermal diffusivity coefficient takes on the form given below in accordance with (16) and (17):

$$a = \frac{\delta h^2}{2\vartheta_0}(1 - \Delta\alpha), \tag{18}$$

where

$$\Delta\alpha = 2 \cdot \frac{h^2}{R_1^2} \cdot \frac{Bi}{2 + Bi} \tag{19}$$

= correction allowing for lateral heat transfer of the specimen.

Expression (19) can be used in selecting the specimen dimensions under which the error in determining thermal conductivity from (18) would not exceed the value given beforehand.

The relationships (18) and (19) derived above can also be used for the case when heat transfer in the air collar layer is simultaneously carried out by thermal conductivity and radiation. Here the thermal flux at the lateral surface is found from the expression

$$Q_{pac} = (\sigma_\delta + 2\sigma_T + \sigma_\Lambda) \cdot \bar{\vartheta}, \tag{20}$$

where

$$\sigma_\Lambda = 4\varepsilon_n \sigma_0 \left(\frac{273+t}{100}\right)^3 \cdot F_1. \qquad (21)$$

The reduced blackness ratio ε_{red} entering into (21) is evaluated from the formula

$$\frac{1}{\varepsilon_n} = \frac{1}{\varepsilon_1} + \frac{F_1}{F_2}\left(\frac{1}{\varepsilon_2} - 1\right). \qquad (22)$$

We will evaluate the values of the correction Δ_α for the example of a Teflon specimen with the following original data: $2h = 6 \cdot 10^{-3}$ m; $R_1 = 1 \cdot 10^{-2}$ m; $\lambda = 0.26$ w/m·deg; $a = 1 \cdot 10^{-7}$ m^2/sec; $\varepsilon_1 = 0.9$; $t = 200°C$; $r_2 = 2.5 \cdot 10^{-2}$ m; $\varepsilon_2 = 0.1$; $\lambda_b = 0.039$ w/m·deg; $F_1 = 3.78 \cdot 10^{-4}$ m^2; $F_2 = 42.4 \cdot 10^{-4}$ m^2. For $\bar{H} = 0.5$ and $\bar{R}_2 = 2.5$, from the graph of (8) we find $\sigma_\delta = 0$ and $\sigma_T = 4.1 \cdot 10^{-3}$ w/deg. From (22) we find $\varepsilon_{sur} = 0.52$, and from (21) $\sigma_\Lambda = 4.7 \cdot 10^{-3}$ w/deg.

The heat transfer coefficient at the lateral surface: $\alpha = (2\sigma_T + \sigma_\Lambda)/F_1 = 34$ w/m^2·deg; $Bi = \alpha R_1/\lambda = 1.3$; the unknown correction is

$$\Delta\alpha = 2\frac{h^2}{R_1^2}\frac{Bi}{2+Bi} = 7.1\%.$$

The method proposed for calculating thermal flux at the lateral surface of the specimen can be applied also for a system of bodies for which the temperature distribution differs from the parabolic. The conditions indicated prevail in a calorimeter for comprehensive measurement of thermophysical parameters [7] and in a calorimeter for measuring thermal conductivity [8].

Symbols

τ = time; t = temperature; t_{av} = temperature of medium; r and z = running coordinates; a and λ = coefficients of thermal diffusivity and thermal conductivity of the specimen; λ_b = thermal conductivity coefficient of air; b = heating rate; α = heat transfer coefficient from lateral surface of specimen; Bi = Biot criterion; $H = 2h$ and R_1 = thickness and radius of specimen; R_2 = radius of external surface of insulating layer; $\bar{R}_2 = R_2/R_1$,

$\bar{H} = H/R_1$; F_1 and F_2 = areas of specimen surface and of the surfaces of the layer surrounding the specimen; $\upsilon_{i,k}$ = thermal conductivity between the surfaces i and k; $Q_{i,k}$ = thermal flux between surfaces i and k; ε_1 and ε_2 = degrees of blackness of specimen and layer surfaces; ε_{rud} = reduced degree of blackness of the surfaces; σ_o = Stefan-Boltzmann constant; $\Psi_{sur} = \pi n/H$; $\Psi_m = \pi(2m - 1)/H$; $\bar{\theta}_{i,k}$ = mean temperature drop between the surfaces i and k.

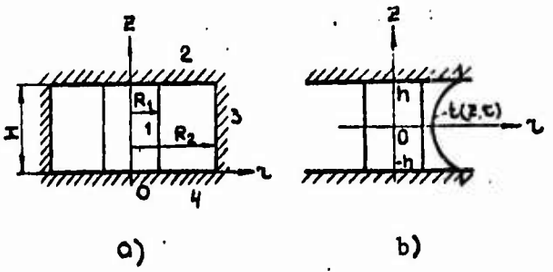

Figure 1. Layout of a-calorimeters

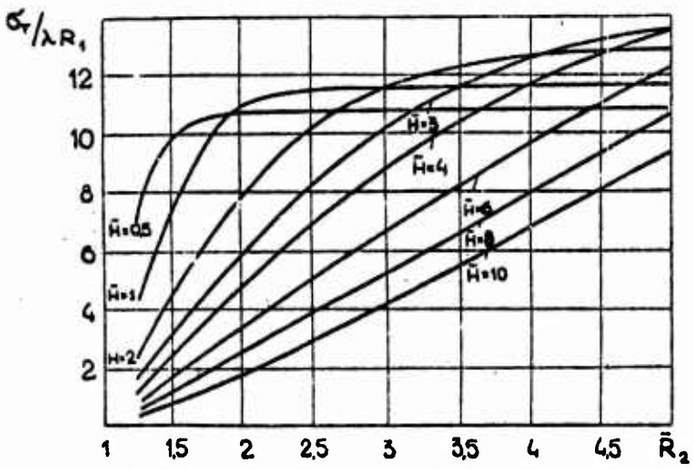

Figure 2. Graph for calculating conductivity σ_δ

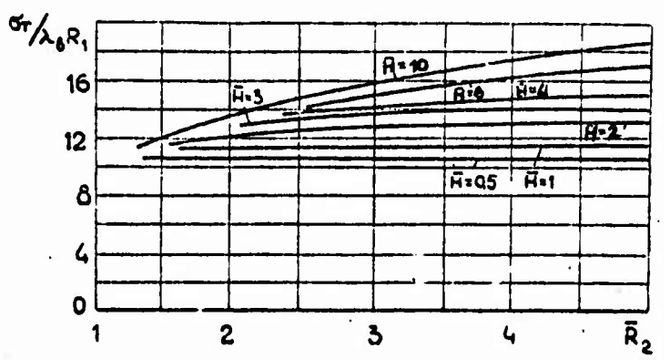

Figure 3. Graph for calculating the conductivity σ_T

References

1. Platunov, Ye. S., *Izvestiya Vuzov. Priborostroyeniye*, Vol. 4, No. 1, 1961.
2. Barskiy, Yu. P. *Trudy NIIStroykeramika*, No. 20, 1962.
3. Poluboyarinov, D. N. and I. G. Duderov, *Zavodskaya Laboratoriya*, No. 14, 1965.
4. Rosser, W. A., S. H. Inami, and H. Wise., *Avia Journal*, Vol. 4, No. 4, 1966.
5. Kurepin, V. V. and Ye. S. Platunov, *Izvestiya Vuzov. Priborostroyeniye*, Vol. 9, 1966.
6. Lykov, A. V., *Teoriya Teploprovodnosti, (Theory of Thermal Conductivity)*, GITTL Press, Moscow, 1952.
7. Platunov, Ye. S., *Izvestiya Vuzov. Priborostroyeniye*, Vol. 4, No. 4, 1961.
8. Eiermann, K: and K. Hellurge, *Kolloid Zeitschrift*, Vol. 174, No. 2, 1961.

MULTI-PURPOSE INSTRUMENT FOR PRECISION AND SIMULTANEOUS DETERMINATION OF TWELVE PROPERTIES OF MATERIALS

V. Leydenfrost

A knowledge of the properties of materials over wide ranges of pressure and temperature is essential to present-day technology.

The scientist who tries to predict property values of materials by statistical mechanics requires information in the form of accurate property values to verify and check his models.

To determine all properties of materials is practically speaking impossible, because new materials are continually being developed. Furthermore, data are sometimes required under conditions where it is practically speaking infeasible to carry out measurements.

Some of the available data fail to agree with each other for many reasons. One of these is that different properties of the same materials (or properties of different materials tested) as a rule are not measured under identical conditions as to pressure and temperature. This occurs in the case when the same property is investigated by different instruments. Oftentimes experiments on different instruments are conducted with specimens of the same material which, however, are not identical to each other. In the first place, impurities cannot be identical and, in addition, in the course of the various tests, material properties can change in different ways. Therefore it is very difficult to make a comparison of measurement results.

These difficulties can be lessened or avoided by using multi-purpose instruments capable of determining simultaneously several properties of a material under identical conditions of pressure, temperature, and impurity content. Moreover, simultaneous determinations of more than one property can improve the precision of measurements, because the single property measured

can be used to correct another property measured on the same instrument under identical conditions.

The advantages of using a multi-purpose instrument have already been briefly outlined by the author [1], where an instrument for investigating thermal conductivity is described.

Figure 1 shows this instrument only schematically with such detail as is necessary in discussing the potentialities of its use in determining other properties.

The instrument consists of a cylindrical heater element (hot body) with hemispherical ends placed and centered by means of a centering rod within a similarly shaped but slightly larger cavity of a cold body. The test liquid or gas fills the gap between the two bodies. The arrangement operates without guard-heaters and therefore allows steady state to be reached in a short time, important in avoiding effects of temperature fluctuations.

The thermal conductivity k can be readily obtained from Fourier's law

$$q_K = K \frac{A}{L} (T_h - T_k) \tag{1}$$

where

$$q_K = (V+\Delta V)(I+\Delta I) - q_r - q_c \pm q_L \pm (q_a)_r \pm (q_a)_a - \\ - (q_u)_r - (q_u)_k - (q_u)_a \pm \cdots \tag{1a}$$

is heat flow by conduction and equal to the electric power input allowing for corrections for, in order, radiation, convection, lead-in losses and heat flow due to nonsteady-state conditions and inhomogeneities. T_{hot} and T_{cold} are the surface temperatures of the hot and cold bodies.

For absolute measurements, it is necessary to determine the geometric constant of the arrangement, that is, the ratio of overall heat transfer area to the mean thickness of the fluid layer. This value is influenced by surface and other inhomogeneities. Determination of the geometric constant can be

done most accurately by measuring the electrical capacitance because in this case all disturbances will be included. The capacitance measured will be

$$C = \epsilon_0 \cdot \epsilon_r \cdot B \tag{2}$$

where B = A/L, geometric constant, ε_v = capacitance of vacuum = 8.8541735 + + 10^{-10} farad/cm; ε_g = dielectric constant of the gas, = 1 for vacuum.

In a vacuum we obtain the geometric constant

$$B = \frac{C}{\epsilon_0} \tag{2a}$$

directly and accurately when the centering rod enclosing the electric wires is built in such a way that lead-in capacitances have no effect. This was achieved by a three-lead measurement technique [2].

If the axis of the hot body coincides with that of the cold body, the capacitance is only a function of vertical displacement. The almost parabolic capacitance curve has a minimum at a location of least disturbance, that is, in the case of the most homogeneous field. This setting then will be the best location of the hot body within the cavity of the cold body. For this setting, the value of the capacitance measured (and therefore, the geometric constant) can be readily taken from the curve.

True curves are given in Figure 3 of the study [1]. The dimensionless curve is described below and shown in Figure 2.

Dielectric Constant and Index of Refraction

Measurements of the capacitance when the instrument is filled with test fluid affords the determination of the dielectric constant of the test material with the aid of equation (2). This feasibility has been demonstrated earlier in [1]. The results of observations are given in the Table.

The dielectric constant of many substances is proportional to the square of the index of refraction, which then is the third property of a material that is simultaneously determinable on the instrument. Knowledge of the refractive index is of importance in evaluating radiant heat transfer, which

in turn is needed for calculating the amount of heat transferred solely by conduction when measuring thermal conductivity (cf. equation (1a)).

Table. Dielectric Constants of Several Test Fluids of Highest Purity Under Normal Conditions

Material	Argon	CO_2	Toluene
Temperature	25.04	24.00	--
Pressure, mm Hg	746,76	775.14	--
Capacitance (measured)	1.0004932	1.000899	2.3787
Values obtained by the National Bureau of Standards and corrected for the same temperature and pressure	1.0004996	1.0009038	2.379 (not corrected
Deviation	$-6 \cdot 10^{-6}$	$-5 \cdot 10^{-6}$	--

Electrical Conductivity (ac)

The capacitance bridge used for the measurements just discussed will yield a precision of six figures only if the loss is balanced precisely. The bridge then provides the dissipation factor and the conductance of the specimen for a particular frequency

$$D = \omega RC \qquad (3)$$

Therefore, the electrical conductivity of the specimen can be determined for the respective frequency range.

Electrical Conductivity (dc)

The electrical wiring necessary to measure capacitance or ac conductance affords determination of the dc conductance of the test fluid by applying Ohm's law

$$i = \lambda B \Delta P \qquad (4)$$

where i = current flowing through the test layer of geometry B under a potential difference ΔP of the hot and cold bodies.

Thermal Expansion Coefficient of Instrument Materials

Measuring in vacuum the capacitance of the arrangement as a function of temperature yields the geometric constant as a function of temperature due to the change of the geometrical arrangement as a result of the thermal expansion of the hot and cold bodies. Equation (1) shows that the change in capacitance or geometric constant is directly proportional to the linear thermal expansion coefficient. But this is valid only when the temperature change does not introduce at the same time a change in the position of the hot body with respect to the cold body surrounding it, since this would disturb the field, resulting in an apparent increase of C or B. To hold the hot body in the same place with respect to the cold body under varying temperatures is possible only when the centering rod changes its length with change in temperature by an identical amount as does the cold body material.

This can be achieved under the condition when those two instrument parts are made of the same material. As already emphasized, the centering rod must be built as a double electrical shield, must satisfy many additional and partially controversial requirements (this will be discussed later), and cannot be made of materials used for the cold body. As a result, there will be a displacement of the hot body within the cavity of the cold body.

The error as a function of this eccentricity is shown in Figure 2, where the dimensionless capacitance is plotted as a function of eccentricity. The curve of this figure represents the error due to eccentricity for the case of the geometrical arrangement shown in Figure 1 and for the case when eccentricity exists only in the spherical part. It can be seen that axial

displacement of 0.05 mm (that is, 10 percent of the thickness of the test fluid layer) results in an increase of capacitance and the geometric constant of only 0.15 percent. A displacement by a value less than 0.015 mm leads to errors of the order of 0.01 percent and become negligibly small.

The discussion of the design of the centering rod shows that it can be designed in such a way as to have a thermal expansion coefficient equal to that of the cold body material, but only for a certain temperature range. It can be expected that the thermal expansion coefficient for other temperature ranges will be similar, but not identical to the thermal expansion coefficient of the cold body material. Its true value can be determined with a high degree of accuracy by measuring the capacitance of the geometrical arrangement of the multi-purpose instrument first when the hot body is holding the centering rod and, second, when the hot body rests on a piece of ceramic plate of such thickness (the centering rod acts then only as a centering device and allows axial motions) that minimum capacitance is achieved corresponding to Figure 2. This thickness is nominally 0.5 mm. Pure alumina changes its length in a 1000°C temperature range by a few thousandths of a millimeter. This expansion would dissipate the hot body in the cold body cavity, but according to Figure 2 this displacement would have practically no effect on the capacitance values measured, so that the true thermal expansion coefficient of the material would be obtained.

Comparison of true capacitance measurements with measurements obtained when the centering rod fixes the position of the hot body yields the thermal expansion coefficient of the rod. This value is of interest only for determining the effect of variable inhomogeneities on measurements of all properties where the geometric constant B is a major quantity.

Knowing the thermal expansion coefficient of the material with the precision with which capacitance measurements can be made makes it possible to determine the true volume occupied by the test fluid within the multi-purpose instrument at any temperature if the volume has been measured accurately at one temperature. This fact offers yet another possibility for use of the multi-purpose instrument.

Thermodynamic Properties of Gases and Vapors

Determinations of thermodynamic relations are usually very strongly influenced by thermal expansion, introducing deviation from isochoric conditions. The multi-purpose instrument affords the possibility of measuring the thermal expansion coefficient of the material with high precision, such that values of thermodynamic properties can be also obtained accurately enough. The effect of pressure on volume is much less than the temperature effect and can be made small by making the instrument walls strong enough (of sufficient thickness or of material of high strength over the operating ranges of temperature).

Change of volume as a function of pressure can be determined accurately by capacitance measurements, when the instrument is charged with a gas of well known pressure dependence of its dielectric constant. If, in addition, its temperature dependence is known, the capacitance measurements will make it possible to determine change of volume as a function of pressure and temperature. Finding the thermal expansion coefficient as a function of temperature makes it possible to determine the volume change at different temperatures as a function solely of pressure. With the aid of this data, we can obtain Young's modulus of the wall material and its temperature dependence.

The effect of pressure on volume can be made negligibly small when the apparatus is held under the same pressure outside as exists inside. In this case only the compressibility of metals must be considered. Enclosing the apparatus in a high-pressure vessel makes the setup somewhat more complex. The high-pressure vessel must remain near ambient temperatures, and only the instrument temperature can change. The thermal insulation of the instrument will experience the effect of pressure and owing to the increasing free convection becomes more and more ineffective with decreasing temperature and rising pressure. As a result, the temperature range of measurements using the instrument can be reduced to such a temperature where the thermal load cannot any longer be insured by the thermostat.

The volume occupied by the test fluid within the multi-purpose instrument must be small to measure all the properties indicated above. But for determining thermodynamic data, a larger volume is more feasible. Here the

best way is to add yet another cavity to the instrument, most suitably in spherical form, as indicated in Figure 1 by dashed lines.

Thermodynamic measurements of gases and vapors can be easily obtained only when no condensation occurs. Also, fluctuations in volume in the manometric section must be eliminated. A device measuring vapor pressure and operating under isochoric conditions was described in [1]. A similar but more improved device will be used in the multi-purpose instrument, which then obviously can be used to determine vapor pressure of liquids. In determining vapor pressure there is no need to know the structure of the liquid and vapor fractions.

Compressibility and Thermal Expansion Coefficient of Liquids

Connecting the multi-purpose instrument with external instrumentation by means of thin capillaries, as shown schematically in Figure 3, makes it possible to observe the change of liquid level resulting from changing temperature and pressure of the test fluid within the instrument. Accounting for change of volume due to thermal expansion or the pressure of the instrument material affords the possibility of determining the thermal expansion coefficient or the coefficient of compressibility of the test fluid.

Errors in the determinations can be reduced to a minimum by avoiding change of volume with pressure and temperature of the external instrumentation, and also by eliminating the effect of surface tension on the liquid level observed.

Specific Heats c_p and c_d of Liquids

E. O. Schmidt and the author have described an adiabatic calorimeter [3] working in a quasi-steady state condition under continuous heating. The specific heat for this case is given by the equation

$$C = \frac{1}{m}\left(\frac{q}{\dot{T}} - W_c\right) \tag{5}$$

where $\dot{T} = dT/dt$ is the temperature change with time of the test material observed under constant heat input q into a specimen of heat capacity mc enclosed in a calorimeter body of heat capacity W_c.

The measurement of specific heat capacity in such an instrument will be of high accuracy whenever the constant and continuous heat input produces at any location within the specimen the same temperature rise with time, and whenever the temperature difference in the specimen is so small that the specific heat capacity can be assumed to be constant, but large enough to determine the temperature change accurately.

These conditions can be provided [3] by solving the partial differential equation describing the temperature field in the sample of spherical geometry under the assumptions that the heat input to the specimen takes place only at the surface of the heater element located at the center of the sphere, that there are no heat losses from the outer surface and, finally, that at a time zero there is uniform temperature distribution within the specimen.

On this basis, the multi-purpose instrument can also be used to determine specific heat capacities. The hot body in this case will be replaced by a calorimetric container of similar external configuration enclosing the specimen of known mass. The cold body acts as an adiabatic envelope; its temperature must change with time at the same rate as the temperature of the exterior of the calorimeter changes, and the temperature difference between the two bodies must remain at zero. For measurements of specific heat capacity c_p, the calorimeter container must accommodate a bellows or other flexible device separating the test liquid from a gas at constant pressure and allowing the test material to freely change its volume with temperature.

For measurements of c_v, the same calorimeter can be used, but the flexible device must either be removed or rendered inactivated. Here isochoric conditions must be maintained.

Thus, the instrument can simultaneously measure six properties (k, ε, n, λ_{ac}, λ_{dc}, p-V-T) of the eleven listed properties when gases and vapors are tested, and seven properties (k, ε, n, λ_{ac}, λ_{dc}, β and k) when liquids are tested. Simultaneity in this respect means that all measurements are made on the test liquid which initially fills the instrument, which is possible by altering only the outside connections as is schematically shown in Figure 4, a, the specimen always remaining the same. Therefore the different properties will be observed under perfectly identical conditions.

These ideal conditions cannot be provided for the other measurements. For specific heat capacity determinations the instrument itself must be modified, and this necessitates moving the specimen out of the cell. Relocating the specimen can be done by filling the calorimeter with the test substance being removed from the instrument. Here, great caution must be observed so that the specimen is not damaged, and if the calorimeter walls and those of the multi-purpose instrument being wetted by the test fluid show no effects, then a quasi-simultaneous determination of the properties is possible. Here all values measured with the multi-purpose instrument will be obtained under practically identical conditions of pressure, temperature and extent of contamination.

The techniques of measuring the various properties with the multi-purpose instrument discussed above represent the first information towards developing a preliminary instrument design. But a whole series of problems still remain to be taken up for development of a final design and construction of the instrument.

Basic Design Considerations

Temperature and Pressure Ranges

One of the main requirements which must be met with the multi-purpose instrument is obtaining data of high precision. The temperature and pressure ranges must be selected in such a way that accurate measurements will not only be possible, but also be made over a broad range of these variables. As to temperature, the working range of the instrument must lie within the limits 190-650°C, because in this range the platinum resistance thermometer is presently recognized as standard for the international temperature scale. Selecting the temperature range limits to some extent the pressure range, due to the strength of the instrument material. Pressure range from vacuum to 500 atm was chosen, which is sufficiently wide, since the pressure dependence of many properties is small.

The ranges selected will influence the design of the instrument, but even more so, measurements with this instrument, since all quantities that must be obtained in calculating the various properties from the respective equations must be determinable accurately at any pressure and temperature.

Pressure and temperature, in addition, must be precisely maintained during measurement for at least that length of time needed to achieve steady-state conditions and to make the readings.

Generating, changing, holding and measuring the necessary pressure can be done in most cases without difficulties, with the exception of vapor pressure under isochoric conditions. This will be discussed in more detail when we deal with the instrument design. Pressure within the instrument must be uniform at any time and under any circumstances.

Still greater difficulties prevail in respect to temperature and much effort must be applied in developing theory, design and fabrication to overcome these difficulties or to minimize errors.

Thermostating the Instrument

Temperature regulation by means of electrical heating wires is insufficient because it is practically impossible to produce the same amount of heat per each length of heating wire element and, most importantly, uniform contact between wire and walls of the instrument cannot be achieved. Furthermore, electrical heaters are useful only at temperatures above the ambient; cooling by means of the Peltier effect is not adequate in most cases.

Boiling point arrangements make it possible to provide excellent temperature control, but changing from one temperature to another requires pressure regulation over wide ranges for the use of different media. Available liquid thermostats function quite satisfactorily, but normally only in narrow temperature ranges and, in addition, also require use of different fluids for different temperature ranges, but these ranges are not as wide as those needed for the multi-purpose instrument.

It was therefore necessary to develop a new thermostat capable of operating with the same working medium was recognized as gas, namely helium, since its high thermal conductivity and low viscosity offer good prospects for heat transfer.

The thermostat is shown schematically in Figure 5. The helium is circulated by means of a pump in a closed loop consisting of a bifilar coil

and a heating section. A platinum resistance thermometer is used as the sensing element in an automatic control system, making it possible to change heat input or cooling when the temperature deviates from the set value. Heating is regulated by changing the electrical power of the heater; cooling -- by means of two solenoid valves activated by the automatic control unit changing the amount of working fluid passing through the cooling coil or bypassing it. To achieve high heat transfer, the heat capacity of helium is increased by pressure which is maintained by means of a storage tank. The pump has to overcome only the pressure drop of the high velocity flow within the closed loop.

Providing Isothermal Conditions at Surfaces Wetted by Test Fluid

To use the possibilities offer by the thermostat, it is necessary to bring the helium in equal heat contact with every section of the apparatus. This is possible when the material of the instrument is wetted directly by the heat carrier. This can be achieved by cutting channels into the surfaces shown in Figure 6, left. Then the part of the surface occupied by the channel is in contact with the gas, and the bridges between the channels do not produce a different temperature at these points, and consequently, an uneven temperature distribution at the surface.

The assumption that the temperature of the thermostating body flowing through neighboring channels is the same (heat loss or gain is small) makes it possible to replace this distribution by a sine or cosine function, which affords analytical determination of the thickness necessary for dampening the uneven temperature distribution at the surface to negligibly small values at sections within the instrument lying in contact with the test material. The plot of the field in the righthand part of Figure 6 shows that damping of temperature fluctuations increases rapidly with greater thickness. The one-dimensional temperature distribution at the inner surface can be expressed as

$$T_{y=0} = T_0 - \frac{q}{k_w} B + \frac{T_m}{\cosh \frac{\pi}{L} b} \cos \frac{\pi}{L} x \qquad (6)$$

for a flat plate arrangement in the design shown in Figure 7.

The third member in the righthand side of equation (6) indicates that damping of temperature fluctuations is not dependent on wall material, but rises proportionally to the hyperbolic cosine as a function of wall thickness. For a thickness that is four times greater than the depth of the channels, temperature at the inner surface will fluctuate with an amplitude T_m a 100,000 times smaller than at the outer surface. In addition, there will be a decrease in amplitude due to the two-dimensionality of the heat flow.

The walls of the multi-purpose instrument can be easily made thick enough to insure practically isothermal conditions at surfaces wetted by the test fluid. This will satisfy the important requirement of attaining high precision, especially in determining thermodynamic properties. Isothermal surfaces are necessary also in measuring thermal conductivity for the simple reason that, otherwise, the geometric constant must be a greater value than is observed when isopotential conditions are set up (for a selected geometry and smooth surfaces). To achieve isothermicity of the surfaces, it is also necessary that the heat flux emanating from the heated body to the cold encounter identical thermal resistance everywhere. This can be achieved to a large extent by providing equal distances, that is, the outer contour of the instrument must be identical to the contour of the heating element -- the hot body. The heater, moreover, must be heated in such a way as to insure uniform heat flux from its surface.

Abiding by the considerations just considered in designing the instrument provides conditions favorable for precision measurements. However, these ideal isothermal conditions must not be distorted by the temperature transducers placed within the wall of the instrument and necessary, above all, in determining the surface temperature in measuring thermal conductivity.

Allowing for heat transfer by radiation and losses along lead-in wires, and also using the new method of eliminating errors when surface temperature is determined, together with careful designing of the instrument will boost the precision of the resulting data.

Above, we discussed essential steps for transforming the instrument initially designed to measure thermal conductivity into a multi-purpose instrument, and also approaches that lead to attaining reliable simultaneous measurement of different properties. The discussion given also shows that drawing up a design for such an instrument is possible, but this does not mean that the instrument can be built, this above all refers to the centering rod, the most critical and most important part of the instrument. Therefore, before beginning work on the design it is necessary to investigate the possibilities of manufacturing the centering rod.

Centering Rod

As already pointed out, the centering rod must satisfy many often contradictory requirements. It will enclose all lead inputs to the hot body and must be made in the form of a double electrical shield. The rod must have thin walls and a small cross-sectional area in order to reduce to the minimum heat losses from the hot body. (For the same reasons, a specific amount of heat must be generated within the centering rod.) It must be strong enough in order to withstand external pressures up to 500 atm and temperatures up to 650°C, and must not be bent under heavy axial loads. It is no less important that its coefficient of linear expansion must be equal to or, at least, close to the coefficient of linear expansion of the material of the cold body surrounding it. Making, from the instrument used to measure thermal conductivity, a multi-purpose instrument would be impossible if the requirement of the double electrical screening was not met. Therefore, we must consider precisely this problem above all else.

Electrical screening requires combining conductive and insulating materials. The pressure and temperature ranges selected for performance of the instrument make it necessary to use high-strength metals and ceramics. The latter must have very good electrical and mechanical properties, and also good chemical stability. High-purity aluminum oxide satisfies these requirements. Combination of this ceramic with metal for attaining good hermeticity in all the temperature ranges requires a hard soldering process. This soldering can be done when the coefficients of thermal expansion of the two components referred to are commensurable throughout the entire temperature range. Iron-nickel-cobalt alloys fulfill this requirement closely, and

the best combination for our temperature range is represented by the alloys Vacon 70 and the A18 type aluminum oxide (98 percent). Making thin-walled parts of a shape which allows some spring action from Vacon 70 assures good operation even when the thermal expansion coefficients are not exactly identical.

Aluminum oxide insulators hard soldered to Vacon 70 occupy a certain length of the centering rod and for this section the thermal expansion coefficient is very much smaller than for the cold body material. To fulfill the requirement of least heat loss from the hot body it was necessary to make the connecting tube thin walled, and this in turn dictated selection of the material for strength considerations. Nimonic 90 was chosen, but this material has a thermal expansion coefficient that is smaller than Nimonic 80A. To compensate for this difference, it is necessary to use for the extension of the centering rod another material (ATS 15), which has a very much higher thermal expansion coefficient than Nimonic 80A, and also to choose the length of parts made out of Nimonic 90 and ATS 15 in such a way that for the total length of the centering rod, the resulting thermal expansion coefficient is equal to the termal expansion coefficient of Nimonic 80A. They will be equal only at a specific temperature. For other temperatures there cannot be a good agreement, since the temperature dependence of the thermal expansion coefficients of the materials used is different. However, they are close enough for the centering rod not to change its length with change in temperature differently than does the cold body, and only a small displacement of the hot body relative to the surrounding parts will occur. This will change the geometric constant, but this change can be measured, and its true value will be known at any temperature. The rise in content of inhomogeneities will have a small effect on determination of properties. The small difference in thermal expansion is also important to insure that the hot body never can be displaced to such an extent that it leads to contact with the cold body, which would make measurement impossible and would damage the instrument.

Combining the different metallic parts (most of which are thin-walled) can be done only by electronic-beam welding. The feasibility of the design

just described was tested on a pilot device, and then a working plan of the apparatus was drawn up, as shown in Figure 7. The centering rod is fully centered and attached to the hot body by means of its base held in place by a screw arrangement.

The centering of the hot body within the cavity is achieved by means of an aperture in the axis of the cold body which accommodates the extension of the centering rod with minimum clearance. The geometry is insured by a 60° tapered seat and a gold gasket whose thickness is chosen from the conditions of best placement of the gasket in the axial direction and for achievement of minimum capacitance value. Sealing forces on the gasket are applied by means of a sleeve and screw allowing the centering rod to be pulled in an upward direction (Figure 7).

Final Design of the Instrument

The design of all the other assemblies of the multi-purpose instrument was examined in less detail than development of the centering rod and made it possible to develop the design shown in Figure 8. The depicted cross section is a reproduction of the engineering drawing somewhat modified for easier reading.

The instrument consists of four main parts: the hot body and three parts comprising the cold body. The cold body has two cavities -- the upper one which is of a shape that makes it possible to accommodate the hot body, and the lower spherically shaped cavity added to increase the volume and for placement of the standard platinum resistance thermometer necessary in measuring the temperature of the test liquid and in calibrating the resistance thermometers placed in capillary tubes. At the outer surfaces of these three parts of the cold body channels have been cut for the thermostating working body. The channels between the different parts are connected by vertical and horizontal bores.

The three parts of the cold body are centered with respect to each other and held together by means of ring nuts. Sealing forces are applied by means of screws in the ring nut and act on the gold rings placed between the parts of the cold body.

All surfaces in contact with the test fluid are made of inert materials bonded by a special process to the base metal. This material is gold for most of the area, but a gold platinum alloy is used at those locations where sealing forces will be applied and where inertness and mechanical strength are required.

The lower part of the cold body accommodates two valve seats and the vapor pressure measuring device. This device is not used for the valve arrangement shown. The test fluid in this case is in contact with the outside instrumentation. For isochoric measurements another valve stem must be inserted, which allows the instrument to be evacuated in an open position, and is seated so that the vapor pressure measuring device is connected with the test fluid. The pressure transducer is always at the specimen temperature; therefore, pressure changes due to condensation or evaporation do not occur.

The upper part accommodates the centering rod and devices for flushing the instrument or to feed in a precisely known mass of specimen, especially in determining thermodynamic relationships.

The hot body held and centered by the centering rod at its upper end is also centered at its lower end by means of a centering pin made of pure alumina.

Figure 8 also shows the arrangement, insulation and screening of the instrument.

All instrument parts have been machined, the only task remaining is attaching the gold lining. The multi-purpose instrument is shown in Figure 9 in assembled form.

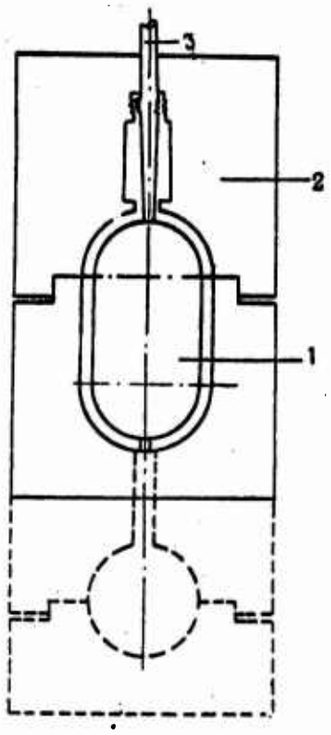

Figure 1. Diagram of instrument for measurement of thermal conductivity: 1, Hot body; 2, Cold body; 3, Centering rod.

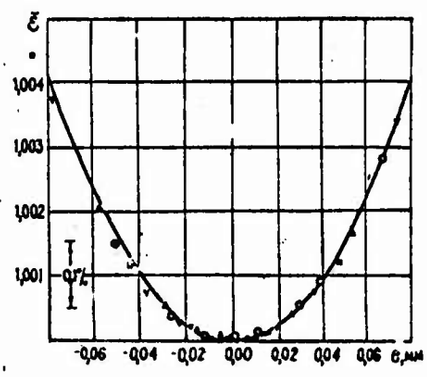

Figure 2. Dimensionless capacitance $\bar{\varepsilon}$ as a function of the eccentricity: —, Theoretical curve; ∇, ○, Values measured by moving the heater element downward; □, Δ, Values measured by moving heater element upward.

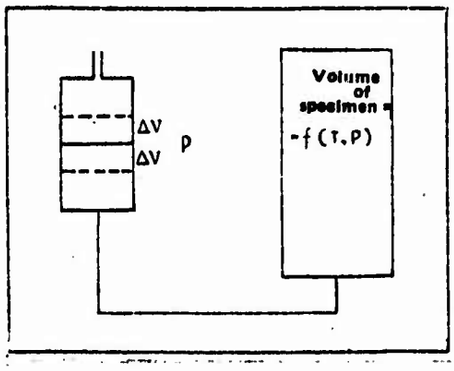

Figure 3. Schematic representation of experimental arrangement for measurement of coefficient of thermal expansion and compressibility.

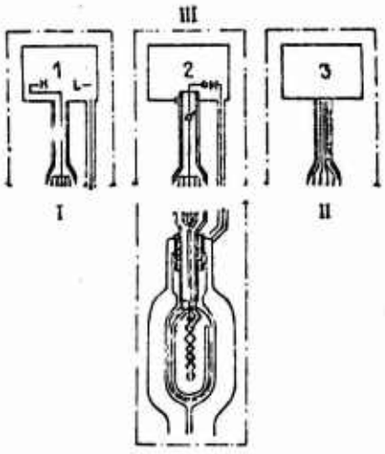

Figure 4. Wiring diagram and switching arrangement for measurement of different properties: 1, Capacitance bridge; 2, Bridge for measuring low resistances; 3, Seven-dial potentiometer and Mueller bridge; I, Electrical conductivity (alternating current) of liquids and gases, capacitance of geometric arrangement, thermal expansion coefficient of instrument material, dielectric constant, index of refraction of liquids and gases; II, Thermal conductivity of liquids and gases, thermodynamic properties of gases and vapors, heat capacities of liquids, vapor pressure of liquids, compressibility of liquids, coefficient of thermal expansion of liquids; III, Electrical conductivity (direct current) of liquids and gases.

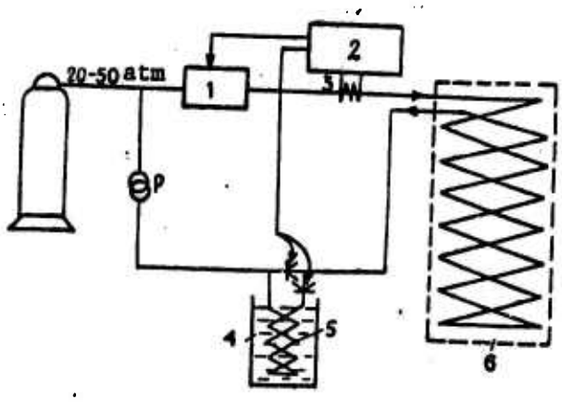

Figure 5. Thermostat: 1, Heater; 2, Automatic control unit; 3, Platinum resistance thermometer; 4, Water, liquid nitrogen, or other liquids; 5, Cooling coil; 6, Bifilar coil.

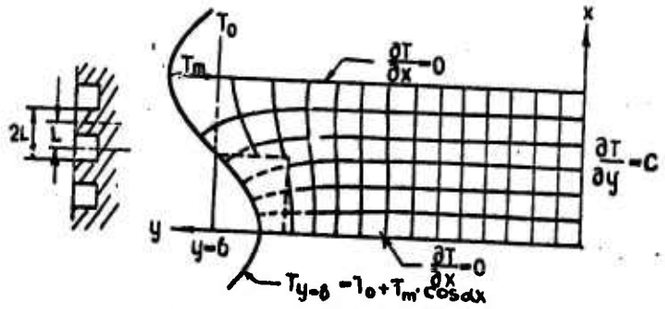

Figure 6. Effect of wall thickness on temperature distribution.

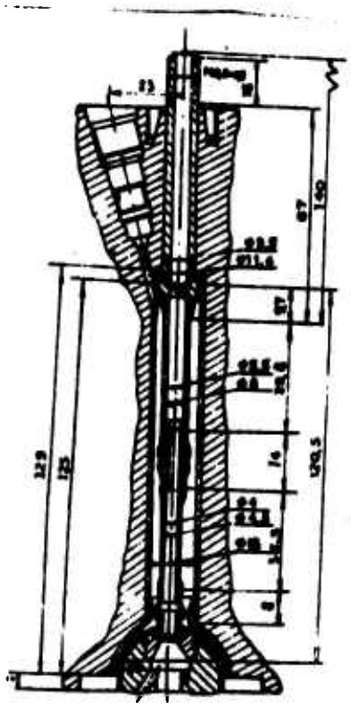

Figure 7. Design of centering rod assembly

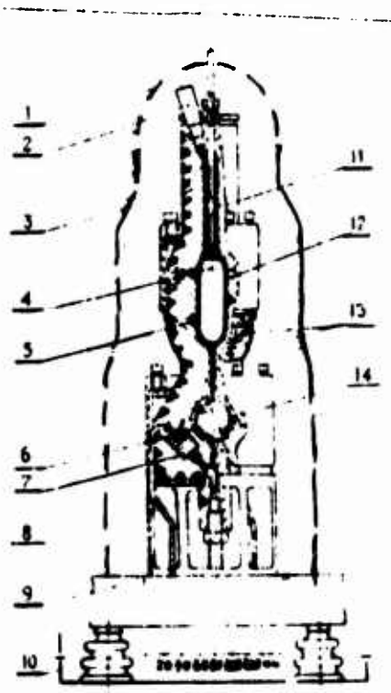

Figure 8. Multi-purpose instrument: 1, Inner contour of pressure vessel; 2, Device for filling instrument; 3, Centering rod; 4, Heating element; 5, Platinum resistance thermometer enclosed in coiled capillary; 6, Standard platinum resistance thermometer; 7, Pressure measuring device; 8, Valve arrangement; 9, Bottom closure of pressure vessel; 10, Electric shield; 11, Test liquid or gas; 12, Layer of test medium 0.5 mm in thickness; 13, Thermostating medium; 14, Gold sheath, 1 mm thick; ▬, Pt-Au alloy.

Figure 9. External view of multi-purpose instrument.

References

1. Leidenfrost, W., *Int. J. Heat and Mass Transfer*, Vol. 7, pp. 447-478, 1964.

2. Mc Gregor, M. C., I. F. Hersh, R. D. Cutkosky, F. K. Harris, and F. R. Kotter, *JRE Trans. On Instrumentation*, Vol. I-7, pp. 253-261, 1958.

3. Schmidt, E. O. and W. Leidenfrost, *Int. J. Heat and Mass Transfer*, Vol. 5, pp. 267-275, 1962.

THEORY OF NONSTEADY-STATE METHODS OF MEASURING THERMOPHYSICAL CHARACTERISTICS

V. K. Li-Orlov and V. N. Volkov

Known nonsteady-state methods of measuring thermophysical characteristics, in particular, the regular regime methods, rely on solving the thermal conductivity equation with constant coefficients. This has greatly limited the scope of application of nonsteady-state methods, because the working temperature range must be narrow enough and all the more so the more strongly thermophysical characteristics depend on temperature.

Accordingly, efforts to find solutions to the thermal conductivity equation in the case of thermophysical characteristics that are temperature-dependent and solutions that have simple analytical expression have gained greatly in theoretical and practical importance. By relying on the solutions the scope of applicability of nonsteady-state methods could be expanded.

Simple analytical solutions can be found by using certain approximation methods of solution. The methods, in particular, include the small parameter method and the integral method of the Karman boundary layer theory [1], which has found satisfactory use in the solution of thermal conductivity problems by Yu. L. Rozenshtok (USSR) [2-4], and by Goodman (US) [5, 6].

Using the somewhat modified Karman method [7], we obtained a solution to the thermal conductivity equation with thermophysical characteristics that depend linearly on temperature for the case of simple cooling of bodies under third-order boundary conditions. Analytical solutions were found by the small parameter method.

To evaluate errors of analytical solutions, the unknowns of the problem were solved numerically using the A. P. Vanichev method [8, 9] on a high-precision electronic digital computer. The agreement realized was fully satisfactory.

Small Parameter Method

Let us examine the cooling of an unbounded plate, the heat transfer on the surface of which follows the Newton law, and the thermophysical characteristics of which are a function of temperature.

We will write the thermal conductivity equation in dimensionless variables

$$M\frac{\partial\theta}{\partial\tau}=\frac{\partial}{\partial\xi}\left(\lambda\frac{\partial\theta}{\partial\xi}\right). \tag{1}$$

Boundary conditions are in the form:

$$\lambda(\theta(\pm1,\tau))\frac{\partial}{\partial\xi}\theta(\pm1,\tau)=\mp Bi_0\theta(\pm1,\tau). \tag{2}$$

We take θ here to denote the relative temperature, the initial value of which equals unity.

We will seek an asymptotic solution corresponding to the regular regime with constant coefficients.

Because for many materials thermophysical characteristics are observed to be linearly dependent on temperature [10], we assume that

$$M=1+m\theta, \qquad \lambda=1+l\theta \tag{3}$$

l and m are small quantities for most materials and as a rule do not exceed the value of 0.1 for temperature drop of 50°.

We will seek a solution to the problem (1-2) in the form

$$\theta=\theta_1+m\theta_2+l\theta_3+\dots \tag{4}$$

assuming that l and m are small parameters.

On such an assumption, in the solution we can limit ourselves to first-order infinitessimals with respect to l and m.

Substituting (4) in (1) and equating the coefficients for the corresponding powers of l and m to zero, we obtain the solution in the form:

$$\theta = A_1 \exp\left[-\mu^2\tau\right]\cos\mu\xi + \left[\left(A_2\cos\sqrt{2}\mu\xi - \frac{1}{2}\sin^2\mu\xi\right)m + \right.$$
$$\left. + \left(A_3\cos\sqrt{2}\mu\xi - \frac{1}{2}\cos 2\mu\xi\right)l\right] A_1^2 \exp\left[-2\mu^2\tau\right] + \ldots, \tag{5}$$

where

$$A_2 = \frac{\mu\sin 2\mu + Bi_0\sin^2\mu}{2\left(Bi_0\cos\sqrt{2}\mu - \sqrt{2}\mu\sin\sqrt{2}\mu\right)}, \tag{6}$$

$$A_3 = -\frac{\mu\sin 2\mu - Bi_0\cos 2\mu}{2\left(Bi_0\cos\sqrt{2}\mu - \sqrt{2}\mu\sin\sqrt{2}\mu\right)}, \tag{7}$$

A_1 is determined from the initial condition,
μ is the smallest root of the equation

$$\mu\,\mathrm{tg}\,\mu = Bi_0 \tag{8}$$

Solution of (5) when $l = m = 0$ transforms into the well known solution of the regular regime [11, 12], that is, formula (5) is an expansion in powers of l and m of the asymptotic solution.

Let us examine the temperature in the center of the plate

$$\theta_u = A_1\exp\left[-\mu^2\tau\right] + \left[mA_2 + l\left(A_3 - \frac{1}{2}\right)\right]A_1^2\exp\left[-2\mu^2\tau\right] \tag{9}$$

l and m are small, therefore from (9) after several transformations and determination of A_1, we get

$$\frac{\ln\theta_u - \ln\theta_{0u}}{\theta_u - \theta_{0u}} - B(l,m,\mu) = -\mu^2\frac{\tau - \tau_0}{\theta_u - \theta_{0u}} \tag{10}$$

We have shown that solution of the form (5) and (10) occur for a sphere, an unbounded cylinder, and a parallelepiped. The functions $B(l, m, \mu)$ have been determined for each case. They are somewhat more complex in form than for the plate.

When $Bi_0 = \infty$, solution of (10) takes on the form

$$\tilde{\theta}_\psi + 0{,}835m - 0{,}335l = -\frac{\pi^2}{4}\tilde{\tau} \qquad (11)^1$$

Integral Method

The problem (1-2) can be solved by an integral method. Well known integral methods (the integral heat balance method and the Karman method) provide inadequate precision. Errors in these methods compared to the familiar precision solutions amount to 20 percent and higher.

We have formulated an improved integral method affording a reduction in the deviation between the approximational and familiar precision formulas down to 1-5 percent. In contrast to the Karman method, the original differential equation is subjected not to one integration, but to two integrations with respect to the coordinate. This is attained by excluding from the integral relationship derivatives with respect to the coordinate. The presence of these derivatives in equations obtained by the Karman method is the main source of error.

For example, in solving the problem (1-2) by the Karman method, in general the coefficient of thermal conductivity is not found as a function of temperature, while the method of double integration does lead to a satisfactory result.

Double integration of equation (1) with account taken of (2) gives

$$\int_0^1 d\xi \int_0^\xi M \frac{d\theta}{\partial\tau} d\xi = \int_0^1 \mathcal{K} \frac{\partial\theta}{\partial\xi} d\xi \qquad (12)$$

[1] See p. 358

When calculating integrals in (12), we represent the function Θ in the form

$$\Theta = \Theta_{ц}(\tau) \cdot \varphi(\xi) \tag{13}$$

The true temperature profile does not exhibit this property. But it does exhibit a temperature profile in the problem with constant coefficients, and if M and L as a function of Θ is not very strong, in the relationship (12) averaged over coordinates the property (13) can be used without substantial error.

The function $\phi(\xi)$ can be approximated by a parabola or any other function satisfying the conditions.

For small l and m in problem (1-2), the function ϕ is more validly approximated by a cosinusoidal corresponding to the precision solution for constant coefficients.

Substituting (13) in (12), we get an equation with respect to Θ_{ctr}

$$(\alpha_1 + \alpha_2 \Theta_{ц}) \dot{\Theta}_{ц}^{1} = \beta_1 \Theta_{ц} + \beta_2 \Theta_{ц}^{2} \tag{14}$$

where α_1, α_2, β_1 and β_2 = functions of ϕ.

The solution of (14) with account of the smallness of l and m is

$$\tilde{\Theta}_{ц} + c(l, m, \mu) = -\mu^2 \tilde{\tau} \ , \tag{15}$$

where

$$c = \frac{\mu^2 + \sin^2\mu}{4(1-\cos\mu)} m - \frac{1+\cos\mu}{2} l \tag{16}$$

μ is the smallest root of equation (8).

A solution of the form (1) has been obtained for a sphere, unbounded and bounded cylinders, and a parallelepiped.

---

[2]See p. 358

As we can see, solution by the small parameter method (10) differs from solution by the integral method (15) only by the small correctional members $B(\zeta, m, \mu)$ and $C(\zeta, m, \mu)$, the numerical values of which, as calculations have shown, are very close to each other.

Mathematical Experiment

To verify the analytical solutions and to evaluate the errors, the unknowns of the problem were solved by us using the A. P. Vanichev numerical method [8, 9] on a high-precision electronic digital computer.

By integrating the numerical solution as a precise experiment after appropriate treatment, we obtained a function analogous to the analytical solution of (10).

The errors of the cooling rate of the central point usually do not exceed one percent, and the error of the small correctional member $B(\zeta, m, \mu)$ -- five percent for the small parameter method, and ten percent for the integral method for any $|\zeta| \leq 0.2$ and $|m| \leq 0.2$.

Example 1. Let us examine the cooling of a plate at $Bi_0 = \infty$ and $M = 1 + 0.2\theta$, $L = 1 - 0.2\theta$. The machine solution gives

$$\tilde{\theta}_4 + 0{,}24 = -2{,}47\,\tilde{\tau}$$

Analytical solutions by the small parameter method and the integral method are of the form

$$\tilde{\theta}_4 + 0{,}234 = -2{,}46\,\tilde{\tau}$$
$$\tilde{\theta}_4 + 0{,}26 = -2{,}46\,\tilde{\tau}$$

Example 2. Cooling of a plate (example 1) when $Bi_0 = 20$. We then will have:

$$\tilde{\theta}_4 + 0{,}26 = -2{,}26\,\tilde{\tau},$$
$$\tilde{\theta}_4 + 0{,}25 = -2{,}24\,\tilde{\tau},$$
$$\tilde{\theta}_4 + 0{,}28 = -2{,}24\,\tilde{\tau}.$$

The solutions (10) and (15) we found make it possible to present several remarks about the potentialities of their use in practice when measuring thermophysical parameters.

If formula (10) is rewritten in the form

$$\frac{\ln\Theta_y - \ln\Theta_{oy}}{\Theta_y - \Theta_{oy}} + B(l, m, \mu) = -\frac{\mu^2 a_o}{R^2} \cdot \frac{t - t_o}{\Theta_y - \Theta_{oy}} \qquad (17)$$

then the experimental points in the coordinates

$$\frac{\ln\Theta_y - \ln\Theta_{oy}}{\Theta_y - \Theta_{oy}} \quad \text{and} \quad \frac{t - t_o}{\Theta_y - \Theta_{oy}}$$

must obviously lie on a straight line, the tangent of whose slope to the X-axis makes it possible to calculate the cooling rate of the central point

$$\frac{\mu^2 a_o}{R^2}$$

and from it also the coefficient of thermal diffusivity a_o, if the experiment is made when $Bi_o = \infty$.

The segment cut off by the experimental line on the Y-axis allows us to find the value of $B(l, m, \mu)$ in evaluating the coefficients of heat capacity and of thermal conductivity as a function of temperature.

Symbols

$\psi = x/r$, relative dimensionless three-dimensional coordinate, where R = semithickness of plate; $\tau = a_o t/R^2$, Fourier's criterion (dimensionless time). Here a_o = coefficient of thermal diffusivity at the temperature of the medium; $\Theta = (T - T_c)/(T_o - T_c)$, relative temperature, where T_o = initial temperature of plate; T_c = temperature medium which is kept constant; $\Theta_{ctr} = (T_{ctr} - T_c)/(T_o - T_c)$, relative temperature in mid-plate; τ_o and $\Theta_{rel\text{-}ctr}$ = time and relative temperature in center of sheet corresponding to the onset of the asymptotic solution; $M = c/c_o$, $L = \lambda/\lambda_o$, relative heat capacity and thermal conductivity, where c_o and λ_o correspond

to the value of the heat capacity and of thermal conductivity at the temperature of the medium; $Bi_o = \alpha R/\lambda_o$, Biot criterion, α = heat transfer coefficient, taken as constant; $l = \beta\Delta T/\lambda_o$, $n = \gamma\Delta T/c_o$, relative linear coefficients of heat conductivity and heat capacity as functions of temperature, where β and γ = absolute linear coefficients of the corresponding quantities.

Footnotes

1. To p. 353 Here for brevity of formulation, we introduce the following symbols of the complexes

$$\tilde{\theta}_4 = \frac{\ln\theta_4 - \ln\theta_{04}}{\theta_4 - \theta_{04}}; \quad \tilde{\tau} = \frac{\tau - \tau_0}{\theta_4 - \theta_{04}}$$

2. To p. 354 $\dot{\theta}_{ctr}$ = the period over the symbol designates the derivative with respect to time.

References

1. Shlikhting, G., *Teoriya Pogranichnogo Sloya,* [Theory of the Boundary Layer], IL Press, Moscow, 1956.
2. Rozenshtok, Yu. L., *IFZH,* No. 3, 1963.
3. Rozenshtok, Yu. L., *IFZH,* No. 6, 1965.
4. Rozenshtok, Yu. L. and A. F. Chudnovskiy, *Teplo-Massoperenos, t. 6,* [Heat and Mass Transfer, Volume 6], Nauka i Tekhnika Press, Minsk, 1966.
5. Goodman, T. R., *Trans. ASME,* Vol. 80, No. 2, 1958.
6. Goodman, T. R., *Trans. ASME,* Vol. 84 C, No. 4, 1962.
7. Volkov, V. N., *IFZH,* No. 5, 1965.
8. Vanichev, A. P., *Izv. AN SSSR,* Otdel Tekhnicheskikh Nauk, No. 12, 1946.
9. Yushkov, P. P., *Tr. Instituta Energetiki AN BSSSR,* No. 6, Moscow, 1958.
10. Chudnovskiy, A. F., *Teplofizicheskiye Kharakteristiki Dispersnykh Materialov,* [Thermophysical Characteristics of Disperse Materials], GIFML Press, Moscow, 1962.
11. Kondrat;yev, G. M., *Regulyarnyy Teplovoy Rezhim,* [Regular Thermal Regime], GITTL Press, Moscow, 1954.
12. Lykov, A. V., *Teoriya Teploprovodnosti,* [Theory of Thermal Conductivity], GITTL Press, Moscow, 1952.

METHOD AND APPARATUS FOR COMPREHENSIVE STUDY OF THERMOPHYSICAL CHARACTERISTICS OF MATERIALS IN A WIDE RANGE OF TEMPERATURES

A. V. Lykov, A. G. Shashkov, Yu. Ye. Frayman,
G. M. Volokhov and V. P. Kozlov

One of the methods of attaining quasi-steady-state heat condition in material is to heat the latter in a medium whose temperature varies linearly [1]. Theoretical fundamentals of an absolute method of comprehensive determination of thermophysical characteristics of materials in a wide temperature range are set forth in [2, 3]. Based on regularities of the quasi-steady-state heating regime, the method makes it possible to investigate thermophysical characteristics without using reference material in measuring heat flux, the value of which must be known when calculating the coefficient of thermal conductivity. This is attained by introducing it to the specimen, a heat source of known and constant intensity, which produces a heat flux directed toward the main flux, resulting in the specimen being heated at a constant rate.

The experimental arrangement that has been put together made it possible to conduct comprehensive studies of thermophysical properties of nonmetallic materials in a wide temperature range (400-1500°K) by using the zonal method of calculation.

The method was realized in its cylindrical version; however, the theory is set forth in [4], where working formulas of the flat variant of the method are derived.

Two main variants of the method of conducting experiments have been advanced. The first variant provides for conducting two heatings of the test material. As a result of the first heating (with the constant-power source switched off) the quantity is determined along with the temperature dependence of the coefficient of thermal diffusivity. The second heating of the

material (with the constant-power source switched on) provides an opportunity to calculate the value and the temperature dependence of the coefficient of thermal conductivity.

The second variant of the method consists in periodically supplying the specimen with a constant-power source as the specimens being heated up throughout the entire temperature range investigated. Corresponding measurements for the opportunity of calculating coefficients of thermal diffusivity and thermal conductivity as the result of a single heating.

Both versions have several disadvantages. When the first version is put into effect, the need to conduct two heatings increases the time of the experiment. Execution of the second variant affords no possibility of obtaining a large number of working points, because a good deal of time is taken up in establishing the quasi-steady state regime after each switching on and switching off of the constant-power source.

Accordingly, a new method of conducting the experiment has been developed and proposed, making it possible to bypass the disadvantages noted above. Essentially, its difference from the earlier used method lies in the temperature measurements being made not at two points over the thickness (radius) of the specimen, but at three. This makes possible during a single heating continuous establishing of all quantities necessary in calculating coefficients of thermal diffusivity and thermal conductivity.

To derive working formulas under the new method, we will reproduce the formulation and solution of the problem (the flat version of the method is under consideration).

Formulation of the Problem

An unbounded plate of 2R thickness, at an initial temperature t_{in}, was heated in a medium whose temperature was a linear function of time. Heat transfer between the plate surfaces and the ambient medium occurred under first-order boundary conditions. The constant-power source operated in the plane $x = 0$. It is required to find the temperature field of the plate in the established quasi-steady-state heat regime.

The mathematical formulation of the problem:

$$\frac{\partial t(x,\tau)}{\partial \tau} = a \frac{\partial^2 t(x,\tau)}{\partial x^2} , \tag{1}$$

$$t_{cp} = t_H + b\tau , \tag{2}$$

$$t(x,\tau)|_{x=R} = t_H + b\tau , \tag{3}$$

$$-\lambda \frac{\partial t(x,\tau)}{\partial x}|_{x=0} = q . \tag{4}$$

Solutions of the problem are of the form

$$t = t_H + b\tau + \frac{bx^2}{2a} - \frac{qx}{\lambda} - \frac{bR^2}{2a} + \frac{qR}{\lambda} . \tag{5}$$

Let us write expressions for the temperature difference between points with coordinates x_0, x_1 and x_2 at the same moment in time:

$$t_1 - t_0 = \Delta t_{1-0} = \frac{b}{2a}(x_1^2 - x_0^2) - \frac{q}{\lambda}(x_1 - x_0) , \tag{6}$$

$$t_2 - t_1 = \Delta t_{2-1} = \frac{b}{2a}(x_2^2 - x_1^2) - \frac{q}{\lambda}(x_2 - x_1) , \tag{7}$$

$$t_2 - t_0 = \Delta t_{2-0} = \frac{b}{2a}(x_2^2 - x_0^2) - \frac{q}{\lambda}(x_2 - x_0) , \tag{8}$$

We assume that $x_0 = 0$, $x_1 = R/2$, and $x_2 = R$.

Then

$$\Delta t_{1-0} = \frac{bR^2}{8a} - \frac{qR}{2\lambda} , \tag{9}$$

$$\Delta t_{2-1} = \frac{3\beta R^2}{8a} - \frac{qR}{2\lambda}, \tag{10}$$

$$\Delta t_{2-0} = \frac{\beta R^2}{2a} - \frac{qR}{\lambda}, \tag{11}$$

Let us find the coefficient of thermal conductivity λ from expressions (9)-(11):

$$\lambda = \frac{qR}{\frac{\beta R^2}{4a} - 2\Delta t_{1-0}}, \tag{12}$$

$$\lambda = \frac{qR}{\frac{3\beta R^2}{4a} - 2\Delta t_{2-1}}, \tag{13}$$

$$\lambda = \frac{qR}{\frac{\beta R^2}{2a} - \Delta t_{2-0}}. \tag{14}$$

Let us substitute (12) in (10) and solve (10) for a, getting

$$a = \frac{\beta R^2}{4(\Delta t_{2-1} - \Delta t_{1-0})}. \tag{15}$$

Substituting (12) in (11), we obtain

$$a = \frac{\beta R^2}{4(\Delta t_{2-0} - 2\Delta t_{1-0})}. \tag{16}$$

After substitution of (13) in (11), we obtain:

$$a = \frac{\beta R^2}{4(2\Delta t_{2-1} - \Delta t_{2-0})}. \tag{17}$$

Substituting successively (13) in (9), (14) in (9), and (14) in (10), we obtain, respectively, the formulas (15), (16) and (17).

Thus, the working formulas for determining the coefficients of thermal diffusivity are of the form:

$$a=\frac{bR^2}{4(\Delta t_{2-1}-\Delta t_{1-0})}=\frac{bR^2}{4(\Delta t_{2-0}-2\Delta t_{1-0})}=\frac{bR^2}{4(2\Delta t_{2-1}-\Delta t_{2-0})} \tag{18}$$

Substituting successively (15), (16) and (17) in (12), (13) and (14), we obtain the following working formulas for determining the coefficient of thermal conductivity:

$$\lambda=\frac{qR}{\Delta t_{2-1}-3\Delta t_{1-0}}=\frac{qR}{\Delta t_{2-0}-4\Delta t_{1-0}}=\frac{qR}{4\Delta t_{2-1}-3\Delta t_{2-0}}=$$
$$=\frac{qR}{2\Delta t_{2-1}-2\Delta t_{1-0}-\Delta t_{2-0}}=\frac{qR}{3\Delta t_{2-0}-6\Delta t_{1-0}-2\Delta t_{2-1}} \tag{19}$$

The specific heat is determined from the relationship

$$c=\frac{\lambda}{a\gamma} \tag{20}$$

Formulas (18), (19) and (20) are the main working formulas of the proposed method.

All formulas that are part of (18) and (19) are equivalent. Treatment of the data obtained as a result of the experiment by any of these formulas makes it possible to conduct an inter-verification, and subsequently, to raise the precision of the results obtained.

Layout of Automatic Temperature Control

Realization of the broad-temperature method of investigating thermophysical characteristics of materials in a quasi-steady-state heating regime at constant rate requires that a reliable scheme of temperature control

following a linear law established beforehand be formulated. The wholly obvious advantages of quasi-steady-state methods (possibility of obtaining a temperature dependence of thermophysical characteristics in principle in any temperature range in combination with simplicity and, at the same time, correctness of theoretical fundamentals) have often remained unutilized precisely owing to the lack of a reliable scheme of temperature control.

In our view, this scheme must satisfy the following properties: 1) be automated, which increases precision of regulation, excludes the effect of any subjective factors, and considerably simplifies the work of the experimenter; 2) insure continuous heating of the material at a linear rate throughout the temperature range required; 3) afford the possibility of conducting the heating at any required rate; 4) insure adequate precision of temperature maintenance; 5) be simple enough in order that it can be realized in any laboratory that is in need of it.

A description of one of the temperature control schemes formulated in the Heat Physics Laboratory of the Institute of Heat and Mass Transfer of the Academy of Sciences Belorussian SSR, and satisfying the requirements postulated above is given below. The structural scheme of the automatic temperature control system of the high-temperature furnace is shown in Figure 1.

The scheme includes the following units:

1) The furnace temperature data pickup, sending a pulse U_{out} to a measuring instrument; it is a thermocouple, the hot arm of which lies at a specific point within the furnace;

2) The measuring instrument is the PS1-01 automatic electronic potentiometer with supplementary slide wire, the output signal of which U'_{out} is proportional to the true value of the furnace temperature;

3) A programmed master device of the RU5-02 type, the slide wire of which is connected with the supplementary slide wire of the measuring instrument by a bridge circuit and which generates the signal U_{des} that is proportional to the desired value of the quantity regulated;

4) An automatic electronic recording device RU4-16A, to which the unbalance signal ΔU is fed, when $U_{des} \neq U'_{out}$, arriving in the summation circuit, and then at the phase-sensitive electronic amplifier;

5) A slave mechanism (RD-09 reversible motor) which rotates as a function of the phase of the unbalance signal arriving from RU4-16A;

6) A regulating unit (automatic transformer) actuating the slave mechanism and carrying out change of voltage on the furnace winding.

The process of temperature control occurs as follows.

The sensing element of the programmed master unit -- a photo resistor with a flash lamp -- continually keeps track of the master heating program recorded by shading on RU5-02 diagram film. The value of the regulated parameter set by the program -- temperature -- is transformed into an electrical signal proportional to it.

The furnace temperature transducer is a thermocouple, the hot arm of which is centered to a metal plate lying in the furnace, and the transducer emits a second electrical signal proportional to the actual value of the parameter being regulated. This signal arrives at the input of the PS1-01 measuring instrument, which records the actual furnace temperature value on its diagram film.

A supplementary slide wire with a hundred percent proportionality zone made of calibrated manganin 0.2-mm-diameter wire is attached to the axis of the main slide wire of the measuring instrument. It is obvious that the potential of the sliding contact of this slide wire will be proportional to the actual value of the parameter being regulated, and the position of the slide wire will correspond to the true temperature value.

The slide wire of the programmed master unit and the supplementary slide wire of the measuring instrument are connected by a bridge circuit (cf. 2 and 3 in Figure 2)[1], and the shifting contacts of the sliders of both slide wires are connected to one of the diagonals of this circuit. The power supply of the bridge circuit comes from the RU4-16A regulator through

[1]See p. 374

adjustable resistances serving to bring into agreement the beginning and end of the programmed unit scale with the scale of the measuring instrument.

If electrical signals from the programmed master unit and thermocouples measuring the furnace temperature arriving at the bridge circuit are equal in absolute value, they compensate each other, and the bridge circuit is in equilibrium. This evidences that the actual furnace temperature value corresponds to the desired value.

In the opposite case, an unbalance signal ΔU appears, proportional to the difference of potentials on the sliders of the slide wires. This signal passes from a diagonal of the bridge circuit and is sent to the input of the RU4-16A regulating unit. Phase of the input signal will depend on the slide wire from which the large potential is removed, that is, on whether the true value of the quantity regulated at a given moment of time is greater or less than the value specified by the program.

The unbalance voltage in the regulating RU4-16A device arrives at the summation circuit, and then at the phase-sensitive electronic amplifier. A feedback bridge circuit is also present in the RU4-16A, one of the elements of which is the feedback rheostat R_{32} feeding back from the shaft of the regulating unit.

After amplification, the signal arriving at the regulator actuates one of the relays P_1 or P_2 of the RU4-16A regulator, through the contacts of which activation of the relay P_{max} or P_{min} controlling the slave mechanism is activated (Figure 2).

The control circuit of the slave mechanism is shown in Figure 2. One winding of the reversible motor is supplied with 127 v of ac current. The second winding is connected through a distributing condenser of one microfarad capacitance and further through normally open contacts of the relay P_{min} or P_{max}. The normally closed contacts k_{min} and k_{max} of the relay p_{min} and p_{max} serve to block the circuit when there is simultaneous activation of two relays. In order to change the direction of motor rotation, it is necessary to change the polarity on the clips 2 and 1. This is carried out by normally open contacts k_{min} and k_{max}. Rotation of the shaft of the slave mechanism produces shifting of the regulating unit, in this case the shifting

contact of the automatic transformer, which leads to an increase or decrease in the voltage fed to the furnace winding.

Shifting of the feedback rheostat slider occurs simultaneously and synchronously with shifting of the regulating unit up to equality of unbalance voltage and feedback voltage. Shifting of the regulating unit halts on attainment of this equality.

In the program control regime with advance (proportional-integral-differential regime), when there is proper choice of control parameters, specifically, the isodrome time T_n, the advance time T_n, and the proportionality range, the regulator periodically controls departure of the quantity regulated from the desired value and strives to reduce this departure to zero with the smallest expenditure of time.

All the units considered above are mounted on the same stand. The stand includes, in addition, the regulating unit position indicator, an electromagnetic system instrument, the winding of which is connected in parallel to the feedback rheostat, and the control panel, making it possible to also execute manual control of the furnace temperature. When the switch is turned to the "manual" position, the RU4-16A regulator is switched off, and control of the relays p_{max} and p_{min} of the slave mechanism is carried out by means of the "add-decrease" switch.

High-Temperature Furnace

A diagram of the high-temperature furnace designed to investigate thermophysical properties of flat specimens is shown in Figure 3.

Four plates (1) 60 × 60 × 6 mm in size with surfaces carefully ground with respect to each other are placed between two plates (2) of grade 1Kh18N9T grade stainless steel, on the outer surface of which channels have been cut. The heater winding made of nichrome wire wire 0.6 mm in diameter is placed in these grooves enclosed in 4-mm-diameter porcelain tubing. Depending on the heating conditions required, the upper and lower heaters can be connected either in series, or in parallel. To reduce heat transfer from the lateral surface, the plates are surrounded by stainless steel screens (4). The heater winding is compressed by plates (5), which in turn are

securely connected to plates (6), to which supplementary screens (7) are secured. The upper and lower halves of the furnace after placement of the specimens are pressed together by means of the plate (8) sliding along the guides (9) when the wing nut (10) is tightened.

The furnace is placed in a housing of sheet steel, the inner surface of which is lined with sheet asbestos.

The symmetry of the temperature field within the furnace is attained in two ways. The first method provides for placing two supplementary heaters alongside the main heater (for this purpose the porcelain tubing must be of the two-channel type). A differential thermocouple measures the temperature difference at the upper and lower plates (2). A signal corresponding to this temperature difference is fed to the amplifier input, which actuates the voltage regulator varying the intensity of the supplementary heaters until the signal from the differential thermocouple disappears. The second method provides for continuous rocking of the furnace during the experiment by a 90° angle to either side of the vertical position. For this purpose, the furnace is centered in the middle of the housing in bearings. The rocking is executed by an RD-09 motor placed on a fixed yoke in which the furnace is secured, and functions through a simple gear transmission.

The physical meaning behind provision of symmetrical heating conditions lies in eliminating additional uncontrolled heat fluxes over the height of the specimen, which can distort the experimental results. Furnaces usually employed in the practice of thermophysical investigations are of considerable size, in order for a zone with uniform temperature field to be selected. An increase in furnace dimensions is extremely undesirable, for this produces a corresponding rise in power consumed, which hampers regulation and maintanence of required conditions. The working volume of the furnace described above is determined by the height and diameter of the test specimens, therefore the maximum power required to attain a rate of 1000° per hour does not exceed 2 kw. The presence of a system of screens surrounding the specimen insures that during the experiment there will be small temperature differences between the lateral surface of the specimen and the surrounding medium. This is necessary to fulfill conditions of one-dimensionality of heat fluxes in the central parts of the specimen [5, 6].

The proposed quasi-steady-state research method does not exhaust the possibilities of the experimental apparatus: its design insures attainment of practically any thermal regime (steady-state, temperature waves, etc.).

Symbols

t = temperature; τ = time; x = coordinate; t_{med} = temperature of medium; t_{in} = initial temperature of medium (plate); b = heating rate; a = coefficient of thermal diffusivity of the plate; λ = coefficient of thermal conductivity of the plate; q = specific heat flux, constant-power source.

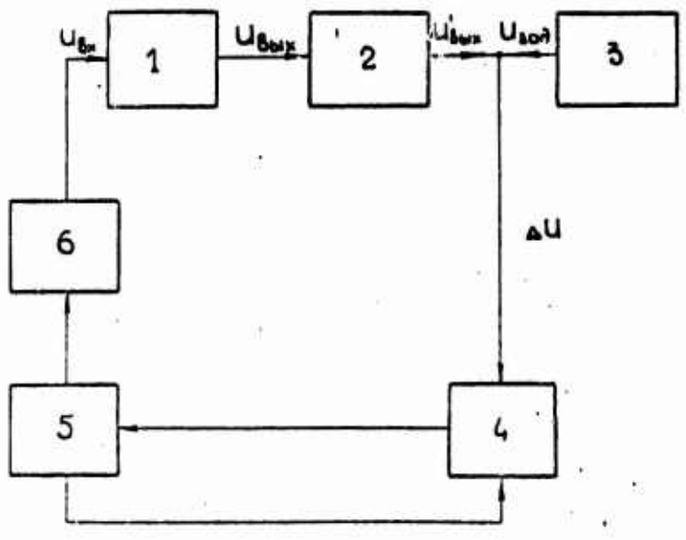

Figure 1. Structural diagram of programmed automatic control of furnace heating: 1, Object (furnace) controlled; 2, PS1-01 automatic electronic potentiometer with built-in rheostat data pickup; 3, RU5-02 master electronic regulating unit; 4, RU4-16A automatic electronic regulator; 5, Slave mechanism (RD09); 6, Regulating unit (automatic transformer).

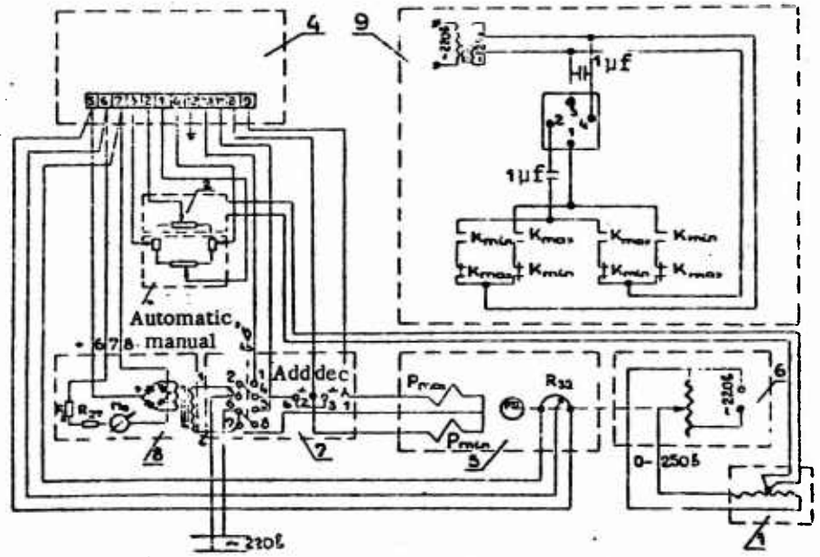

Figure 2. Assembly-switching diagram of furnace temperature programmed regulation: 1, 6, as in Figure 1; 7, Control panel; 8, Regulating unit position indicator; 9, Diagram of slave mechanism control.

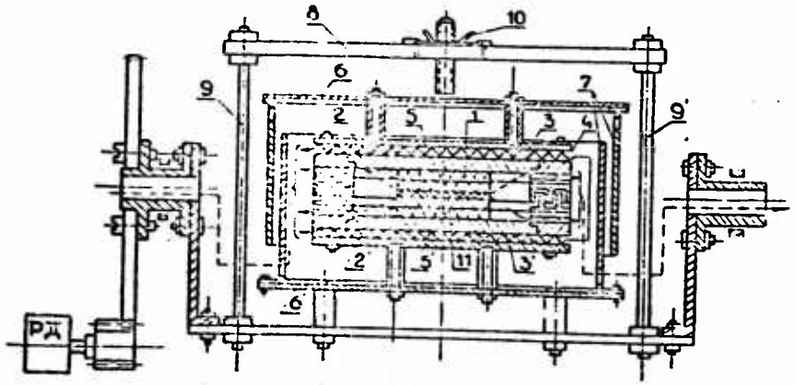

Figure 3. High-temperature furnace for plate-shaped specimens. 1, Test specimen; 2 and 2', Compressing plate; 3 and 3', Main heater; 4, Screen; 5 and 5', 6 and 6', 8, Stainless steel plates; 7, Supplementary screen; 9 and 9', Guides; 10, Wing nut; 11, Inner specimen heater. РД indicates the Slave mechanism.

Footnotes

1. To p. 366 The numbered sections of instruments and units in Figure 2 correspond to the numbered sections in Figure 1.

References

1. Lykov, A. V., *Teoriya Teploprovodnosti,* [Theory of Thermal Conductivity], Vysshaya Shkola Press, Moscow, 1967.

2. Frayman, Yu. Ye., *IFZh,* No. 10, 1964.

3. Frayman, Yu. Ye, *Trudy Mezhvuz. Nauch. Konferentsii po Problemam Stroit. Teplofiziki,* Proceedings of the Inter-institutional Scientific Conference on Problems of Construction Heat Physics], Vysshaya Shkola Press, Minsk, 1964.

4. Frayman, Yu. Ye., *Kandid. Dissertatsiya,* [Candidate's Dissertation], Minsk, 1965.

5. Frayman, Yu. Ye. and G. A Surkov, *IFZh,* Vol. 8, No. 5, 1965.

6. Volokhov, G. M., *Sb. Issledovaniye Nestatsionarnogo Teplo- i Massо-obmena,* [Collection: Research on Nonsteady-state Heat and Mass Transfer], Nauka i Tekhnika Press, Minsk, 1966.

NONSTEADY-STATE METHOD OF MEASURING CONTACT THERMAL RESISTANCES AND THERMAL CONDUCTIVITY COEFFICIENTS

I. G. Meyerovich and I. Yu. Kertselli

The regular regime in a multi-layer system is employed in measuring R and λ, when on one face the temperature changes at a constant rate, and on the other it is kept constant. In this regime, called quasi-steady-state, when there are nonsymmetrical boundary conditions [1] the overall temperature field is made up of distributions of temperatures induced by the passage of the so-called "absorption" flux and the "transit" flux. The latter changes with variation in temperature at the face, but at each moment of time is identical to the steady-state temperature distribution. By finding temperature distributions of the transit flux experimentally, we can determine R and λ as continuous functions of the temperature by the customary formulas of the steady-state regime methods. The distribution of temperatures from the transit flux is found from the general distribution by excluding temperature values from the absorption flux, which is achieved by successive execution of heating and cooling at the same rate, or by introducing corrections into the field of the absorption flux according to the formulas in [1]. The calculation requires prior knowledge (even though approximate) of the values of the parameters being measured, therefore it is simpler to determine the corrections experimentally by finding once for a series of such specimens temperature deviations in the quasi-steady-state regime from the steady-state regime at the same temperatures on the faces.

An apparatus with a system of programmed automation of temperature change has been developed for conducting the experiments using the method proposed, affording measurements in vacuum (up to $2 \cdot 10^{-3}$ N/m^2) or an inert atmosphere for different specimen compressive forces.

A diagram of the device is shown in Figure 1. The hermetic chamber (2) houses a system consisting of the test specimen (5), a heat measurer -- reference specimen (8), heater (11) with which linear temperature rise at the upper surface of the system is provided, and refrigerator (15) maintaining a constant temperature at the lower face. Mechanical stress is transmitted to specimens through the bellows (9) and the rod (10) with the aid of a system of levers and loads (1). The stress value can be varied without violating the hermeticity of the chamber within the limits 50-8000 N.

A shielding cylinder (13) on the upper section of which the heater is wound is provided to eliminate heat losses from the lateral surface of the test specimens and the heat measure. The design of the shielding cylinder insures the distribution of temperatures along its height in agreement with the distribution of temperatures in the test specimens and the heat-measure. The specimens and the shielding cylinder are surrounded by thermal insulation (3). The linear temperature rise at the upper surface of the system is insured by a programmed automatic unit [2], and an electronic potentiometer (22) serves as the regulator, which depending on the emf difference of the regulating thermocouple (12) and the voltage drop at the linear temperature rise transducer (21) switches off or switches on heater (11) with the aid of the magnetic starter (23). A tracking automated system, similar to the one described above, but without the regime transducer, is present to control the temperature of the shielding cylinder: a signal from the differential thermocouple (7), whose arms are calked at the same level in the shielding cylinder and on the specimen surfaces is fed to the input of the regulating electronic potentiometer (19).

Temperature is recorded by means of the EPP-09M3 multipoint electronic potentiometer (18) designed to measure voltage sources of 0-10 mv with a zero-resetting device (17). Cold arms of the thermocouples are placed in a Dewar flask (16). An evacuation system with forevacuum and diffusion pumps and an inert gas supply system are part of the apparatus.

Thermograms with temperature recordings on the diagramed film of the potentiometer are obtained as a result of experiments. Treatment of experiments leads to finding temperatures by the emf of the thermocouples, making

corrections for the absorption flux, and calculation according to the formulas:

$$q=\frac{\lambda_э}{\delta_э}\Delta t_э;\quad \lambda=\frac{q\cdot\Delta t}{\delta};\quad R_к=\frac{\Delta t_к}{q} \tag{1}$$

Though formulas (1) are extremely simple, calculation of a large number of measurement points for plotting the continuous function R = f(t) and λ = f(t) by the method indicated above takes a great deal of time and proceeds in contradiction to the high-speed measurement method. We have proposed a method that makes it possible to read off directly from the diagramed film the values of the specific heat flux and the temperature differences for test specimens, where λ_ε as a function of temperature is more precisely allowed for in determination of q. The function λ = f(t) of the steel Kh18N10T of which the heat-measure is made is described by the following equation with adequate precision:

$$\lambda=a+\beta t \tag{2}$$

We introduce the provisional temperature Ψ:

$$\Psi=\left(t+\frac{a}{\beta}\right)^2 \tag{3}$$

Then the expression for the specific heat flux is written in the form:

$$q=\left|\beta\sqrt{\Psi}\,\frac{d\sqrt{\Psi}}{dx}\right| \tag{4}$$

Separating the variables in (4) and integrating, we get

$$q=k(\Psi_1-\Psi_2) \tag{5}$$

where $k = b/2\delta_э$.

Using (3) and (5), we can calibrate a nomogram that makes it possible to find the quantity q directly from temperature differences in the heat-measure. A second nomogram is calibrated with respect to temperature. Thus, treatment of the experiments amounts to the following operations: plotting directly on the thermogram of corrected curves for the previously found values of the corrections, determination of Δt and q with aid of the nomograms, and calculation of the sought-for quantities λ and R from formulas (1).

Experimental error comprises two components: errors inherent in the corresponding steady-state methods of measuring λ and R, and supplementary error -- owing to imprecise linear temperature rise. The automated system we used insures observance of constancy of rate at the boundary that is so precise, such that the second component of error is negligibly small compared to the first. When measuring λ the error was 8-10 percent, and when measuring R -- 10-12 percent.

The proposed method was verified for specimens made of Duralumin, the end surfaces of which were planed to the fifth class of surface finish. The chemical composition of the Duralumin is as follows: Cu -- 3.63, Mg -- 1.35, Fe -- 0.3 and Mn -- 0.56 percent.

The test results in air using the proposed method and the steady-state method are shown in Figure 2. These values agree well with each other and satisfactorily agree with literature data [4].

The main advantage of the proposed method -- obtaining continuous functions of parameters measured in a wide temperature range with small amount of time spent in the experiment -- shows up in study of materials whose properties change appreciably with temperature and which have special points (inflection, minima and maxima). Materials of the following kind have been investigated in the study: semiconductors based on copper chalcogenides -- $Cu_2Tl_{0.5}S_{0.7}$; $Cu_2Tl_{0.5}S_{0.5}$; Cu_2S was graciously given us by L. D. Dudkin.

Due to technological considerations, specimens had to be made not more than 1.5-1.8 mm thick. Precise measurement of the temperature drop in brittle and solid semiconductors of such a small thickness is fairly

complicated task. We selected the following method: a copper layer was deposited on the end surfaces of specimens made in the form of 20-mm-diameter disks; the specimens were brought into contact with copper disks of the same diameter. In each, the copper disk was connected to two weighed chromel-aluminum thermocouples to a depth of 10 mm. A contact thermal resistance R_{Cu} was thus generated between the copper and test disks, which was measured separately. These transitional contacts could not be eliminated by soldering, since the solder at high temperatures can diffuse into the semiconductor and modify its properties. The above-mentioned R_{Cu} and the temperature drop within the copper disks were taken into account in calculating the λ of the semiconductors.

The measurement data are given in Figure 3. Measurements were made by the steady-state method for some of the temperatures, and the λ values found good agreement. It is clear from the figure that the function $\lambda = f(t)$ for Cu_2S has a maximum whose value and the value of the temperature corresponding to it were measured precisely.

Symbols

$\lambda_э$ = mean thermal conductivity coefficient of the heat-measure; $\Delta t_э$ and Δt = temperature differences for the heat-measure and the test specimen; $\delta_э$ and δ = distances between the thermocouples on the heat-measure and the specimen; $\Psi_1 - \Psi_2$ = difference of provisional temperatures corresponding to $\Delta t_э$; a and d = known coefficients [3]; q = heat flux passing through the specimens and the heat-measure.

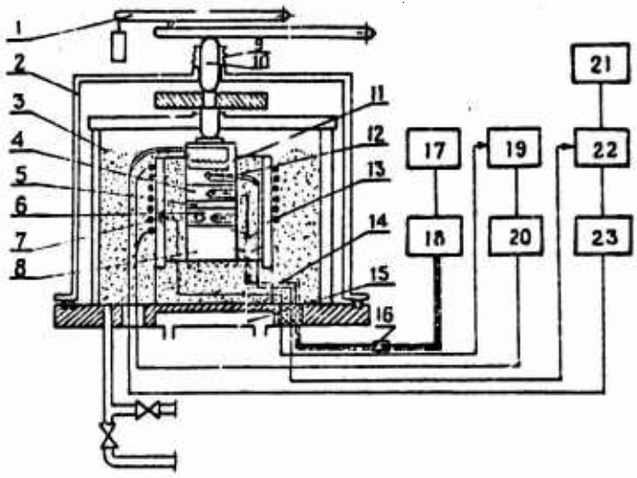

Figure 1. Diagram of experimental apparatus: 1, Lever system; 2, Hermetic chamber; 3, Thermal insulation; 4, Upper copper disk; 5, Specimen; 6, Lower copper disk; 7, Differential thermocouple; 8, Heat-measure; 9, Bellows; 10, Rod; 11, Heater; 12, Regulating thermocouple; 13, Shielding cylinder; 14, Measuring thermocouples; 15, Refrigerator; 16, Dewar vessel; 17, Zero-resetting device; 18, 19, 22, Electronic potentiometers; 20, 23, Magnetic starters; 21, Regime transducer.

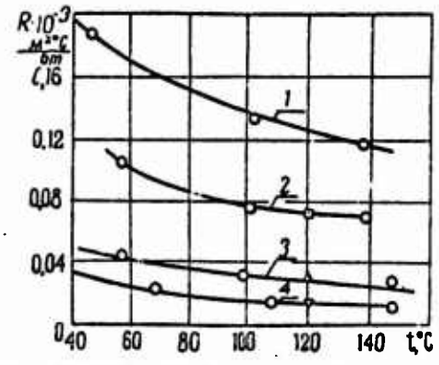

Figure 2. Contact thermal resistance of the D-16 -- D-16 pair as a function of temperature and of pressure (surface finish 7): ——, Quasi-steady-state method: 1, $P = 1 \cdot 10^6$ N/m^2; 2, $P = 2 \cdot 10^6$ N/m^2; 3, $P = 5 \cdot 10^6$ N/m^2; 4, $P = 10 \cdot 10^6$ N/m^2; ○, Steady-state method. Data [4]: □, $P = 1 \cdot 10^6$ N/m^2; △, $P = 5 \cdot 10^6$ N/m^2; ▽, $P = 10 \cdot 10^6$ N/m^2.

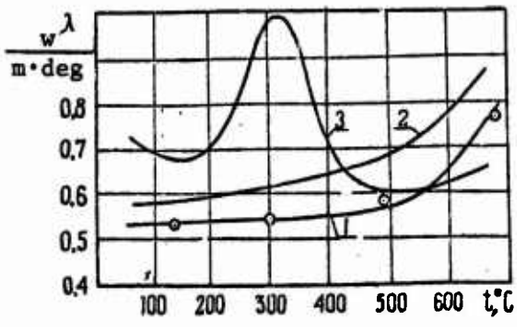

Figure 3. λ of semiconductors as a function of temperature: ——, Quasi-steady-state method: 1, $Cu_2Tl_{0.3}S_{0.7}$; 2, $Cu_2Tl_{0.5}S_{0.5}$; 3, Cu_2S. ○, Steady-state method, semiconductor $Cu_2Tl_{0.3}S_{0.7}$.

References

1. Meyerovich, I. G., *Teplo- i Massoperenos, T. 8,* [Heat and Mass Teansfer, Volume 8], Nauka i Tekhnika Press, Minsk, 1968.

2. Meyerovich, I. G. and I. Yu. Kertselli, *Teplofizika Vysokikh Temperatur,* Vol. 3, No. 5, 1965.

3. Vargaftik, N. B., *Teplofizicheskiye Svoystva Veschestv,* [Thermophysical Properties of Compounds], GEI Press, Moscow, 1956.

4. Shlykov, Yu. P. and Ye. A. Ganin, *Kontaktnyy Teploobmen,* [Contact Heat Transfer], GEI Press, Moscow, 1963.

METHODS OF MEASURING THE COEFFICIENT OF THERMAL CONDUCTIVITY OF MATERIALS WITH LOW THERMAL CONDUCTIVITY

I. N. Petrov

Customarily used methods for measuring thermal conductivity of semiconductor materials [1, 2] have proved inapplicable for materials with low thermal conductivity or materials that are transparent to thermal radiation. Many studies in which the thermal conductivity of such materials have been measured -- polycrystalline oxides of alkali-earth metals [3-5] -- contain obvious methodological errors: pyrometry of the transparent material surface, cementing in of thermocouples, etc., which casts doubt on the reliability of the result. The studies [6, 7] in which transparency of oxide layers to thermal radiation was allowed for, are also not free of several shortcomings. Thus, in [6] there is a description of the instrument design, which does not allow us to estimate whether possible errors in measurements owing to design features of the instrument were allowed for. In [7] there is no consideration given to possible losses of heater power, and imprecise equations are used in determining the radiation factor. The study [8], free of the above-indicated shortcomings, affords a clear idea of the mechanism of thermal conductivity of oxides of alkali-earth metals and the values of the thermal conductivity coefficient. However, a common shortcoming of the above-indicated studies [6-8] is the measurement of ξ for large temperature drops (200-300°), which for many materials, as in the case of oxides and alkali-earth metals, is undesirable owing to the strong temperature dependence of the thermal conductivity coefficient.

The aim of this study is to develop an improved method of measuring the thermal conductivity coefficient of such materials.

Experimental Method

Measurement of the thermal conductivity coefficient was carried out in a vacuum. A diagram of the instrument used in the measurement is shown in Figure 1. A specimen of the test material up to 200 μ thick was pressed by springs between two metal (for example, nickel) disks 5 mm in diameter, the temperature of which near the specimen was measured by platinum-platinum-rhodium thermocouples 50 μ in diameter. To reduce heater power losses, two thermal shields were used; the outer shield was made of thin sheet material of low thermal conductivity (invar). In the case of highly porous materials, of the type of alkali-earth metal oxides or alundum, thermal contact with the metal core was achieved by applying a coating employing technological procedures usually adopted for such materials (pulverization or cataphoresis). In the case of more compact materials, reliable thermal contact can be achieved by the same methods as are usually employed [1, 2].

Measurement of the thermal conductivity coefficient was carried out as follows: at identical core temperatures, which in the case of semiconductor materials can be controlled, in addition to thermocouples, also by the absence of a thermo-emf at the specimen, the temperature of both cores was recorded as a calibrated function of incandescence power fed to the heaters (Figure 2). The incandescence power, determined from the current and voltage at the heaters, must be measured with high precision (D-57 ammeter of the 0.1 class and the R-56 alternating current potentiometer).

However, not all the power fed to the heaters is expended directly in heating up the cores. In order to determine this "useful" component of the incandescence power, the same core temperature was established (T_x in Figure 2) and then, with incandescence power unchanged, the specimen was heated by alternating current. The Joule power Q_j supplied to the specimen leads to heating up of the cores to the temperature T_γ and the incandescence power of each core necessary to heat it to the same temperature T_γ is found from the calibration curve. The relationship of these power intensities (γ) shows by how much direct heating of cores is more effective than increase in heater power, that is, determines the "useful" component of heater power:

$$\gamma = \frac{Q_{g\text{н}}/2}{P(T_r) - P(T_x)} \qquad (1)$$

In the reduced expression (1) it is presupposed that the power supplied to the specimen is distributed in heating each core uniformly. If the cores are heated unevenly, this power can be divided proportionally to the temperature change of each core.

The coefficient γ can change somewhat with temperature change, therefore it must be determined for each range of temperature change.

In measuring the thermal conductivity of a specimen, after identical core temperatures are established, the temperature of one of the cores (to be specific, the upper core) is raised with incandescence power of the second (lower) core unchanged. However, owing to the thermal flux from the hotter core, the temperature of the lower core also rises, and from the calibrated graph we find the change in incandescence power corresponding to this temperature change. Because thin specimens are used, losses to the side owing to radiation of the specimen itself can be neglected. Then the thermal conductivity coefficient of the specimen can be determined from the equation:

$$\text{æ} \frac{S}{l}(T_r - T_x') = \gamma\left[P(T_x') - P(T_x)\right] \qquad (2)$$

This measurement is repeated for the same mean temperature upon switching the hot and cold cores (that is, the lower core is heated, and the incandescence power of the upper remains unchanged) and ξ is found as the mean of these two measurements.

Experimental Results and Their Discussion

Verification of the method was conducted on specimens of berium-strontium-calcium oxide 75-150 μ thick. A suspension of carbonate $(BaSrCa)CO_3$ was applied on both cores by pulverization, then the cores were placed and compressed by springs. Further evacuation and treatment of the vacuum instrument and the specimen were conducted following the technology customary for oxide cathodes [9, 10].

The effective thermal conductivity ξ as a function of temperature for oxide layers of different thicknesses is shown in Figure 3. The graphs presented demonstrate that in the low temperature range the thermal conductivity depends weakly on temperature; however, starting with temperatures of approximately 600°K there is a strong temperature dependence of ξ.

The data obtained is in good agreement with the results in [8]. In the high temperature range, the thermal conductivity was determined mainly by core radiation through an almost transparent oxide layer. Actually, the high-temperature sections of the temperature dependence of ξ demonstrate that $\xi \sim T^n$, where n lies within the limits 4-4.5, as should be anticipated in the case when radiation predominates in the overall thermal flux through the oxide layer.

In the low-temperature region, where radiation proved to be considerably weaker, the thermal conductivity was determined by oxide grains.

The measurements made allow us to calculate the mean radiation factor of nickel under oxide. Actually, because at high temperatures heat transfer occurs via radiation from core to core, then according to [8]

$$Q_{изм} = \gamma_0 [P(T_x') - P(T_x)] = \sigma_0 \bar{n}^2 S (T_r^4 - T_x'^4) \varepsilon. \qquad (3)$$

The resulting dependence of ε on T, shown in Figure 4, shows that the radiation factor of nickel under oxide is ~ 0.2-0.25, 1.5-2 times different from the reduced radiation factor of two polished nickel surfaces calculated according to a formula in [11]:

$$\varepsilon_{пр} = \frac{\varepsilon_r \varepsilon_x}{\varepsilon_r + \varepsilon_x - \varepsilon_r \varepsilon_x}. \qquad (4)$$

The results obtained on measurement of the thermal conductivity coefficient of oxide in a wide temperature range show that the proposed can be applied in measuring the thermal conductivity coefficient of electroconductive materials.

In the case of nonconductive materials, preliminary calibration of the instrument for determination of the coefficient γ is necessary.

This instrument design is suitable, if simultaneously with thermal conductivity electrical properties also have to be measured -- electroconductivity and thermo-emf -- in the absence or for small temperature drop in the specimen.

The radiation factor values of nickel under oxide obtained in the study, ~ 0.2-0.25, evidence some blackening of the nickel surface compared to the polished surface, which must be taken into account in calculating radiation from oxide cathodes.

Symbols

ε = radiation factor of nickel under oxide; ε_γ and ε_x = radiation factor of polished nickel at temperatures of hot and of cold cores, respectively; ξ = thermal conductivity coefficient; σ_o = Stefan-Boltzmann constant; $\bar{n}$ = mean index of refraction of oxide ($\bar{n}^2 = 1.3$); S = specimen area; l = specimen thickness; T_γ = temperature of hotter (upper) core; T'_x = equilibrium temperature of colder (lower) core; Q_j = power supplied to the specimen; $P(T_x)$ = incandescence power of one of the cores up to specimen heating; $P(T_\gamma)$ = incandescence power of the same core determined from the calibrated graph for the core temperature reached after the power Q_j is fed to the specimen; T_x = temperature of lower core in the absence of thermal flux from the upper core (equal core temperatures); $P(T'_x)$ and $P(T_x)$ = incandescence temperature of the colder core for the corresponding temperatures (from the calibrated graph).

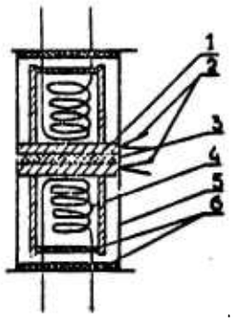

Figure 1. Diagram of experimental instrument: 1, Metal (nickel) core; 2, Thermocouples; 3, Test specimen; 4, Heater; 5, Thermal shield; 6, Ceramic washers.

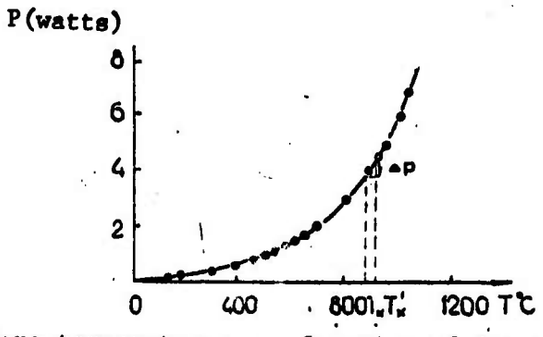

Figure 2. Core temperature as a function of incandescence power.

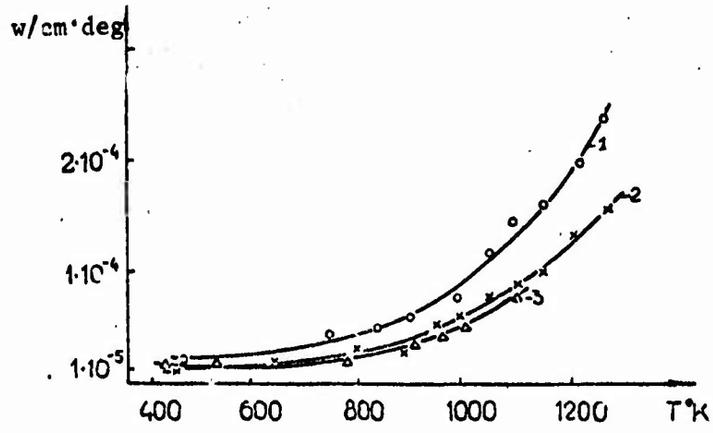

Figure 3. Thermal conductivity coefficient as a function of temperature for different specimens $(BaSrCa)O_2$, specimen thickness ℓ: 1, 150 μ; 2, 100 μ; 3, 75 μ.

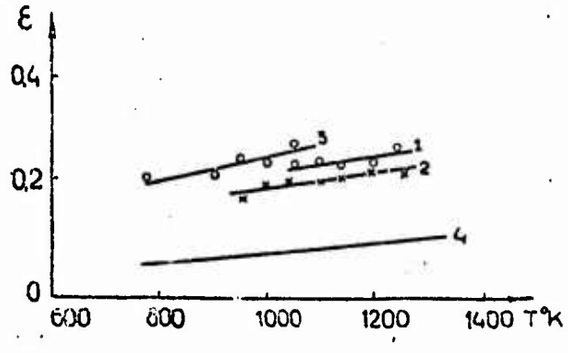

Figure 4. Radiation factor of nickel under oxide as a function of temperature: 1, 2, 3, Same specimens as in Figure 3; 4, Theoretical ε_{max} calculated from formula (4).

References

1. Egli, P. H., (Ed), *Thermoelectricity*, N-Y-L, 1960.
2. Petrov, A. V., *Sb. Thermoelektricheskiye Svoystva Poluprovodnikov*, [Collection: Thermoelectric Properties of Semi-conductors], Academy of Sciences Belorussian SSR Press, Moscow-Leningrad, 1963.
3. Clausing P. and I. Ludwig, *Physica*, Vol. 13, p.193, 1933.
4. Patai, E., and A. Tomashek, *Kolloid A.*, Vol. 74, p. 253, 1936.
5. Zingerman, Ya. P., *Ukr. Fiz. Zhurnal*, Vol. 1, p. 308, 1956.
6. Weston, J. E., *Nature*, Vol. 166, No. 4234, p. iiii, 1956.
7. Pengelly A. E., *Brit. J. of Appl. Phys.*, Vol. 6, p. 18, 1955.
8. Chudnovskiy, F. A., *IFZh*, Vol. 10, p. 106, 1966.
9. German, G. and S. Vagener, *Oksidnyy Katod*, [Oxide Cathodes], Gostekhizdat Press, 1949.
10. Moyzhes, B. Ya., I. N. Petrov, O. V. Sorokin and E. M. Sher, *Radiotekhnika i Elektronika*, Vol. 11, p. 1674, 1966.
11. Blokh, A. G., *Osnovy Teploobmena Izlucheniyem*, [Fundamentals of Radiative Heat Transfer], Gosenergoizdat Press, Moscow-Leningrad, 1962.

METHODS OF QUASI-STEADY-STATE REGULAR AND STEADY-STATE REGIMES IN DETERMINING HEAT TRANSFER COEFFICIENTS AT ELEVATED TEMPERATURES

V. G. Petrov-Denisov, I. B. Zasedatelev and L. A. Maslennikov

The wide use of heat-resistant concrete has required determination of heat transfer coefficients of these materials in a wide temperature range. Specific feature of concrete and conditions of its use have led to the necessity to develop new designs of experimental devices and the use of different research methods.

To put into effect a method of heating the specimen at constant rate proposed by A. V. Lykov [1, 2], and in the regime of temperature waves in the 300-1200°K range, an experimental device with radiation heating of the specimen was devised, consisting of a radiation chamber (Figure 1), systems of automatic regulation and programmed control, a temperature recording unit, and a protective device.

An iodine lamp made of quartz tubing 10 mm in diameter and 400 mm long served as the heating element for the panel and the radiation chamber.

The most successful solution for reinforcement of iodine lamps was to weld the lamp bases to copper tubes, which served as a supporting framework, a busbar for passage of electric power to the lamps, and for removal of heat from the lamp bases. The latter was attained by circulating water through the tubes.

An electronic system of automatic regulation with programmed control was developed to provide the required conditions at the specimen surface.

By using the programmed-master unit operating under the principle of tracking the photo head from the program graph plotted on the tape of the electronic regulator and the RNO-20-250 automatic transformer, the temperature of the specimen surface was controlled. The other side of the specimen

by means of the second automatic transformer. To provide feedback, a surface thermocouple connected to the main electronic temperature regulator on the RPIB series was placed on the controlled surface of the specimen. The regulator equalized the signal of the programmed-master unit with the thermocouple signal and through intermediate RS-13 relays sent signals simultaneously to both automatic transformers insuring their synchronicity.

In the case of temperature unbalance at the specimen surfaces, the auxiliary RPIB was activated, which introduced the appropriate correction into the performance of the second automatic transformer by means of the differential thermocouple.

Experiments on determining the coefficient of thermal conductivity by quasi-steady-state regime methods were carried out on plates 80 and 50 mm thick and with top view dimensions of 400 × 400, made of heat-resistant concrete using Portland cement and chamotte filler.

The dimensions of the concrete specimens modeling an unbounded plate were selected on the basis of numerical calculations of the temperature field made on analog computers.

After manufacture, the concrete specimens were steamed in forms, then dried to constant weight at 105°, then tested.

Initially, experiments were conducted with each specimen using the method of heating and cooling at a constant rate in the following ranges: 20-100, 100-200, 200-300, 300-400, 400-500, 500-600, 600-700, 700-800, and 800-900° (three cycles), and then one cycle of heating following a sinusoidal law was carried out for the same temperature ranges.

The A-calorimeter for determination of thermal diffusivity in the regular regime [3] in the temperature range 0-160°C consisted of two thermostats and a modernized EPP-09 potentiometer. In both thermostats the temperature of the liquid (water, oil) was kept constant with a previously determined drop.

Two spherical specimens 100 mm in diameter were tested simultaneously, each of which was placed in a corresponding thermostat. When the temperature in the center of the specimen equaled the ambient temperature, the specimens were switched. After testing, the specimens were covered with moisture

insulation, the following being used: nitroemal, organic glass soluble in dichloroethane, epoxide resin, and latex. The best results were obtained when envelopes were used.

To discover the coefficient of thermal diffusivity as a function of temperature in the 0-100°C range, the teste were conducted for a 25° temperature drop in the thermostats and at a mean experimental temperature of 12.5, 37.5, 62.5, and 87.5°C.

Determination of thermal diffusivity at temperatures of 300-400°C was made on a special device in which liquid thermostats were placed on heat baths containing molten tin.

Temperature control was carried out with the aid of an automatic control system used in the apparatus to determine the coefficient of thermal diffusivity by the quasi-steady-state regime method. Forced mixing of molten tin was performed by a propeller type mixer. To avoid large heat losses from the surface of the melt when the specimens were rearranged, the open area of the bath was heaped over with fine perlite sand. This made it possible, by not exposing the melt surface, to place and remove spceimens from the bath.

Experimental results on determination of the coefficient of thermal diffusivity of heat-resistant concrete in quasi-steady-state and regular regimes throughout the entire temperature range studied quite closely group around the mean curve (Figure 2). The scatter of experimental points does not exceed 10 percent. If the large anisotropicity of structure of the test material is borne in mind, the precision of experimental data must be regarded as satisfactory.

Reliability of the methods developed and the experimental data obtained for heat-resistant concrete is confirmed by results obtained upon investigating a reference body. The latter was a chamotte brick, since a great deal of experimental material on heat transfer coefficients is available for it in the literature.

As can be established (Figure 3), the results obtained find good agreement with the data in [4-6].

Bearing in mind the importance of direct determination of the thermal conductivity coefficient of materials at elevated temperatures under steady-state conditions, a method and instrument design were developed for determining the thermal conductivity coefficient of building materials of the 50-800° range, in which many shortcomings of similar existing instruments were eliminated.

This refers above all to avoidance of a liquid cooling agent. An instrument operating on the two-plate method has a central heating element and two end-face heaters. This makes it possible to produce the desired temperature drop in specimens.

Intensification of heat removal from the external side of the end-face heaters is attained by installing small-size axial fans, as the result of which the temperature difference within specimens can be regulated over wide ranges.

To preserve the linearity of the thermal flux in the specimens, a shielding envelope was provided in the form of a diametrical tubing containing local heaters placed along its outer surface in the areas where the main heaters were located. This design afforded a temperature field at the inner surface of the envelope similar to the temperature field at the outer cylindrical surface of specimens.

To eliminate the effect of convection on the thermal conductivity coefficient for coarse-porous materials, the possibility of rotating the specimens during the experiment was provided for.

The value of the thermal flux passing through the specimen was determined by the consumption of electric power used up in maintaining the temperature of the central heater.

The main distinguishing feature of the instrument is the possibility of automatically setting and maintaining any required temperature drop between the cold and hot surfaces of the specimen throughout the entire range of measurements.

The instrument was equipped with an automatic control system, by means of which determination was made of the thermal conductivity coefficient automatically in the 100-800° ranges.

At present an experimental design of the instrument has been developed and is being tested.

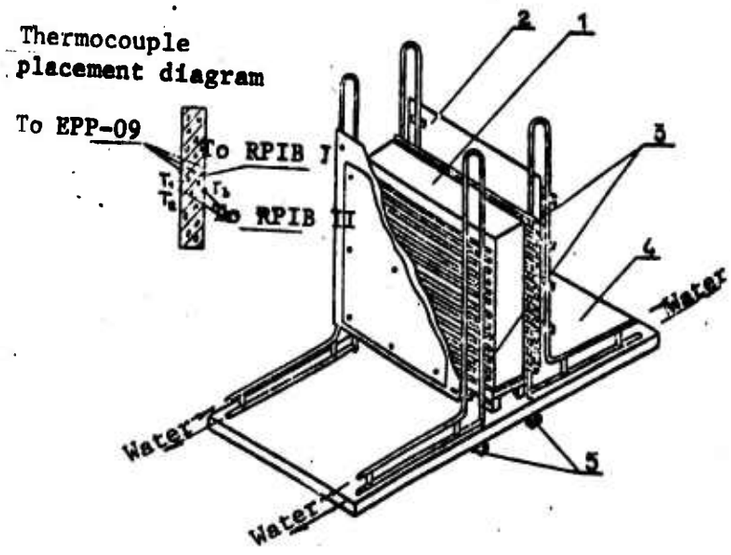

Figure 1. Diagram of radiation chamber: 1, Specimen; 2, Screen; 3, Incandescent lamp; 4, Plate; 5, Power conduit

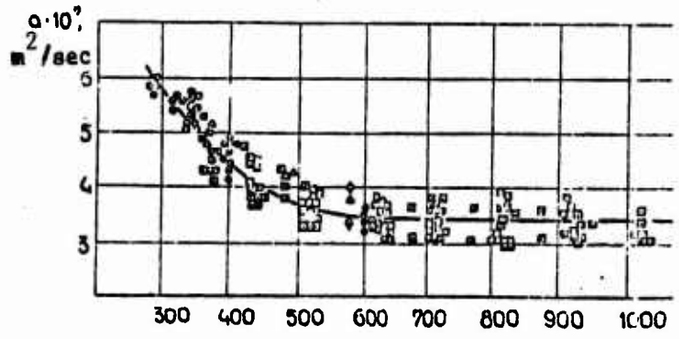

Figure 2. Thermal diffusivity of heat-resistant concrete as a function of temperature. Regular regime: ⊙ in [illegible]; ○, In spindle oil; ⊗, In molten tin. Quasi-steady-state regime: ⊡, Rectilinear radiation; □, Sinusoidal radiation; Δ, Rectilinear [illegible]

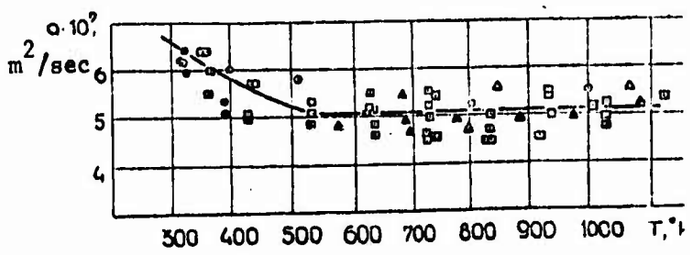

Figure 3. Thermal diffusivity of chamotte as a function of temperature: ⊗, Regular regime; ⊡, Quasi-steady-state regime; Δ, Chamotte brick of the Borovichi Plant [4]; Δ, Chamotte brick of the Latnaya Plant [4]; Δ, Chamotte ceramic [6]; ⊙, Chamotte ceramic [5].

References

1. Lykov, A. V., *ZhETF*, Vol. 5, p. 171, 1935.

2. Lyl[illegible] V., *IFZh*, No. 10, 1960.

3. Kondrat'yev, G. M., *Teplovoy Regulyarnyy Reshim*, [Regular Thermal Regime], Gostekhizdat Press, Moscow, 1954.

4. Kolechkova, A. F., and V. V. Goncharov, Ogneupory: a) No. 10, 1949; b) No. 9, 1948.

5. Vasil'yev, L. L. and Yu. Ye. Frayman, *IFZh*, No. 6, 1965.

6. Zalkind, I. Ya., *Teploenergetika*, No. 8, 1964.

GENERALIZATION OF REGULAR THERMAL REGIME METHODS FOR THE CASE OF VARIABLE THERMOPHYSICAL COEFFICIENTS

Ye. S. Platunov

Almost all methods of determining thermophysical properties of materials available at present are based on regularities of the linear theory of thermal conductivity. Only in several studies [1-6] are concrete recommendations given for taking into account corrections for the temperature dependence of thermophysical coefficients.

Various procedures are known for an approximational solution of the nonlinear thermal conductivity equation: for example, by means of integral substitutions [2], by the method of successive approximations (small-parameter method) [4-6], by finding the temperature field in the form of an exponential [1] or functional [3] series. At present, the procedure of successive approximations is employed for generalizing thermophysical methods, since it provides rapid convergence of solutions when there is a simple structure of corrections and has some universality.

Thermophysical studies are conducted mainly on specimens of simple configuration with a one-dimensional temperature field $t(r, \tau)$ at sufficiently small values of temperature drop $\vartheta(r, \tau)$. Their temperature field (excluding internal heat sources) is governed by the equation

$$\operatorname{div}(\lambda \cdot \operatorname{grad} t) = c\gamma\beta \qquad (1)$$

Thermophysical coefficients of specimen materials within the limits of the temperature drop $\vartheta(r, \tau)$ can usually be represented with required precision by relationships of the form

$$\lambda=\lambda_0\cdot(1+\kappa_\lambda\cdot\vartheta+n_\lambda\cdot\vartheta^2+\ldots);\quad a=a_0\cdot(1+\kappa_a\cdot\vartheta+n_a\cdot\vartheta^2+\ldots);$$
$$c\gamma=c\gamma_0\cdot(1+\kappa_c\cdot\vartheta+n_c\cdot\vartheta^2+\ldots) \qquad (2)$$

An exception here is represented only by zones of phase transitions, where the monotonic temperature dependence characteristic of coefficients is violated. The number of members actually taken into account in the relationships (2) depend on $\vartheta(r, \tau)$. When $|\vartheta| < 50°$, the functions (2) approximate linearity, therefore it is often sufficient to have a solution of equation (1) to the first approximation. The second and subsequent approximations become necessary when thermophysical tests are conducted near the phase transition zones, where the values of the coefficients k and n rise sharply and the following conditions are not observed:

$$|\kappa_\lambda\cdot\vartheta|<0{,}1;\quad |\kappa_a\cdot\vartheta|<0{,}1;\quad |\kappa_c\cdot\vartheta|<0{,}1; \qquad (3)$$

$$|n_\lambda\cdot\vartheta^2|<0{,}01;\quad |n_a\cdot\vartheta^2|<0{,}01;\quad |n_c\cdot\vartheta^2|<0{,}01 \qquad (4)$$

Under ordinary conditions, the second approximation is required only for a more substantiated evaluation of the precision of the first approximation.

Second-Order Regular Regime

A distinguishing feature of the regime considered is the condition b = const. However, in actuality it can never be strictly complied with owing to difficulties that are purely technical and owing to the inconstancy of thermophysical coefficients. The rate of temperature rise $b(r, \tau)$ proves to be a monotonic function of r and τ, where, like the functions (2), the partial increments of $b(r, \tau)$ with respect to the coordinate and time within the limits of the temperature drop $\vartheta(r, \tau)$ and the temperature increment commensurable with them Δt are usually close to the linear and can be represented in the form of the relationship

$$b(r,\tau)=b_0\cdot(1+\kappa_{b,r}\cdot\vartheta+n_{b,r}\cdot\vartheta^2+\ldots) \qquad (5)$$

$$b(a\tau)=b_0\cdot(1+\kappa_{b,\tau}\cdot\Delta t+n_{b,\tau}\cdot\Delta t^2+\ldots) \qquad (6)$$

To simplify working formulas, it is desirable to place the following restrictions on the experimental regime:

$$|\kappa_{b,\tau} \cdot \vartheta| < 0{,}1 \qquad \text{and} \qquad |n_{b,\tau} \cdot \vartheta^2| < 0{,}01 \tag{7}$$

The coefficients $k_{b,r}$ and $k_{b,\tau}$ in (5) and (6) are interrelated. The primary and independent coefficient here is $k_{b,\tau}$. It takes account of characteristics of heat transfer of the specimen from the medium.

The following functions are valid between coefficients k_λ, k_a, k_c and n_λ, n_a and n_c:

$$\kappa_\lambda = \kappa_a + \kappa_c \qquad \text{and} \qquad n_\lambda = n_a + n_c + 2\kappa_a \cdot \kappa_c \tag{8}$$

To find an analytical relationship between the coefficients $k_{b,r}$ and $k_{b,\tau}$, it is sufficient to transform equation (1) into the form

$$\nabla^2 \vartheta + \frac{1}{\lambda} \cdot \frac{d\lambda}{dt} \cdot (\operatorname{grad} \vartheta)^2 = \frac{b}{a}$$

and to differentiate both of its members with respect to τ at the base point with t_o, taking into account the above-adopted conditions (3)-(7) and the assumptions of the constancy of the coefficients k_λ, k_a, $k_{b,\tau}$ and $k_{b,r}$.

We have

$$\frac{d}{d\tau}\left(\frac{b}{a}\right)_{t_o} = \frac{b_o^2}{a_o} \cdot (\kappa_{b,\tau} - \kappa_a);$$

$$\frac{d}{d\tau}\left[\nabla^2 \vartheta + \frac{1}{\lambda} \cdot \frac{d\lambda}{dt} \cdot (\operatorname{grad} \vartheta)^2\right]_{t_o} = \kappa_{b,\tau} \cdot b_o \left[\nabla^2 \vartheta + 2\kappa_\lambda \cdot (\operatorname{grad} \vartheta)^2\right]_{t_o}$$

from whence the following relationship is valid with an error of not more than ±10%:

$$\kappa_{b,\tau} = \kappa_{b,a} - \kappa_a \tag{9}$$

This error for (9) is usually wholly acceptable, because it serves to relate correctional members.

The relationship (9) is marked by some universality. It can be used not only in analyzing single-dimensional temperature fields, but also two- and three-dimensional fields, if they are isotropic with respect to the coefficient $k_{b,r}$.

If the specific thermal flux $w(\tau)$ at the specimen surface is given, differentiation of the equation $w \cdot F = c\gamma_v \cdot b_v \cdot V$ with respect to τ, taking into account the restrictions (3)-(7), gives the relationship

$$K_{\beta,\tau} = K_w - K_c \tag{10}$$

which is valid with an error of not more than 10 percent at all specimen points.

In the particular case, when the heat transfer of the specimen from the medium is governed by Newton's law $w = \alpha \cdot t_F$ (here and in what follows the thermostated medium has $t_c = 0$), for k_w we have:

$$K_w = K_\alpha + 1/t_F \tag{11}$$

If the specimen is cooled in a vacuum-treated medium according to the law

$$w = \varepsilon \cdot \sigma_0 \cdot T_F^4$$

then

$$K_w = K_\varepsilon + 4/T_F \tag{12}$$

Below are presented the results of a solution of the thermal conductivity equation (1) to the second approximation applicable to a plate, cylinder, and a sphere. Solutions to the first approximation for these forms are found in [4-6].

Plate. Equation (1) for the plate is

$$\frac{d^2\vartheta}{d\tau^2}+\frac{1}{\lambda}\cdot\frac{d\lambda}{dt}\cdot\left(\frac{d\vartheta}{d\tau}\right)^2=\frac{b}{a} \tag{13}$$

upon the assumptions (2)-(7) at an arbitrary moment of time τ, is transformed to the following form with a precision up to members of the second order of smallness:

$$\frac{d^2\vartheta}{d\tau^2}=\frac{b_e}{a_e}-\left[\frac{b_e}{a_e}\cdot\left(K_a-K_{b,\tau}\right)\cdot\vartheta+K_\lambda\left(\frac{d\vartheta}{d\tau}\right)^2\right]-\left[\left(K_a\cdot K_{b,\tau}-\right.\right.$$

$$\left.\left.-K_a^2+n_a-n_{b,\tau}\right)\cdot\frac{b_e}{a_e}\cdot\vartheta^2+\left(2n_\lambda-K_\lambda^2\right)\cdot\vartheta\cdot\left(\frac{d\vartheta}{d\tau}\right)^2\right] \tag{14}$$

The members of the first and second orders of smallness, respectively, are collected within the square brackets.

The boundary conditions

$$\vartheta(0,\tau)=0 \qquad \text{and} \qquad \vartheta(R,\tau)-\vartheta(-R,\tau)=\vartheta_{R,-R}(\tau) \tag{15}$$

Equation (14) in the null approximation (without correctional members) has the following solution with (15) taken into account:

$$\vartheta^0=\left(\vartheta_{R,-R}/2R\right)\cdot\tau+\left(b_0/2a_0\right)\cdot\tau^2 \tag{16}$$

After independent determination of numbers of the first order of smallness in equation (14), the solution of (14) can be obtained through ϑ^0 from (16) to the first approximation

$$\vartheta^I=\vartheta^0+\Delta\vartheta^\tau, \tag{17}$$

where

$$\Delta\vartheta^{I} = \frac{1}{3}(2K_{\lambda} + K_{\alpha} - K_{\beta,\tau})(b_{0}/2a_{0})\left[(\vartheta_{\tau,-R}/2R)(R^{2}-\tau^{2})\tau - \right.$$

$$\left. -(b_{0}/2a_{0})\cdot\frac{1}{2}\tau^{4}\right] - \frac{1}{2}K_{\lambda}\cdot(\vartheta_{R,-R}/2R)^{2}\cdot\tau^{2} \qquad (18)$$

For a solution to the second approximation, members of the first order of smallness in equation (14) are determined through ϑ^{I} from (17) and (18), and members of the second order of smallness -- through ϑ^{O} from (16). Thereupon, equation (14) yields the solution

$$\vartheta^{II} = \vartheta^{*} + \Delta\vartheta^{I} + \Delta\vartheta^{II}, \qquad (19)$$

where

$$\Delta\vartheta^{II} = \frac{1}{6}\cdot(2n_{\lambda} - 3K_{\lambda}^{2})(\vartheta_{R,-R}/2R)^{3}(R^{2}-\tau^{2})\cdot\tau - \frac{1}{3}\cdot(2K_{\lambda}^{2} + K_{\lambda}\cdot K_{\alpha} -$$

$$K_{\lambda}\cdot K_{\beta,\tau})(\vartheta_{R,-R}/2R)^{2}(b_{0}/2a_{0})\cdot R^{2}\tau^{2} + \frac{1}{9}(2K_{\lambda} + K_{\alpha} - K_{\beta,\tau})^{2}\cdot(\vartheta_{R,-R}/2R)\cdot \qquad (20)$$

$$\cdot(b_{0}/2a_{0})^{2}R^{2}\cdot(R^{2}-\tau^{2})\cdot\tau + \frac{1}{12}(13K_{\lambda} + 2K_{\alpha}^{2} + 3K_{\lambda}\cdot K_{\alpha} - 3K_{\lambda}\cdot K_{\beta,\tau} - 2K_{\alpha}\cdot K_{\beta,\tau} -$$

$$10n_{\lambda} - 2n_{\alpha} + 2n_{\beta,\tau})(\vartheta_{R,-R}/2R)^{2}(b_{0}/2a_{0})^{2}\cdot\tau^{4} + \frac{1}{30}(28K_{\lambda}^{2} + 7K_{\alpha}^{2} + K_{\beta,\tau}^{2} +$$

$$+10K_{\lambda}\cdot K_{\alpha} - 10K_{\lambda}\cdot K_{\beta,\tau} - 8K_{\alpha}\cdot K_{\beta,\tau} - 24n_{\lambda} - 6n_{\alpha} + 6n_{\beta,\tau})\cdot\left[(\vartheta_{R,-R}/2R)(R^{2}-\tau^{4})\tau + \right.$$

$$\left. +\frac{1}{5}\cdot(b_{0}/2a_{0})\tau^{6}\right]\cdot(b_{0}/2a_{0})^{2}$$

If the plate is heated in symmetrical conditions ($\vartheta_{R_1-R} = 0$), its temperature field becomes

$$\vartheta^{II} = (b_{0}/2a_{0})\cdot\tau^{2}\left[1 - \frac{1}{6}(2K_{\lambda} + K_{\alpha} - K_{\beta,\tau})\cdot(b_{0}/2a_{0})\cdot\tau^{2} + \right.$$

$$\frac{1}{90}(28K_{\lambda}^{2} + 7K_{\alpha}^{2} + K_{\beta,\tau}^{2} + 10K_{\lambda}\cdot K_{\alpha} - 10K_{\lambda}\cdot K_{\beta,\tau} - 8K_{\alpha}\cdot K_{\beta,\tau} - \qquad (21)$$

$$\left. 24n_{\lambda} - 6n_{\alpha} + 6n_{\beta,\tau})\cdot(b_{0}/2a_{0})^{2}\cdot\tau^{4}\right]$$

If the temperature field of the plate is close to the steady-state and the following inequality is fulfilled

$$|(b_{0}/2a_{0})\cdot\tau^{2}| < q1\cdot|(\vartheta_{R,-R}/2R)\cdot\tau| \qquad (22)$$

then we have

$$\vartheta^{II} = (\vartheta_{R_1-R}/2R)\cdot r + \Delta\vartheta^{I} + \Delta\vartheta^{II}$$

where

$$\Delta\vartheta^{I} = (b_0/2a_0)\cdot r^2 - \frac{1}{2}K_\lambda\cdot(\vartheta_{R_1-R}/2R)^2\cdot r^2$$

$$\Delta\vartheta^{II} = \frac{1}{3}(2K_\lambda + K_a - K_{\beta,\tau})(\vartheta_{R_1-R}/2R)(b_0/2a_0)\cdot(R^2-r^2)r - \frac{1}{6}(2K_\lambda + K_a - K_{\beta,\tau})(b_0/2a_0)^2\cdot r^4 + \frac{1}{6}\cdot(2n_\lambda - 3K_\lambda^2)\cdot \cdot(\vartheta_{R_1-R}/2R)^3\cdot(R^2-r^2)\cdot r \qquad (23)$$

Cylinder. Thermal conductivity equation:

$$\frac{d^2\vartheta}{dr^2} + \frac{1}{r}\cdot\frac{d\vartheta}{dr} = \frac{b_0}{a_0} - \left[\frac{b_0}{a_0}(K_a - K_{\beta,\tau})\cdot\vartheta + K_\lambda\cdot \cdot\left(\frac{d\vartheta}{dr}\right)^2\right] - \left[\frac{b_0}{a_0}(K_a\cdot K_{\beta,\tau} - K_a^2 + n_a - n_{\beta,\tau})\vartheta^2 + (2n_\lambda - K_\lambda^2)\cdot\vartheta\left(\frac{d\vartheta}{dr}\right)^2\right] \qquad (24)$$

Boundary conditions:

$$\vartheta(0,\tau) = 0 \quad \text{and} \quad \frac{d\vartheta(0,\tau)}{d\tau} = 0 \qquad (25)$$

The temperature field is governed by a function of the form (19) where

$$\vartheta^{I} = (b_0/4a_0)\cdot r^2, \quad \Delta\vartheta^{I} = -\frac{1}{4}(K_\lambda + K_a - K_{\beta,\tau})(b_0/4a_0)^2\cdot r^4,$$

$$\Delta\vartheta^{II} = \frac{1}{36}\cdot(8K_\lambda^2 + 5K_a^2 + K_{\beta,\tau}^2 + 5K_\lambda\cdot K_a - 5K_\lambda\cdot K_{\beta,\tau} - 6K_a\cdot K_{\beta,\tau} - 8n_\lambda - 4n_a + 4n_{\beta,\tau})\cdot(b_0/4a_0)^3\cdot r^6 \qquad (26)$$

Sphere. The temperature field is governed by functions of the type (19), where

$$\vartheta^{0}=(b_0/6a_0)\cdot\tau^2;\quad \Delta\vartheta^{I}=-\frac{1}{10}(2K_\lambda+3K_a-3K_{\beta,\tau})(b_0/6a_0)^2\tau^4;$$

$$\Delta\vartheta^{II}=\frac{1}{210}\cdot(20K_\lambda^2+39K_a^2+9K_{\beta,\tau}^2+30K_\lambda\cdot K_a-30K_\lambda\cdot K_{\beta,\tau}-$$

$$-48K_a\cdot K_{\beta,\tau}-8n_\lambda-30n_a+30n_{\beta,\tau})(b_0/6a_0)^3\cdot\tau^6 \qquad (27)$$

Analytical functions of the second-order regular regime find wide acceptance in methods of determining the thermal diffusivity. In particular, as applied to flat specimens with symmetrical temperature field, a formula for calculating $a(t_0)$ is obtained from (21)

$$a_0=(b_0R^2/2\vartheta_R)(1-\Delta\sigma_a),\ \text{where}\ \Delta\sigma_a=\frac{1}{6}(2K_\lambda+2K_a-K_{\beta,\tau})\vartheta_R^1 \qquad (28)$$

We will show with the example of this formula several additional features of generalized second-order regular regime regularities relating to measurements of a(t) directly after the time delay $\Delta\tau_R$ [1, 4].

Thus, if at moment of time τ_0 the temperature $t(R, \tau_0)$ coincides with the set temperature level t

$$t=t(R,\tau_0)=t_0(\tau_0)+\vartheta_R(\tau_0) \qquad (29)$$

the center of the plate attains the temperature t after the interval of time $\Delta\tau_R(t)$:

$$t=t_0(\tau_0+\Delta\tau_R)=t_0(\tau_0)+b_0(\tau_0)\Delta\tau_R+\frac{1}{2}K_{\beta,\tau}b_0^2(\tau_0)\cdot\Delta\tau_R^2 \qquad (30)$$

From (29) and (30), we have:

$$\vartheta_R(\tau_0)=b_0(\tau_0)\cdot\left[1+\frac{1}{2}\cdot K_{\beta,\tau}\cdot\vartheta_R(\tau_0)\right]\cdot\Delta\tau_R \qquad (31)$$

After substituting (31) for the main member of formula (28) and the conversion from $a(t_0)$ to a(t) by the relationship

$$a(t)=a(t_0)\cdot(1+K_a\cdot\vartheta_R)$$

and also the customary assumptions given (3) and (7), we obtain the sought-for working formula for a(t):

$$a(t)=(R^2/2\Delta\tau_R)\cdot(1-\Delta\sigma_a),\quad \Delta\sigma_a=\frac{1}{3}(K_\lambda-2K_a+K_{\beta,\tau}). \tag{32}$$

In this same way we can obtain working formulas for a(t) in other cases as well:

-- a plate with nonsymmetrical temperature field

$$a(t)=[R^2/(\Delta\tau_R+\Delta\tau_{-R})]\cdot(1-\Delta\sigma_a) \tag{33}$$

where

$$\Delta\sigma_a=\left[\frac{1}{6}\cdot(K_\lambda-2K_a+K_{\beta,\tau})(\Delta\tau_R+\Delta\tau_{-R})+\frac{1}{4}\cdot K_{\beta,\tau}\cdot(\Delta\tau_R-\Delta\tau_{-R})-\right.$$
$$\left.-\frac{1}{8}\cdot(4K_a-K_\lambda)\cdot(\Delta\tau_R-\Delta\tau_{-R})^2/(\Delta\tau_R+\Delta\tau_{-R})\right]\cdot b_0$$

-- cylinder:

$$a(t)=(R^2/4\Delta\tau_R)\cdot(1-\Delta\sigma_a),$$

where (34)

$$\Delta\sigma_a=\frac{1}{4}\cdot(K_\lambda-2K_a+K_{\beta,\tau})b_0\cdot\Delta\tau_R;$$

-- sphere:

$$a(t)=(R^2/6\Delta\tau_R)\cdot(1-\Delta\sigma_a),$$

where (35)

$$\Delta\sigma_a=\frac{1}{5}\cdot(K_\lambda-2K_a+K_{\beta,\tau})\cdot b_0\cdot\Delta\tau_R$$

Example. A test was made of a flat specimen made of polymethylmethacrylate (organic glass) with 2R = 8 mm, for which at 20°C a = $= 1.1\cdot10^{-7}$ m^2/sec, $k_\lambda \approx 1\cdot10^{-3}$ deg^{-1}, $k_a \approx -2.5\cdot10^{-3}$ deg^{-1}. The heating rate $b_0 = 0.2$ deg/sec, and the nonlinearity $k_{b,\tau} = 3\cdot10^{-3}$ deg^{-1}.

From (32) in the null approximation, we have $\Delta\tau_R$ = 73 sec, so that $\Delta\sigma_a$ = 0.044 = 4.4 percent.

Formulas analogous to (32) and (34) have been found earlier for the plate (rod) and the cylinder [1] using another method of solving the problem and have found wide acceptance. Accordingly, it is convenient to direct attention to finding discrepancies between the corrections of formulas (32), (34) and the Krayev formulas. Verification of the Krayev solutions shows that in deriving the formulas he put up with errors. The corrected results agree with (32) and (34).

First-Order Regular Regime

The basic feature of this regime is the existence of the function

$$\theta(r,\tau)=-m\cdot t(r,\tau), \tag{36}$$

where m = const.

However, the inconstancy of the coefficients $\lambda(t)$, $a(t)$, $c\gamma(t)$ and $\alpha(t)$ lead under actual experimental conditions to violation of function (36). For a generalized analysis of the problem, as in previous cases, use can be made of the relationships (2)-(4), adding to these analogous functions for $\alpha(t)$ and $m(r, \tau)$ within the limits of temperature drop $\vartheta(r, \tau)$ in the specimen

$$\alpha=\alpha_0\cdot(1+\kappa_\alpha\cdot\vartheta+n_\alpha\cdot\vartheta^2+\dots); \tag{37}$$

$$m(r,\tau)=m_0\cdot(1+\kappa_{m,r}\cdot\vartheta+n_{m,r}\cdot\vartheta^2+\dots);$$

$$m(0,\tau)=m_0\cdot(1+\kappa_{m,r}\Delta t+n_{m,r}\cdot\Delta t^2+\dots) \tag{38}$$

with the restrictions

$$|\kappa_\alpha\cdot\vartheta|<0{,}1;\quad |\kappa_{m,r}\cdot\vartheta|<0{,}1;\quad |\kappa_{m,\tau}\cdot\vartheta|<0{,}1, \tag{39}$$

$$|n_\alpha\cdot\vartheta^2|<0{,}01;\quad |n_{m,r}\cdot\vartheta^2|<0{,}01;\quad |n_{m,\tau}\cdot\vartheta^2|<0{,}01 \tag{40}$$

The relationships (2)-(4) and (36)-(40) make it possible to solve the thermal conductivity equation (1) by means of the above-used procedure of successive approximations.

We can obtain the following relationships from equations (1) and (39) with account taken of (2)-(4), and from equations (40)-(43), with account similarly taken of (9)-(11), we can obtain the following relationships:

$$K_{m,\tau}=K_{m,\tau}-K_a\,; \qquad K_{\delta,c}=K_{m,\tau}+1/t_o \tag{41}$$

Plate. Equation (1) given the assumptions (2)-(4) and (36)-(40) with precision up to members of the second order of smallness becomes

$$\frac{d^2t}{d\tau^2}=-\nu_o^2 t+\left[\nu_o^2(K_o-K_{m,\tau})\cdot\nu\cdot t-K_\lambda\left(\frac{dt}{d\tau}\right)^2\right] \text{ where } \quad \nu_o^2=m_o/a_o \tag{42}$$

The condition of regularity

$$\delta(r,\tau)=-m_o(\tau)\cdot(1+K_{m,\tau}\cdot\nu)\cdot t(r,\tau) \tag{43}$$

Boundary and initial conditions:

$$\left|\lambda\frac{dt}{dr}+\alpha\cdot t\right|_{r=R}=0;\ \frac{dt(0,\tau)}{dr}=0;\ t(0,\tau)=t_o(\tau);\ t(0,0)=t_H \tag{44}$$

The combined solution of equations (42)-(44) in the null approximation gives the well known function

$$t^\circ(r,\tau)=t_o(\tau)\cdot\cos\nu_o r=t_H\cdot\cos\nu_o r\cdot\exp(-m_o\tau) \tag{45}$$

where

$$\varphi_o\cdot tg\,\varphi_o=Bi_o;\ \varphi_o=\nu_c\cdot R \quad \cup\ Bi_o=\alpha_o\cdot R/\lambda_o$$

An approximational function of the following form can be used in determining the correctional members in (42) in place of function (45):

$$t^{*}(r,\tau)=t_{o}(\tau)\cdot(1-p\cdot r^{2}),\ p\cdot R^{2}=Bi_{o}/(2+Bi_{o}) \tag{46}$$

which satisfies the boundary conditions (44).

After substituting (46) into the correction of equation (42), the latter becomes

$$\frac{d^{4}t}{dr^{2}}+\nu_{o}^{2}\cdot t=-\left[\nu_{o}^{2}(K_{a}-K_{m,r})(1-p\cdot r^{2})\cdot pr^{2}+4p\cdot K_{\lambda}\cdot pr^{2}\right]\cdot t_{o}^{2} \tag{47}$$

Its solution allowing for (43) is

$$\begin{aligned}t(r,\tau)=t_{o}(\tau)\cdot\cos\nu_{o}r+\Big\{\Big[\big[4(K_{\lambda}+3K_{a}-3K_{m,r})\cdot(p/\nu_{o}^{2})+\\+(K_{a}-K_{m,r})\big]\cdot\big[(2p/\nu_{o}^{2})(1-\cos\nu_{o}r)-pr^{2}\big]+\\+(K_{a}-K_{m,r})\cdot p^{2}\cdot r^{4}\Big\}\cdot t_{o}^{2}(\tau)\end{aligned} \tag{48}$$

where for $m_{o}\cdot\tau < 0.2$

$$t_{o}(\tau)=t_{H}\left[1-2K_{m,c}\cdot t_{H}\cdot m_{o}\tau-K_{m,c}\cdot t_{H}(m_{o}\cdot\tau)^{2}\right]\cdot\exp(-m_{o}\cdot\tau) \tag{49}$$

The condition $m_{o}\cdot\tau < 0.2$ in (49) can always be satisfied, since the point at which τ is read off is arbitrary.

The coefficient ν_{o} in function (48) is sought for from the first boundary condition in (44), and values of ν_{o}^{2} in correctional members (48) can be taken from the results of analyzing this condition in the null approximation.

The coefficient $k_{m,r}$ can be found by differentiation with respect to $t_{o}(\tau)$ by deriving from the symbols for (42) and (45) the relationship

$$m_{o}=(\alpha_{o}/c\gamma_{o}R)(q_{o}/tgq_{o}) \tag{50}$$

We have

$$K_{m,r}=2(K_{a}-K_{\lambda})(\sin 2q_{o})/(2q_{o}+\sin 2q_{o}) \tag{51}$$

If the experiment is conducted in the microcalorimeter regime ($Bi_o \to 0$), the relationship (48) yields a function of the form

$$\vartheta = -(m_o t_o/2a_o)\cdot\tau^2\left[1-\frac{1}{6}(2\kappa_\lambda+\kappa_a-\kappa_{m\tau}-1/t)(m_o t_o/2a_o)\cdot\tau^2\right], \qquad (52)$$

which after identity transformations leads wholly to the earlier derived function (21) in its first approximation. When the plate is cooled in the a-calorimeter regime ($Bi_o \to \infty$), the condition $t(R, \tau) = 0$ obtains, and from function (48) with account taken of the symbols for (42)-(46) a generalized formula is derived for calculating the coefficient a(0):

$$a(0) = (4/\pi^2)\cdot R^2 m_o\cdot(1+\Delta\sigma_a) \qquad (53)$$

where

$$\Delta\sigma_a = \frac{2}{5}\cdot(\kappa_\lambda - 2\kappa_a)\cdot t_o$$

Turning to the preceding example where the specimen was made of polymethylmethacrylate, when t_o = 20 degrees, we have $\Delta\sigma a = 0.048 = 4.8$ percent.

Symbols

r = coordinate; τ = time; R = half-thickness of plate or cylinder radius; $t(r, \tau)$ = temperature (read off from the ambient temperature); $t_o(\tau) = t(0,\tau)$ = temperature of central (base) layer in the body: $b = b(r, \tau) = \partial t(r, \tau)/\partial\tau$; $b_o = b_o(\tau) = \partial t_o(\tau)/\partial\tau$; $\vartheta(r, \tau) = t(r, \tau) - t_o(\tau)$; $\vartheta_R = t(R, \tau) - t_o(\tau)$; $\lambda(t)$, $a(t)$, $c\gamma(t)$ = thermophysical coefficients; $\alpha(t)$ = heat transfer coefficient; $\varepsilon(t)$ = coefficient of blackness; $\lambda_o = \lambda(t_o)$, $a_o = a(t_o)$, $c\gamma_o = c\gamma\cdot(t_o)$; $\alpha_o = \alpha(t_o)$, $\varepsilon_o = \varepsilon(t_o)$; m = rate of regular regime; $k_i = \frac{1}{i_o}\cdot\frac{di}{dt}$ = const, $n_i = \frac{1}{2i_o}\cdot\frac{d^2 i}{dt^2}$ = const = relative temperature coefficients for $i = \lambda, a, c\gamma, \alpha, \varepsilon$: and w; $k_{b,r} = \frac{1}{b_o}\cdot\frac{\partial b}{\partial\vartheta}$ = const, $k_{b,\tau} = \frac{1}{b_o}\cdot\frac{\partial b}{\partial t}$ = const = relative temperature coefficients characterizing the inconstancy of the velocity $b(r, \tau)$ for the coordinate and time, respectively:

$\cap_{\beta,\tau} = \frac{1}{2\beta_o} \cdot \frac{\partial^2 \beta}{\partial \vartheta^2}$ = const and $\cap_{\beta,\sigma} = \frac{1}{2\beta_o} \cdot \frac{\partial^2 \beta}{\partial t^2}$ = const; $\Delta t = b_o \cdot \Delta\tau$ = temperature rise $t_o(\tau)$ for the time interval $\Delta\tau(\Delta t \approx \vartheta)$; F = surface; V = volume.

References

1. Krayev, O. A., *Teploenergetika*, Vol. 3, No. 4, 1956; Vol. 4, No. 12, 1957; Vol. 5, No. 4, 1958.

2. Pak, M. I. and V. A. Osipova, *Teploenergetika*, Vol. 14, No. 6, 1967.

3. Kover'yanov, V. A., *TVT*, Vol. 5, No. 1, 1967.

4. Platunov, Ye. S., *Izv. Vuzov SSSR. Proborostroyeniye*, Vol. 4, No. 1, 1961; Vol. 4, No. 4, 1961; Vol. 7, No. 5, 1964.

5. Platunov, Ye. S., *IFZh*, Vol. 9, No. 4, 1965.

6. Platunov, Ye. S., *TVT*, Vol. 2, No. 3, 1963; Vol. 4, No. 1, 1966.

COMPLEX OF INSTRUMENTS FOR MASS THERMOPHYSICAL MEASUREMENTS AT ROOM TEMPERATURE

Ye. S. Platunov, V. V. Kurepin and L. A. Komkova

In recent years, a complex of instruments has been developed in the Leningrad Institute of Precision Mechanics and Optics for determining thermophysical properties of materials at close to room temperature for specimens of small dimensions. Well known regularities of regular cooling of test specimens in a constant-temperature environment were postulated as the operating basis of the instruments [1, 2]. However, the instruments assembled differ appreciably from former models in design features, nature of heat transfer of specimens from environment, and experimental methods. A massive metal jacket served as the thermostated medium in each of these instruments. Treatment of experimental data was conducted without graphic plots, and the rate of regular cooling was determined directly from timer readings and was calculated from the formula:

$$m = \frac{\ln\left(\frac{n_c}{n_k}\right)}{\Delta\tau_{ik}} \qquad (1)$$

The instruments are marked by simplicity of construction and high reliability.

The make-up of each instrument included the following: calorimeter, vertical galvanometer, timer, thermometer for control of ambient temperature, and furnace for specimen heating.

The furnace was made of textolite and was supplied from an approximately 220-v network. The steady-state temperature in the furnace was 5-10° higher than the ambient temperature.

Calorimeter diagrams are shown in Figure 1. The main component of the calorimeters was a massive dismountable jacket of brass, the inner surface of which was chrome-plated and carefully polished to reduce radiative heat transfer. A reliable thermal contact between upper and lower parts of the jacket was ensured by careful grinding of the contact surfaces. Temperature measurements were made by differential thermocouples of 0.2 mm diameter copper and constantan.

The configurations and dimensions of the test specimens are given in Figure 2. Prior to the beginning of the tests, the specimens were heated in the furnace for 10-15 min and then placed in the calorimeter.

The regular c-calorimeter is shown in Figure 1, a. The working arm of the thermocouple was mounted within the central needle, and the cold arm within one of the two guides on which the upper part of the jacket was placed. When solid materials were tested (metals, semiconductors, plastics, etc.) specimens shown in Figure 2 were used. When liquid materials were tested, light-weight, elastic, air-porous materials, powder and fibrous insulation, the test material was placed in a capsule that agreed in shape and external dimensions with the specimen. The capsule was a thin-walled copper shell with an axial metal tubing. Six radial plastic sheets were soldered between the tubing and the shell walls. When the capsule was placed in the calorimeter, the central thermocouple was located within the left tubing. This capsule design afforded a practically uniform temperature field within the specimen ($\Psi = 1$) of any material.

During the experiment, the specimen was heated on the central needle of the calorimeter and cooled through a closed air pocket 3-6 mm thick.

The well known function for the microcalorimeter [2] is valid in the general case for calculating heat capacity:

$$C = \frac{\Psi}{M}\left(\frac{m_3}{m} \cdot M_3 C_3 - C_K\right) \qquad (2)$$

which when expression (1) is taken into account is transformed to:

$$C = \frac{\Psi}{M}(\varphi_{ik} \cdot \Delta\tau_{ik} - C_k) \qquad (3)$$

where $\varphi_{ik} = \frac{C_k \cdot M_2}{\Delta\tau_{ik}}$ instrument constant for the section (n_1-n_k) of the galvanometer scale determined from a calibrated experiment.

When testing materials placed within the capsule, the criterion is $\Psi = 1$, therefore instead of (3), we have:

$$C = \frac{1}{M}(\varphi_{ik} \cdot \Delta\tau_{ik} - C_k) \qquad (4)$$

If, however, solid materials are tested, the working formula becomes:

$$C = \frac{\Psi}{M}\varphi_{ik} \cdot \Delta\tau_{ik} \qquad (5)$$

The criterion Ψ in (5) is calculated from one of the approximational functions:

$$\Psi = 1 - \frac{mR^2}{8a} \qquad \text{or} \qquad \Psi = 1 - \frac{\alpha_1 \cdot R}{4\lambda} \qquad (6)$$

where the values of the coefficients a and λ are here taken in approximate terms.

The instrument constant ϕ_{ik} is determined from an experiment with a metal (copper) specimen, and the constant C_k -- from an experiment with an empty capsule.

In contrast to the well known calorimeter, the instrument constants Φ_{ik} and C_k exhibit high stability, since the heat transfer of the specimen from the medium is achieved only via thermal conductivity of air. Convection is excluded, and the proportion of radiative heat transfer is relatively small.

The regular ac-calorimeter is designed for comprehensive measurement of heat capacity and thermal diffusivity of solid, mechanically processed heat-insulating materials. Heat capacity and thermal diffusivity are measured simultaneously on the same specimen. To determine heat capacity, the same

principle of relative measurements is employed as for the previous c-calorimeter. The thermal diffusivity is determined by an absolute method.

The diagram of the small ac-calorimeter (Figure 1, d) is similar to the diagram of the c-calorimeter, with the only difference that here for the temperature measurements two differential thermocouples are used, the working arms of which are installed in the side and central needles, and the cold arms -- in the guides. During the test the specimen rests on the needles.

Two time intervals $\Delta\tau_{ob}$ and $\Delta\tau_{ik}$ are measured in the experiment.

The heat capacity of the specimen is calculated from formula (5). The criterion ψ can here be precisely calculated based on experimental data obtained in the experiment using formulas (6) transformed to

$$\psi = 1 - \beta_{ik} \frac{R^2}{2R_5^2} \cdot \frac{\Delta\tau_{o5}}{\Delta\tau_{ik}} \tag{7}$$

where

$$\beta_{ik} = \frac{2(n_i - n_k)}{n_i + n_k} \tag{8}$$

The thermal diffusivity coefficient is calculated from the following formula:

$$a = \frac{R_5^2}{\Gamma \cdot \Delta\tau_{o5}} \cdot \left(1 + \frac{1}{4}\beta_{ik} \cdot \frac{\Delta\tau_{o5}}{\Delta\tau_{ik}}\right), \tag{9}$$

where $\Gamma = 4\left(1 + \frac{k_z}{k_r} \cdot \frac{R}{2H}\right)$ is the instrument constant determined analytically. The complex [2, 391] that is part of this expression is small (~ 0.25), therefore the relationship k_z/k_r can be calculated from the following approximate relationship:

$$\frac{K_2}{K_1} = \frac{\delta_1}{\delta_2}\cdot\left(1+4\varepsilon_n\sigma_0 T^3\frac{\delta_2-\delta_1}{\lambda_\delta}\right) \qquad (10)$$

The regular acλ-calorimeter is designed for independent determination of heat capacity, thermal conductivity, and thermal diffusivity of heat-insulating materials and semiconductors. The calorimter diagram is shown in Figure 1, b. The cold arm of the thermocouple is rigidly mounted in the lower part of the jacket, and the hot arm can be shifted in the vertical direction between the upper and lower sections of the jacket. The thermocouple is insulated with lacquer and placed in a chlorovinyl tube to ensure necessary strength.

In determining thermal diffusivity the specimen is placed between contact surfaces of the dismantable jacket.

The time $\Delta\tau_{ik}$ is recorded during the cooling process.

The thermal diffusivity coefficient is determined from a formula similar to the well known formula of the a-calorimeter [1]:

$$a = 0{,}405H^2\frac{\ln\left(\frac{n_i}{n_k}\right)}{\Delta\tau_{ik}}\left(1+\Delta\sigma_k-\Delta\sigma_a\right) \qquad (11)$$

where $\Delta\sigma_k = 2\frac{\lambda P_k}{H}$ is the correction for contact resistance, $\Delta\sigma_a = 2\frac{H^2}{R^2}\cdot\frac{\alpha_r\beta}{\lambda}$ is the correction for lateral heat transfer.

For this instrument α_r can be taken as equal to 10 $w/m^2\cdot deg$, and P_k, when specimens with ground faces (∇7) and liquid lubricant are used, is about $1\cdot10^{-4}$ $m^2\cdot deg/w$. When heat insulators are tested (λ = 0.15-0.4 $w/m\cdot deg$) with specimens 4-6 mm thick, the corrections $\Delta\sigma_k$ and $\Delta\sigma_\alpha$ do not exceed, respectively, 0.06 and 0.036, but when semiconductors are tested (λ = 0.5-0.3 $w/m\cdot deg$) 16-20 mm thick the corrections do not exceed 0.04 and 0.06, respectively.

The method of determining thermal conductivity of materials coincides with the method of the flat symmetrical bicalorimeter [2]. In the tests two identical specimens are used which are placed on both sides of a metal (copper) rod, whose diameter equals the specimen diameter, and whose height

$2H_c$ = 10 mm. The outer surfaces of the specimens are in contact in the experiment with the working planes of the jacket (Figure 1, f).

The time interval $\Delta\tau_{ik}$ is measured directly in the experiment. Thermal conductivity is calculated from the formula:

$$\lambda = \frac{H}{\frac{2\pi R^2}{C_c} \cdot \frac{\Delta\tau_{ik}}{\ln\left(\frac{n_i}{n_k}\right)} \cdot \frac{1}{1+\Delta\sigma_c-\Delta\sigma_\perp} - 2P_k} \qquad (12)$$

where $\Delta\sigma_c = \frac{2}{3C_c} \cdot C \cdot M$ is the correction for heat capacity of specimens, and $\Delta\sigma_\perp = 4\pi \frac{\alpha_r R}{C_c} \cdot \frac{\Delta\tau_{ik}}{\ln\left(\frac{n_i}{n_k}\right)} \cdot (H_c+H)$ is the correction for lateral heat transfer.

The quantities α_r and p_k are close to the values indicated in the preceding case. When 0.5-2-mm-thick heat insulators are tested, the corrections do not exceed the values $\Delta\sigma_c$ = 0.04 and $\Delta\sigma_k$ = 0.015, but when 2-4-mm-thick semiconductors are tested, the corrections are not greater than the values $\Delta\sigma_c$ = 0.15 and $\Delta\sigma_k$ = 0.004.

Specific heats are determined according to the above-indicated principle.

A metal plate with three vertical capron pins (Figure 1, e). The specimen is placed on the pins. The metal blocks of the calorimeter are shifted 10 mm, which is kept constant by means of two hatches in calibration and working experiments. The quantity c is calculated from formula (5). The criterion ψ in this case is found from the expression:

$$\psi = 1 - \frac{1}{3}\alpha_z \cdot \frac{H}{\lambda}, \qquad (13)$$

where for this instrument α_z can be taken as equal to 6 $w/m^2 \cdot deg$.

The regular ac-calorimeter for metals is designed for comprehensive measurement of heat capacity and thermal diffusivity of metals (Figure 1, c). When heat capacity is determined, the principle of comparative measurements is employed, but thermal diffusivity is determined by an absolute method.

Two differential thermocouples are used in the instrument, and their working arms can be shifted vertically, while the cold arms are rigidly mounted in the jacket. During the experiment, the specimen is placed within the calorimeter on a heat-insulating insert cemented to the base with the thermal resistance $P = 1.3 \cdot 10^{-3}$ $m^2 \cdot deg/w$. The working thermocouple arms are placed in specimen apertures. The time lag $\Delta\tau_{oh}$ and the time $\Delta\tau_{ik}$ are measured successively during the cooling process with the upper thermocouple connected.

Heat capacity is calculated from the formula:

$$c = \varphi_{ck} \frac{\Delta\tau_{ik}}{M} \left(1 - \frac{2}{3}\beta_{ck} \frac{H^2}{h^2} \cdot \frac{\Delta\tau_{oh}}{\Delta\tau_{ck}}\right), \qquad (14)$$

and thermal diffusivity is found from the relationship:

$$a = \frac{h^2}{2\Delta\tau_{oh}} \cdot \frac{1}{1 - \frac{1}{2}\beta_{ck} \cdot \frac{\Delta\tau_{oh}}{\Delta\tau_{ck}} + \frac{\alpha_2}{\lambda R} \frac{h^2}{\beta_{ck}} \cdot \frac{\Delta\tau_{ik}}{\Delta\tau_{oh}}} \qquad (15)$$

β_{ck} is determined from (8).

Verification of instrument precision is conducted on materials with known thermal characteristics (water, fused quartz, polymethylmethacrylate, and brass L62).

The error values obtained are shown in Figure 2.

Symbols

a = coefficient of thermal diffusivity of the specimen; c = specific heat of specimen; λ = coefficient of thermal conductivity of specimen; M and M_a = mass of specimen and of reference standard for calibrating c-calorimeter; c_k, c_c and C_B = overall heat capacity of capsule, copper rod for acλ-calorimeter, and reference standard for calibrating the c-calorimeter; m and $m_э$ = rate of regular cooling in working and calibrating experiments; n_i and n_k = established galvanometer scale divisions; $\Delta\tau_{ik}$ = time of swing of "light spot" of galvanometer between the divisions n_i and n_k; $\Delta\tau_{ob}$ and τ_{oh} = time delay of central thermocouple signal with respect to the lateral

thermocouple signal, and time lag of the lower thermocouple signal with respect to the upper thermocouple signal; R and R_b = radius of specimen and place of attachment of lateral thermocouple; 2H and $2H_c$ = height of specimen and of metal rod; α_r and α_z = heat transfer coefficients from lateral surface and specimen face, respectively; k_z - and k_r = effective coefficients of heat transfer through face and lateral air layer; σ_o = Stefan-Boltzmann constant; ϵ_n = reduced degree of blackness; T = ambient temperature, °K; P_k = contact resistance; λ_b = thermal conductivity coefficient of air.

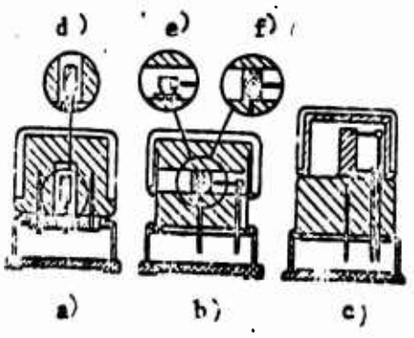

Figure 1. Instrument diagrams: a, c-calorimeter; b, a-calorimeter; c, ac-calorimeter; d, ac-calorimeter; e, c-calorimeter; e, λ-calorimeter

Instrument type	Parameter measured	Measurement error	Specimen shape and dimensions
C-calorimeter RK-C-20	c-solid materials	± 1%	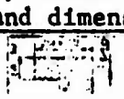
	c-friable, liquid, and fibrous materials	± 3%	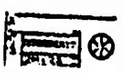
ac-calorimeter RK-ac-20	a c	± 10% ± 3%	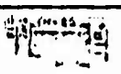
acλ-calorimeter RK-acλ-20	a cλ	± 3%	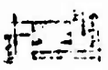
ac-calorimeter for metals RK-III-20	ac	±3%	

Figure 2. Recommended specimen dimensions and measurement errors.

References

1. Kondrat'yev, G. M., *Regulyarnyy Teplovoy Reshim*, [Regular Thermal Regime], GITTL Press, Moscow, 1954.

2. Kondrat'yev, G. M., *Teplovyye Izmereniya*, [Thermal Measurements], Mashgiz Press, Moscow-Leningrad, 1957.

THERMODYNAMIC STUDY OF GASES AND LIQUIDS BY ACOUSTICAL METHODS

A. N. Solov'yev and Ye. P. Sheludyakov

Thermodynamic studies of gases and liquids by acoustical methods have lately found considerably greater acceptance owing to high precision and relative simplicity of these methods. Acoustical methods can be used in a great many cases to obtain information inaccessible by other methods, and also to raise precision of results or to considerably simplify experiments and calculations. To be specific, experimental data on the velocity of sound can be used in plotting entropy diagrams and in calculating specific heat ratios c_p / c_v; data on the velocity of sound can be used to calculate such properties as bulk concentrations of binary molecules in vapors of monatomic metals, the Joule-Thomson coefficient, the heat capacity c_v of water-laden vapor, etc. Study of ultrasonic dispersion affords determination of a whole series of intramolecular parameters, such as heat capacity of vibrational degrees of freedom of molecules, relaxation time, and other quantities.

This study presents results of experimental and theoretical studies conducted by the authors in this area, where the focus of attention was given to studying freons. A low-frequency acoustic apparatus was devised (Figure 1) to secure thermodynamic, that is, frequency-independent, values of the velocity of sound in vapor. The main assembly of the device is a resonator, consisting of a tube 550 mm long and 40 mm in diameter. Sound waves in the resonator are produced with the aid of an electromagnetic radiator; a microphone is used to fix the standing wave in the resonator. Measurements on the apparatus were conducted as follows. By altering the frequency of the acoustic generator transmitting vibrations at the radiator, 10-15 maxima were observed on the oscillograph, each of which corresponded to a standing wound wave. The first maxima corresponded to the half-wavelength, the second to the whole wave, etc. The velocity of sound was determined from

the formula

$$c = \frac{2Lf}{n}.$$

The device makes it possible to study frequencies from 1 to 3 KHz in aggressive media in a wide pressure range 0-05 - 170 bar and a temperature range -50 to +400°C. Studies of the velocity of sound in saturated vapors of water, mercury and several organic compounds were conducted on the apparatus.

Analysis of these, and also several other results, afforded a number of regularities. In particular, Figure 2 presents experimental values of the velocity of sound for water, carbon dioxide, mercury and calculated values for potassium. This same graph gives discontinuity values of the thermodynamic velocity of sound or, which is tantamount to the same thing, the discontinuity of the derivative $\sqrt{(dp/d\rho)_s}$ for these same compounds. The figure makes clear that the discontinuity value of the thermodynamic velocity of sound differs for different substances.

Analysis of the temperature dependence shows that when the temperature rises from the boiling point, the discontinuity of the thermodynamic velocity of sound initially is reduced, reaches a minimum, and then begins to rise, while the velocity of sound, in contrast, initially rises, reaches a maximum, and then begins to decrease; it was also shown that the drop in velocity of sound corresponds to an increase in the discontinuity, and a rise in velocity of sound to a decrease of the discontinuity. From the foregoing we can conclude that the maximum of the velocity of sound coincides with the minimum of the discontinuity of the thermodynamic velocity of sound.

An ultrasonic interferometer (Figure 3) was assembled to investigate the velocity of sound both in liquids, as well as in gases, and also in the critical region. The instrument makes it possible also to investigate the dispersion of ultrasound. The device was built as follows. A radiator and an ultrasonic receiver were secured onto support stands. The receiver was fixed, but the radiator could be shifted vertically by means of a micrometric screw. The electrical signals from the generator amplified by the resonance

amplifier was passed on to the ultrasound radiator, where it was transformed into acoustic signal, passed through the medium under study, and picked up by the ultrasound receiver. The received acoustic signal was again transformed into an electrical signal, amplified by the resonance amplifier, and passed on through the detector to an electronic self-recording potentiometer. The signal frequency was controlled by a heterodyne wave meter. During the period of travel between the radiator and the ultrasound receiver an integral number of semiwaves was periodically induced; the voltage was varied at the receiver. This change was recorded and from this recording the velocity of ultrasound was determined from the formula $c = \lambda f$. Measurements of the velocity of sound (at a frequency of 220 Khz) were made on this apparatus in freons F-11, F-12, and F-142 in liquid and vapor phases at the saturation line (Figure 4). Studies were also made of dispersion in freon F-21 at frequency of 220 KHz and 2100 KHz. Figure 5 presents the dispersion curve at a temperature of 82°C, making it possible to calculate such intramolecular parameters as heat capacity of the vibrational degrees of freedom, relaxation time, etc. Along with experimental study of thermodynamic properties, several calculational methods were developed by acoustic approaches.

Calculation of the velocity of sound and the heat capacity ratio $c_p - c_v$ in saturated vapors of liquids with low discontinuity value of the derivative

$$(\partial p/\partial P)_s$$

To obtain a working formula, we will write an expression for the velocity of sound as one approaches the saturation curve from the side of the single-phase region

$$c^{**} = \sqrt{-gv''^2(\partial p/\partial v)_s} \qquad (1)$$

or allowing for

$$\left(\frac{\partial p}{\partial v}\right)_s = \frac{c_p''}{c_v''}\left(\frac{\partial p}{\partial v}\right)_T \qquad (2)$$

$$c^{o.\varphi} = \sqrt{-g v''^2 \frac{c_p''}{c_v''}\left(\frac{\partial p}{\partial v}\right)_T}$$

The velocity of sound in saturated vapor as one approaches from the region of two-phase states is described by the formula [1]

$$c^{g.\varphi} = v'' \frac{dp}{dT}\sqrt{\frac{gT}{c_v^{g.\varphi}}} \qquad (3)$$

In these equations the index " refers to saturated vapor, and the index "m-p" and "t-p" denote approach, respectively, from the monophase and the two-phase region.

We will write an expression for the discontinuity of the velocity of sound as

$$\Delta c = c^{o.\varphi} - c^{g.\varphi} = \sqrt{-g v''^2 \frac{c_p''}{c_v''}\left(\frac{\partial p}{\partial v}\right)_T} - v'' \frac{dp}{dT}\sqrt{\frac{gT}{c_v^{g.\varphi}}} \qquad (4)$$

Let

$$c_v^{g.\varphi} = c_v^{o.\varphi} + \Delta c_v''$$

As a rule, at a great distance from the critical point $c_v^{g.\varphi} \gg c_v^{o.\varphi}$ and then

$$c_v^{g.\varphi} \approx \Delta c_v''$$

Therefore

$$\Delta c = \sqrt{-g v''^2 \frac{c_p''}{c_v''}\left(\frac{\partial p}{\partial v}\right)_T} - v'' \frac{dp}{dT}\sqrt{\frac{\partial T}{\Delta c_v''}}$$

Using the formula for the discontinuity of heat capacity [2]

$$\Delta c_v'' = -T\left(\frac{\partial p}{\partial v}\right)_T''\left(\frac{dv''}{dT}\right)^2$$

after uncomplicated transformation we can write (3) as

$$\Delta c = c^{0.\Phi} + \frac{g v''^2 \frac{dp}{dv}\sqrt{\frac{c_p}{c_v}}}{c^{0.\Phi}} \qquad (5)$$

or for the relative discontinuity value

$$\frac{\Delta c}{c^{0.\Phi}} = 1 + \frac{g v''^2 \frac{dp}{dv}\sqrt{\frac{c_p}{c_v}}}{(c^{0.\Phi})^2} \qquad (6)$$

If $\Delta c \ll c$, formula (5) can be reduced to

$$c = \sqrt{-g v''^2 \frac{dp}{dv}\sqrt{\frac{c_p}{c_v}}} \qquad (7)$$

In equation (7) all quantities relate to saturated vapor as we approach from the side of the monophase region. Therefore, the indices m-p and t-p are omitted. Comparing (7) with (2), we find that

$$\frac{c_p}{c_v} = \frac{\left(\frac{dp}{dv}\right)^2}{\left(\frac{\partial p}{\partial v}\right)_T} \qquad (8)$$

It is necessary to know calorimetric and thermal quantities only along the saturation line in calculating the velocity of sound from formula (7). Additionally, since c_p/c_v in this formula has a very small effect, this ratio can be taken from preliminary evaluations without appreciable reduction of precision. Calculation of the velocity of sound from the Laplace formula (1, 2) requires, in addition, the availability of thermodynamic data even in superheated vapor close to the saturation line. The velocity of sound in

saturated vapor of benzene and of carbon tetrachloride (Figure 6) was calculated from equation (7). The greatest discrepancy from experimental data did not exceed 1.5 percent, and this discrepancy was evidently due to imprecision of starting data in the calculation. Experimental study of the velocity of sound in freon vapor using the ultrasonic interferometer made it possible to verify formula (7) for this class of compounds as well (cf. Figure 4). The deviation in this case did not exceed 1 percent. The formula derived (8) can be used in calculating the heat capacity ratio c_p/c_v in saturated vapor.

Calculation of Several Thermodynamic Properties Based on the Relationship Between Velocity of Sound and the Differential Joule-Thomson Effect

As we know, the differential Joule-Thomson effect amounts to

$$\alpha = -\frac{T\left(\frac{\partial P}{\partial T}\right)_v + v\left(\frac{\partial P}{\partial v}\right)_T}{c_v\left(\frac{\partial P}{\partial v}\right)_T - T\left(\frac{\partial P}{\partial T}\right)_v} \tag{9}$$

In order to relate the differential Joule-Thomson effect with the velocity of sound, we will use the well known thermodynamic formulas:

$$c_p - c_v = -\frac{T\left(\frac{\partial P}{\partial T}\right)_v^2}{\left(\frac{\partial P}{\partial v}\right)_T}; \tag{10}$$

$$c^2 = -gv^2\frac{c_p}{c_v}\left(\frac{\partial P}{\partial v}\right)_T \tag{11}$$

Substituting in (9) the values of the derivatives from (10) and (11), after uncomplicated transformations we obtain

$$\alpha = \frac{v}{c}\sqrt{g\left(\frac{1}{c_v} - \frac{1}{c_p}\right)T} - \frac{v}{c_p} \tag{12}$$

We can obtain a simple formula for the velocity of sound from the inversion curve $\alpha = 0$ and from (12)

$$C = \sqrt{gT\frac{c_p}{c_v}(c_p - c_v)} \qquad (13)$$

By comparing this formula with the Laplace equation (11) it is clear that only calorimetric parameters are part of it, while formula (11) still includes thermal parameters and, in particular, the derivative $(\partial P/\partial v)_T$. Therefore formula (13) must be more precise than formula (11). Using equation (13) we calculated the velocity of sound on the inversion curve for carbon dioxide in the temperature range 619-1000°C and the pressure range 92-600 bar (Table 1). This same table lists the velocity of sound at 1000°C from the data in [3]. These values agree with each other to a precision of up to 0.2 percent. Formula (12) can be used in calculating the differential Joule-Thomson effect. Additionally, by using equation (12) we can derive a formula for calculating the heat capacity c_v of moisture-laden vapor. Taking into account that in the two-phase state region

$$d = \frac{dT}{dp} = \frac{T(v'' - v')}{r}, \quad c_p = \infty$$

we obtain

$$c_v = \frac{g(rx)^2}{c_x^2 T} \qquad (14)$$

An equation of this type applicable to the critical point has been obtained previously by various methods first by I. I. Novikov [4], and then by V. V. Sychev [1]. Let us express the velocity of sound in moisture-laden vapor c_x as the velocity of sound in saturated vapor. For this we will use the following formula [4]:

$$c_x = \sqrt{\frac{gPv''x}{1 - \frac{Pv'x}{r}\left[2 - \frac{T}{rx}\left(c'_p + x\frac{dr}{dT}\right)\right]}} \qquad (15)$$

For dry saturated vapor, x = 1 and (15) can be written as

$$c''=\sqrt{\frac{gpv''}{1-\frac{pv'}{\tau}\left[2-\frac{T}{\tau}\left(c'_p+\frac{d\tau}{dT}\right)\right]}} \tag{16}$$

Let us take the ratio of velocities of sound in saturated and moisture-laden vapor

$$\frac{c''^2}{c_x^2}=\frac{gpv''}{1-\frac{pv''}{\tau}\left[2-\frac{T}{\tau}\left(c'_p+\frac{d\tau}{dT}\right)\right]}:\frac{gpv''x}{1-\frac{pv''x}{\tau}\left[2-\frac{T}{\tau x}\left(c'_p+x\frac{d\tau}{dT}\right)\right]}$$

From this point, after uncomplicated transformations, bearing in mind that far removed from the critical point $c''_p = c'_p + dr/dT$, we obtain

$$c_x=c''\sqrt{x\frac{1-\frac{pv}{\tau}\left(2-\frac{c''_pT}{\tau}\right)}{1-\frac{pvx}{\tau}\left[2-\frac{Tc''_p}{\tau x}-(1-x)\frac{d\tau}{dT}\right]}} \tag{17}$$

or, bearing in mind that in equation (17) the relationship

$$\frac{1-\frac{pv}{\tau}\left(2-\frac{c''_pT}{\tau}\right)}{1-\frac{pvx}{\tau}\left[2-\frac{Tc''_p}{\tau x}-(1-x)\frac{d\tau}{dT}\right.}$$

where x, close to 1, is also extremely close to 1 [sic -- Tr.], we can write

$$c_x=c''\sqrt{x} \tag{18}$$

Table 1. Velocity of Sound on the Inversion Curve of CO_2

t, °C	669	700	800	900	1000
P, bar	600	556	407	253	92
C, m/sec according to for. (13)	570	567	556	546	542
C, m/sec as /3/	—	—	—	—	543

Table 2. Heat Capacity c_v of Moisture-Laden Vapor of Freon-21

t, °C	c_v, kJ/kg·deg			
	x = 1	x = 0,9	x = 0,8	x = 0,7
- 30	12,788	11,537	10,243	8,983
- 20	11,424	10,268	9,121	8,159
- 10	10,214	9,318	8,397	7,221
0	9,239	8,305	7,388	6,459
10	8,259	7,409	6,568	5,735
20	7,451	6,698	5,936	5,203
30	6,756	6,078	5,396	4,713

Equation (14) is valid at temperatures that are not too close to the critical, and also for very dry states. To verify equation (14), we calculated the heat capacity c_v of saturated water vapor at temperatures from 0 to 200°C. Comparison with known data in [2] shows that the maximum deviation does not exceed 1 percent. So, formula (14) was used in calculating the heat capacity c_v in water-laden freon-21 vapor (Table 2).

Symbols

c_p = heat capacity at constant pressure; c_v = heat capacity at constant volume; c = velocity of sound; c_x = velocity of sound in moist vapor; f = frequency, Hz; n = number of half-waves; P = pressure; ρ = density; S = entropy; λ = wavelength; v = specific volume; T = temperature;

α = Joule-Thomson coefficient; r = heat of vaporization; x = extent of dryness; L = distance between radiator and acoustic receiver.

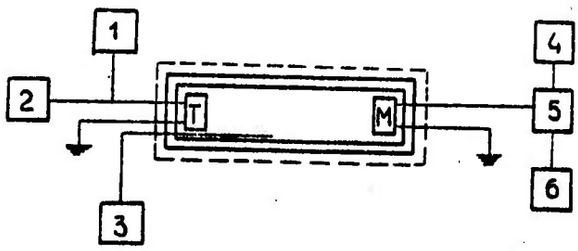

Figure 1. Block diagram of low-frequency device: 1, Audiofrequency oscillator type ZG-14; 2, Type ChZ-4 frequency meter; 3, Temperature measurement circuit; 4, Oscilloscope; 5, Amplifier; 6, Amplifier power supply

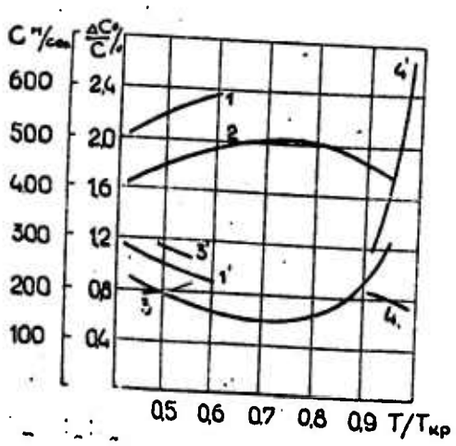

Figure 2. Speed of sound and jump in thermodynamic speed of sound in saturated vapors: 1, and 1', Speed of sound and jump of thermodynamic speed of sound in saturated potassium vapors; 2 and 2', Mercury vapors; 3 and 3', Water vapor; 4 and 4', Carbon dioxide vapor

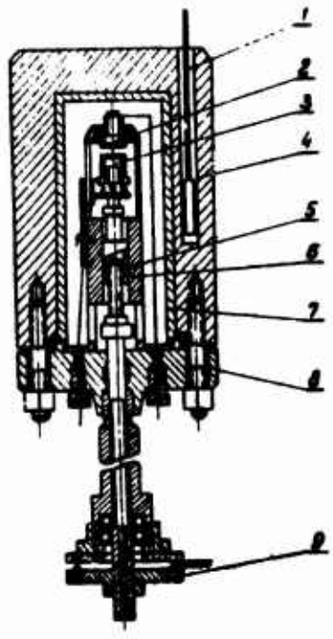

Figure 3. Ultrasonic interferometer: 1, Resistance thermometer; 2, Ultrasonic receiver; 3, Ultrasonic radiator; 4, Copper autoclave; 5, Micrometer screw; 6, Micrometer nut; 7, Stainless steel collar; 8, Autoclave cover; 9, Contact disk

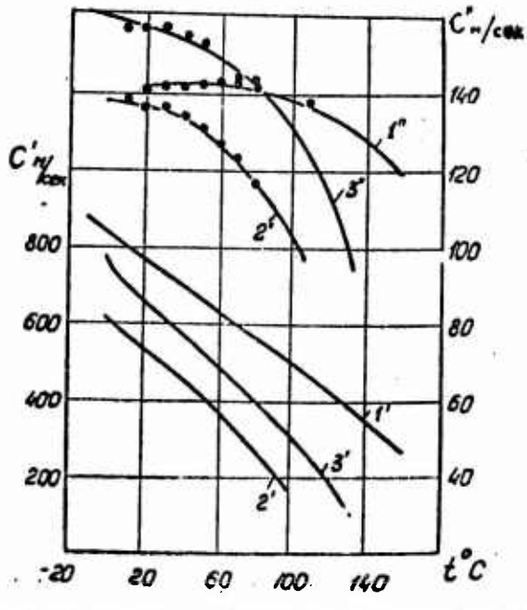

Figure 4. Speed of sound in freon at saturation line: 1', 2', 3', In liquid phase of F-11, F-12 and F-142; 1", 2", 3", In saturated vapors of F-11, F-12 and F-142

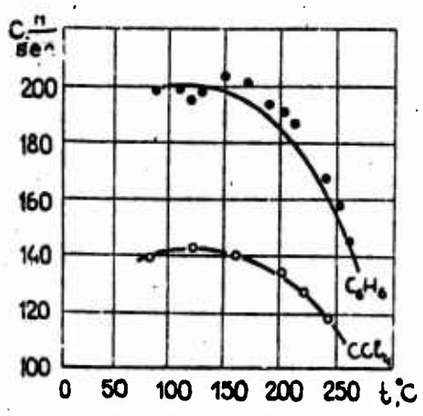

Figure 5. Dispersion curve

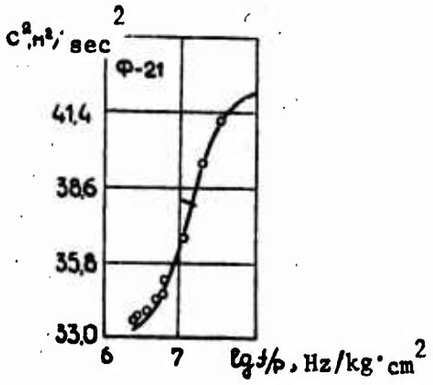

Figure 6. Velocity of sound in saturated vapors of benzene and carbon tetrachloride as a function of temperature

References

1. Sychev, V. V., *PMTF*, No. 6, 1961.

2. Sychev, V. V., *IFZh*, No. 7, 1960.

3. Vargaftik, N. B., *Spravochnik po Teplofizicheskim Svoystvam Gazov i Zhidkostey*, [Handbook on Thermophysical Properties of Gases and Liquids], Fizmatgiz Press, Moscow, 1963.

4. Novikov, I. I., *DAN SSSR*, Vol. 59, p. 1425, 1948.

AUTOMATED INSTRUMENT FOR DETERMINING THERMOPHYSICAL CHARACTERISTICS OF MATERIALS THAT ARE POOR HEAT CONDUCTORS

B. V. Spektor

Each thermophysical characteristic of a material when calculated from experimental data, independently of the method of determination, is a function of several variable quantities characterizing the thermal flux, temperature field of the specimen, and time.

If thermophysical characteristics are determined under conditions when all, except one, quantities entering into the calculation are constants, the sought-for thermophysical characteristic will be a function only of one variable. In this case, the instrument scale used in measuring this quantity can be graduated in units of the sought-for thermophysical characteristic.

This is the basic scheme for automating the determination of thermophysical characteristics of materials used in the instruments described below for determination of coefficients of thermal conductivity, thermal diffusivity and thermal activity.

The following tasks were solved in developing the automated instruments: choice of a method for determining the sought-for thermophysical characteristic and quantities entering into the working formula for which constants had to be adopted; choice of constants of these quantities insuring compliance with boundary conditions corresponding to the method of determination and the necessary temperature field in the test material specimen; automatic maintenance of constancy of selected values of quantities entering into the working formula, and automatic measurement of the variable characteristic.

In determining the thermal conductivity coefficient, the well known method of linear pulsating heater suitable for study both of dry and moist materials was selected. The working formula for calculating the coefficient

of thermal conductivity in measuring temperature at the heater itself is of the form:

$$\lambda = \frac{Q}{4\pi \Delta t} \ln \frac{\tau_1}{\tau_1 - \tau} \qquad (1)$$

The regular regime method was chosen for determining the coefficient of thermal diffusivity. The calculation was made according to the formula:

$$a = K \frac{\ln \Delta t_1 - \ln \Delta t_2}{\Delta \tau} \qquad (2)$$

In determining the coefficient of thermal activity, use was made of the solution of the problem of temperature distribution in an unbounded medium when there is present within the medium a flat heat source whose thickness approaches zero. The formula for calculating the coefficient of thermal activity when measuring the temperature at the heater is of the form:

$$\frac{\lambda}{\sqrt{a}} = \frac{1}{\Delta t} \cdot \frac{Q}{\sqrt{\pi}} \left(\sqrt{\tau_2} - \sqrt{\tau_2 - \tau} \right) \qquad (3)$$

Consideration of the quantities entering into expressions (1)-(3) shows that the quantities most suitable for automatic measurement include Δt as change in heater temperature in expressions (1) and (3), and Δt_2 as the difference between specimen temperature and thermostat liquid temperature in expression (2).

Expressions (1) and (3) are realistic when the heater is placed in an infinite medium. We will regard the condition of infinity of medium as met if change in surface temperature of the specimen, parallel to the heater, does not exceed 0.001° during the experiment.

For averaged values of thermophysical characteristics of nonhomogeneous materials, it is customarily assumed that during the experiment the specimen must be heated at a distance 1.5 cm from the heater for not less than 0.1°.

Based on these considerations, the dimensions of the test material, the size of thermal flux, duration of heating, and measurement time were selected.

Choice of the values for the constants in expression (2) were made by starting from the condition of attainment of the regular heat transfer regime with desired precision upon cooling of specimens of given form and dimension to a temperature Δt_1 °C higher than the temperature of water in the thermostat.

The following instruments were built and operated: the TP-5-66 type for determining the coefficient of thermal conductivity of construction and heat-insulation material, the TP-2-61 type for determining the thermal diffusivity coefficient of the same materials, and the TP-4-65 type for determining the coefficients of thermal conductivity, thermal diffusivity and thermal activity of nonmetallic materials.

The TP-5-66 instrument has a measurement limit 0.03-1.5 w/m·deg, divided into two subranges. The regime under which measurements were made was as follows: τ = 60 sec, τ_1 = 117.2 sec, heating current for measurements in the first subrange I_1 = 0.31 amperes, and in the second subrange I_2 = 0.8 amperes.

A specimen of material for measurements on the TP-5-66 instrument consisted of two plates 10 × 10 cm or 15 × 15 cm in size, and 5 cm thick. The heater was made of manganin wire 0.12 mm in diameter. A resistant thermocouple made of copper wire 0.03-0.04 mm in diameter wound around the central part of the heater was used as a temperature transducer.

Regulation of the heating current, switching it on and off, reading of time, and measurement of the quantity Δt was carried out automatically by the instrument.

The duration of a single measurement was 2 min. The time required to prepare for measurement, which consisted of placing the heater in the specimen and waiting for temperature equalizing throughout the bulk of the specimen and warming up of the electronic amplifier, was about 30 min.

In making the measurements it was necessary after carrying out preparatory operations to place the instrument needle at the null segment by rotating the rheostat knob and then to flick the start switch. The results

of measurements in w/m·deg was indicated by the needle on the instrument scale.

The maximum possible relative error of measurement when the temperature in the room was in the limits 15-25° was 7.6 percent, and when the temperature was 10-30° -- 9.7 percent.

The TP-5-66 type instrument can be assembled on the basis of an electronic automatic bridge or an EMD or EPD type potentiometer.

The TP-2-61 instrument has a measurement limit of from $0.15 \cdot 10^{-7}$ to $25 \cdot 10^{-7}$ m^2/sec. The regime under which measurements are made for a specimen 5 × 5 × 10 cm in size is as follows: temperature of heated specimen 70°, temperature of thermostated liquid 20°, $\Delta t_1 = 10°$, $\Delta\tau = 3$ and 7 min.

To conduct the measurement, the heated spceimen with the temperature transducer is placed in a thermostat containing strongly mixed water and the temperature transducer is connected to the instrument with the current turned on. The results of the determination in m^2/sec is indicated by an instrument scale dial. The duration of the measurement is 10 min. The maximum possible relative error of measurement is 8 percent.

The TP-2-61 instrument is constructed on the basis of the EPV-01 type instrument. Two rotating potentiometer scales afford two readings of the thermal diffusivity coefficient and thus afford checking of the determination.

The TP-4-65 instrument has the following measurement limits: for λ, from 0.03 to 3.0 w/m·deg, divided into two ranges, a from $0.06 \cdot 10^{-7}$ to $18 \cdot 10^{-7}$ m^2/sec, $\lambda/\sqrt{a}$, from 0.17 to 17 $w \cdot sec^{1/2}/m^2 \cdot deg$, divided into two ranges.

The regime under which the measurements are made is as follows: $\tau = 60$ sec, $\tau_1 = 150$ sec, $\tau_2 = 270$ sec, $I_1 = 0.254$, and $I_2 = 0.8$.

The specimen for determination of the thermal conductivity coefficient and the thermal activity consists of two plates that are 10 × 10 × 5 cm in size, and for determination of the coefficient of thermal diffusivity -- a rectilinear prism 5 × 5 × 10 cm in size.

The heater for determination of thermal conductivity is the same as in the TP-5-66 instrument, and for determination of thermal activity it is flat and made of 0.15-mm-diameter manganin wire; the temperature transducer made of 0.03-mm-diameter copper wire is placed in the center of the heater in an area 2 × 2 cm in size.

Determination of the coefficient of thermal conductivity and thermal diffusivity is carried out in the same way as with the TP-5-66 and TP-2-61 instruments. Determination of the coefficient of thermal activity is made just as determination of the coefficient of thermal conductivity, and the time of a single measurement, including preparatory operations, is 30 min; the maximum possible relative measurement error is 10 percent.

Symbols

λ = coefficient of thermal conductivity; a = coefficient of thermal diffusivity; $\lambda/\sqrt{a}$ = coefficient of thermal activity; k = shape factor; Q = heater power; τ, τ_1, τ_2 = time; $\Delta\tau$ = time interval between two measurements; Δt = change of heater temperature; Δt_1 and Δt_2 = difference between temperature of specimen and that of a thermostated liquid.

NONDESTRUCTIVE METHOD OF DETERMINING THERMOPHYSICAL PARAMETERS OF SHEET AND FILM MATERIAL

A. G. Temkin, I. V. Balter and Ya. F. Bazhbauer

Rapid progress in industrial production and the wide use of sheet and film materials (metal and polymer films, vacuum-metallized thin-film compositions, oxide, lacquer-paint, and ceramic coatings, etc.) have stimulated balanced research of their thermal properties.

However, existing methods of determining thermophysical characteristics of film materials [1-9], in spite of their diversity and multiplicity, are not always applicable. This is first of all due to the difficulty of placing the temperature transducer on the surface or in the film itself. In the first case the "roughness" and "nonplanarity" of the surfaces in contact are sharply increased, that is, conditions of ideal thermal contact are violated and the transducer essentially measures the temperature of the contact zone [10, 11]. However, embedding the transducer into the surface of the film studied [5, 7] introduces distortion in the temperature field, as a result of which the intrinsic transducer temperature more or less sharply differs from the temperature of the surface at a sufficient distance from the transducer [12, 13]. In this case the correct evaluation of the thermal flux value along the transducer wires is made difficult. In the second case the film structure is violated, and for most films it is difficult to indicate the coordinate of the temperature transducer, since deformation of the film in the heating process is a substantial function of temperature [14].

In addition it is known that heat transfer parameters of polymeric materials, oxide films and the like depend heavily on temperature [9, 15]. However, the methods proposed for determining λ and c do not make it possible to discover this relationship.

For these reasons it is worthwhile describing a method of comprehensive determination of heat transfer parameters that does not involve violation of the integrity of film materials.

The proposed device consists of two plates (subsequently we will call these etalons in the text), between the end surfaces of which the test material is placed. Heat is conducted to the end surface of one etalon: the law of change of thermal flux supplied with time can be any differentiable function of time.

We must especially emphasize that the etalon need not necessarily be selected from materials with verified and precise λ and c data. If thermophysical parameters of the etalon materials are not known, reconstruction of the hermal field [18] is carried out in two stages.

In the first stage λ and c are determined from the readings of three thermotransducers embedded in the etalon [18, 19]. In the second stage the temperature field is reconstructed [16-19].

If, however, the λ and c of the etalons are known in advance, the latter can serve as experimental quality control (embedding of temperature transducers, surface finish and nonplanarity of surfaces in contact, etc.). Additionally, the etalons can be made of different materials (the steel Kh18N9T and the copper M-3, the steel Yal9T and the aluminum D-3, etc.), which in several cases makes it possible to more readily discover the difference in thermal fluxes at the surfaces of the test film.

1. Reconstruction of the Etalon Temperature Field

When the etalon temperature fields are reconstructed, three local systems of coordinates are used (Figure 1).

For the left etalon

$$N_1=(x-x_{11})/(x_{21}-x_{11}),\quad x_0\leqslant x\leqslant x_1 \tag{1.1}$$

for the right etalon

$$N_2=(x-x_{12})/(x_{22}-x_{12}),\quad x_2\leqslant x\leqslant x_3, \tag{1.2}$$

for the film

$$\xi=(x-x_1)/(x_2-x_1),\quad x_1\leqslant x\leqslant x_2 \tag{1.3}$$

x_{11} and x_{21} are coordinates of left specimen temperature transducers. x_{12} and x_{22} are coordinates of right specimen temperature transducers. It is obvious that

$$N_{11}=(x_1-x_{11})/(x_{21}-x_{11})>1$$

corresponds to $\xi = 0$ and

$$N_{22}=(x_2-x_{12})/(x_{22}-x_{12})<0$$

corresponds to $\xi = 1$.

In the case of an asymmetrical field the temperature at any point of the etalon can be represented in the form of a series expanded with respect to derivatives of the temperatures measured and radial polynomials [16-19]:

$$t(N_i,\tau)=\sum_{n=0}^{m}\left[t^{(n)}(0,\tau)\cdot P_n(N_i,0)+\sum_{i=1,2}t^{(n)}(1,\tau)\cdot P_n(N_i,1)\right](b_0^{2n-1})^n \tag{1.4}$$

where

$$P_n(N_i,\mu)\,[\mu=0,1;\quad i=1,2]$$

are radial polynomials governed by the recurrent relationship

$$P_n(N_i,\mu)=\int_0^{N_i}dN_i\int_0^{N_i}P_{n-1}(\eta,\mu)\,d\eta-N_i\int_0^{1}dN_i\sum_{i=1,2}\int_0^{N_i}P_{n-1}(\eta,\mu)\,d\eta. \tag{1.5}$$

Radial polynomials associated with the first etalon reference point $\mu = 0$, $i = 1.2$:

$$P_0(N_i,0) = -N_i + 1$$
$$P_1(N_i,0) = -\frac{N_i^3}{6} + \frac{N_i^2}{2} - \frac{N_i}{3}$$
$$P_2(N_i,0) = -\frac{N_i^{21}}{120} + \frac{N_i^4}{24} - \frac{N_i^3}{18} + \frac{N_i}{45} \qquad (1.6)$$
$$P_3(N_i,0) = -\frac{N_i^7}{5040} + \frac{N_i^6}{720} - \frac{N_i^3}{360} + \frac{N_i^3}{270} - \frac{2N_i}{945}$$

and the radial polynomials associated with the second reference point $\mu = 1$, $i = 1.2$:

$$P_0(N_i,1) = N_i,$$
$$P_1(N_i,1) = \frac{N_i^3}{6} - \frac{N_i}{6},$$
$$P_2(N_i,1) = \frac{N_i^5}{120} - \frac{N_i^3}{36} + \frac{7N_i}{360} \qquad (1.7)$$
$$P_3(N_i,1) = \frac{N_i^7}{5040} - \frac{N_i^5}{720} + \frac{7N_i^3}{2160} - \frac{31N_i}{15120}$$

Reconstructing the temperature field of a flat etalon with respect to measured temperatures and the polynomials (1.6) and (1.7), we determine the temperatures (1.4) and the thermal fluxes at the faces of the test film.

Thermal fluxes:

at the left face of the film $[\xi = 0, \quad N_{11} = (x_1 - x_{11})/(x_{21} - x_{11})]$

$$q(N_{11},\tau) = -\lambda \partial t(N_{11},\tau)/\partial N_1 =$$
$$= -\lambda \sum^{m} \left[t^{(m)}(0,\tau) \cdot P_n'(N_{11},0) + t^{(m)}(1,\tau) \cdot P_n'(N_{11},1) \right] (\delta^2 \cdot a^{-1})^n \qquad (1.8)$$

and at the left film face $[\xi = 1, N_{11} = (x_1 - x_{11})/(x_{21} - x_{11})]$

$$q(N_{22},\tau) = -\lambda \partial t(N_{22}\tau)/\partial N_2 =$$
$$= -\lambda \sum_{n=0}^{m} \left[t^{(n)}(0,\tau) \cdot P_n'(N_{22},0) + t^{(n)}(1,\tau) \cdot P_n'(N_{22},1) \right] (b^2 \cdot a^{-1})^n \qquad (1.9)$$

in which the derivatives of the radial polynomial for the left etalon are as follows:

for reference point $N_1 = 0$

$$P_0'(N_{11},0) = -1$$
$$P_1'(N_{11},0) = -\frac{N_{11}^2}{2} + N_{11} - \frac{1}{3}$$
$$P_2'(N_{11},0) = -\frac{N_{11}^4}{24} + \frac{N_{11}^3}{8} - \frac{N_{11}}{6} + \frac{1}{45} \qquad (1.10)$$
$$P_3'(N_{11},0) = -\frac{N_{11}^6}{720} + \frac{N_{11}^5}{120} - \frac{N_{11}^4}{72} + \frac{N_{11}^2}{90} - \frac{2}{945}$$

and for reference point $N_1 = 1$

$$P_0'(N_{11},1) = 1$$
$$P_1'(N_{11},1) = \frac{N_{11}^2}{2} - \frac{1}{6}$$
$$P_2'(N_{11},1) = \frac{N_{11}^4}{24} - \frac{N_{11}^2}{12} + \frac{7}{360} \qquad (1.11)$$
$$P_3'(N_{11},1) = \frac{N_{11}^6}{720} - \frac{N_{11}^4}{144} + \frac{7N_{11}}{720} - \frac{31}{15120}$$

For the right etalon the derivatives of the radial polynomials are expressed in a similar way.

2. Determination of Thermal Diffusivity of Film

After reconstruction of the thermal fields of the etalons, assuming that the contact of specimen surfaces and film surfaces was ideal, we will obtain four boundary conditions for the film

$$t(0,\tau) = t(N_{11},\tau) \qquad (2.1)$$

$$t(1,\tau)=t(N_{22},\tau) \tag{2.2}$$

$$q_0=q(N_{11},\tau)=-\lambda\partial t(0,\tau)/\partial N_1 \tag{2.3}$$

$$q_1=q(N_{22},\tau)=-\lambda\partial t(1,\tau)/\partial N_2 \tag{2.4}$$

the problem of finding the temperature field of the film would be indeterminate if λ and a were known.

Distribution of temperatures within the film when the first two conditions (2.1) and (2.2) are used is described by the series (1.4) in which the coordinates of the temperature reference points coincide with the film faces.

Comparing the ratio of thermal fluxes, we obtain the following equation in determining thermal diffusivity

$$\frac{q_0(\tau)}{q_1(\tau)}=\frac{q(N_{11},\tau)}{q(N_{22},\tau)}=\frac{\partial t(0,\tau)/\partial\xi}{\partial t(1,\tau)/\partial\cdot} \tag{2.5}$$

or in more detail

$$\frac{q_0(\tau)}{q_1(\tau)}=\frac{\sum_{n=0}^{m}\left[t^{(n)}(0,\tau)\cdot P_n'(0,0)+t^{(n)}(1,\tau)\cdot P_n'(0,1)\right](\delta^2a^{-1})^n}{\sum_{n=0}^{m}\left[t^{(n)}(0,\tau)\cdot P_n'(1,0)+t^{(n)}(1,\tau)\cdot P_n'(1,1)\right](\delta^2a^{-1})^n} \tag{2.6}$$

We will designate experimental functions of time as follows:

$$\theta_{n0}'=t^{(n)}(0,\tau)\cdot P_n'(0,0)+t^{(n)}(1,\tau)\cdot P_n'(0,1) \tag{2.7}$$

$$\theta_{n1}'=t^{(n)}(0,\tau)\cdot P_n'(1,0)+t^{(n)}(1,\tau)\cdot P_n'(1,1) \tag{2.8}$$

then the equation for determination of thermal diffusivity is written as follows:

$$\frac{q_0}{q_1}=\frac{\theta_{00}'+\theta_{10}'\delta^2a^{-1}+\theta_{20}'(\delta^2a^{-1})^2+\dots}{\theta_{01}'+\theta_{11}'\delta^2a^{-1}+\theta_{21}'(\delta^2a^{-1})^2+\dots} \tag{2.9}$$

the value of the derivatives of the first radial polynomial at the reference points $\mu = 0$ and $\mu = 1$ and the experimental functions of time are tabulated in Tables 1 and 2.

If as a result of reconstruction of the thermal flux it turns out that the temperature at the film faces varies linearly with time, that is, when expanded (2.5) is maintained only with respect to the first two members, and the equation for determination of thermal diffusivity will be

$$\frac{q_0}{q_1} = \frac{\theta'_{00} + \theta'_{10}\delta^2 a^{-1}}{\theta'_{01} + \theta'_{11}\delta^2 a^{-1}} \tag{2.10}$$

and thermal diffusivity

$$a_1 = \frac{\theta'_{10} \cdot q_1 - \theta'_{11} \cdot q_0}{\theta'_{01}(q_0 - q_1)} \tag{2.11}$$

The second approximation can be obtained if the second derivative in the expansion of (2.5) is considerably greater than its error, and the third derivative is commensurable with its error

$$a_1 = a_1\left[0{,}5 + \sqrt{0{,}25 + \frac{(\theta'_{21} \cdot q_0 - \theta'_{20} \cdot q_1)\delta^2}{(\theta'_{11} \cdot q_0 - \theta'_{10} \cdot q_1) \cdot a_1}}\right] \tag{2.12}$$

After we find the thermal diffusivity, the film temperature averaged over film thickness is calculated

$$t_v(\tau) = \int_0^1 \sum_{n=0}^{m} \left[t^{(n)}(0,\tau) \cdot P_n(\xi,0) + t^{(n)}(1,\tau) \cdot P_n(\xi,1)\right](\delta^2 a)\, d\xi \tag{2.13}$$

By relating the thermal diffusivity values found to the mean film temperature, we will determine the function $a = f(t)$.

Table 1. Derivatives of Diverse Radial Polynomials

Polynomial number	Reference point coordinate	$\mu = 0$		$\mu = I$	
		$\xi = 0$	$\xi = I$	$\xi = 0$	$\xi = I$
0	$P'_0(\xi,\mu)$	$-I$	$-I$	I	I
I	$P'_I(\xi,\mu)$	$-I/3$	$I/6$	$-I/6$	$I/3$
2	$P'_2(\xi,\mu)$	$\frac{I}{45}$	$\frac{7}{360}$	$\frac{7}{360}$	$\frac{I}{45}$
3	$P'_3(\xi,\mu)$	$\frac{-2}{945}$	$\frac{3I}{15120}$	$\frac{3I}{15120}$	$\frac{2}{945}$

Table 2. First Experimental Functions of Time

Experimental function of time	Reference point $\mu = 0$	Experimental function of time	Reference point $\mu = I$
θ'_{00}	$-t(0,\tau) + t(1,\tau)$	θ'_{0I}	$-t(0,\tau) + t(1,\tau)$
θ'_{I0}	$\frac{t'(0,\tau)}{3} - \frac{t'(1,\tau)}{6}$	θ'_{II}	$\frac{t'(0,\tau)}{6} + \frac{t'(1,\tau)}{3}$
θ'_{20}	$\frac{t''(0,\tau)}{45} + \frac{7t''(1,\tau)}{360}$	θ'_{2I}	$\frac{-7t''(0,\tau)}{360} - \frac{t''(1,\tau)}{45}$
θ'_{30}	$\frac{-2t''(0,\tau)}{945} - \frac{3It'''(1,\tau)}{15120}$	θ'_{3I}	$\frac{3It'''(0,\tau)}{15120} + \frac{2t'''(1,\tau)}{945}$

3. Determination of Film Thermal Conductivity

Thermal conductivity of film and sheet materials is a substantial function of temperature. For the given case, the thermal conductivity equation

$$c_v \frac{\partial t}{\partial \tau} = \operatorname{div}(\lambda \cdot \operatorname{grad} t) \qquad (3.1)$$

can be reduced to the form

$$\frac{1}{a}\frac{\partial t}{\partial \tau} = \nabla^2 t + (\nabla t)^2 \frac{d \ln \lambda}{dt} \tag{3.2}$$

since the thermal diffusivity for any temperature range $[t_1, t_2]$ is determined, the relative thermal conductivity is found as an exponential function of the integral

$$\frac{\lambda(t_1)}{\lambda(t_2)} = \exp\left\{\int_{t_1}^{t_2}\left[\frac{1}{a}\frac{\partial t}{\partial \tau} - \nabla^2 t\right]\frac{dt}{(\nabla t)^2}\right. \tag{3.3}$$

By way of verification, the absolute value of thermal conductivity can be determined directly from conditions of ideal thermal contact of film and etalon surfaces

$$q_0 = -\frac{\lambda(t_0)}{\delta} \cdot \frac{\partial t(0,\tau)}{\partial \xi} \tag{3.4}$$

$$q_1 = -\frac{\lambda(t_1)}{\delta} \cdot \frac{\partial t(1,\tau)}{\partial \xi} \tag{3.5}$$

or in more detail

$$q_0 = -\frac{\lambda(t_0)}{\delta}\left[\theta'_{00} + \theta'_{10}\delta^2 a^{-1} + \theta'_{20}(\delta^2 a^{-1})^2 + \ldots\right] \tag{3.6}$$

$$q_1 = -\frac{\lambda(t_1)}{\delta}\left[\theta'_{01} + \theta'_{11}\delta^2 a^{-1} + \theta'_{21}(\delta^2 a^{-1})^2 + \ldots\right] \tag{3.7}$$

By referring the thermal conductivity value found to the temperature of the corresponding film face, we establish the function $\lambda = f(t)$.

4. Determination of Film Heat Capacity

The difference between thermal flux values at the left $q_0(\tau)$ and the right $q_1(\tau)$ faces

$$q_0(\tau)-q_1(\tau)=q_a(\tau) \tag{4.1}$$

is absorbed by the film. This accumulated intensity is expended in raising the mean film temperature

$$q_a(\tau)=c\gamma\delta\frac{dt_v}{d\tau} \tag{4.2}$$

where $c\gamma$, $J/m^3 \cdot deg$ is the bulk heat capacity of test material.

From (4.2) we can determine $c\gamma$ after we find the thermal diffusivity and calculate t_v (2.13).

We can also point out another method of determining the bulk heat capacity. After the absolute value of thermal conductivity is determined in the temperature range $[t_1,t_2]$ (3.4) and (3.5), the bulk heat capacity is calculated as the product

$$c\gamma=\frac{\lambda(t)}{a}\exp\left\{\int_{t_1}^{t_2}\left[\frac{1}{a}\frac{\partial t}{\partial\tau}-\nabla^2 t\right]\frac{dt}{(\nabla t)^2}\right\} \tag{4.3}$$

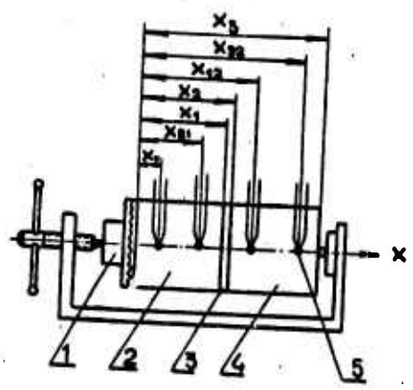

Figure 1. Placement diagram of etalons, test film and temperature transducers: 1, Heater; 2, Left etalon; 3, Film; 4, Right etalon; 5, Thermocouples

References

1. Vol'kenshteyn, V. S., *ZhTF*, Vol. 24, No. 2, 1954.
2. Pengelly, A. E., *Br. J. Appl. Phys.*, Vol. 6, No. 1, 1955.
3. Vozhnyak, A. I., *Ispytaniye Kokil'nykh Krasok na Teploprovodnost'*, [Testing Ingot Mold Paints for Thermal Conductivity], Mashgiz Press, Moscow, 1955.
4. Novichenok, L. N. and A. B. Verzhinskaya, *IFZh*, Vol. 3, No. 9, 1960.
5. Novichenok, L. N., *Sb. Teplo- i Massoobmen v Kapillyarnoporistykh Telakh*, [Collection: Heat and Mass Transfer in Capillary-Porous Bodies], Nauka i Tekhnika Press, Minsk, 1965.
6. Baganov, A. G., Yu. A. Pirogov, and Ya. P. Makarov, *TVT*, No. 1, 1965.
7. Gogel', V. O. and A. G. Alekseyev, *IFZh*, No. 10, 1962.
8. Vartenev, G. M., *Plasticheskiye Massy*, No. 1, p. 56, 1963.
9. Chudnovskiy, F. A., *IFZh*, Vol. 10, No. 1, 1966.
10. Shlykov, Yu. P. and Ye. A. Ganin, *Kontaktnyy Teploobmen*, [Contact Heat Transfer], 1963.
11. Khizhnyak, P. Ye., *Tr. GosNII GVF*, Vol. 39, Report 7627. 1963.
12. Novopavlovskiy, V. S., *IFZh*, No. 5, 1964.
13. Meisenard, V. Ye., V. I. Subbotin, P. A. Ushakov, and A. A. Sholokhov, *Konvektivnyy i Luchistyy Teploobmen*, [Convective and Radiative Heat Transfer], Academy of Sciences USSR Press, Moscow, 1960.
14. Kanavin, I. F. and L. G. Batalov, *Plasticheskiye Massy*, No. 9, p. 50, 1964.
15. Molchanov, Yu. M., *Fizicheskiye i Mekhanicheskiye Svoystva Polietilena, Polipropilena i Poliizobutelena*, [Physical and Mechanical Properties of Polyethylene, Polypropylene, and Poly-isobutylene], 1966.
16. Temkin, A. G., *Izv. Vuzov. Energetika*, No. 5, 1961.
17. Temkin, A. G., *IFZh*, Vol. 4, No. 9, 1961.
18. Temkin. A. G., *IFZh*, Vol. 4, No. 10, 1961.
19. Temkin, A. G. and G. P. Buynyachenko, *Izv. AN Latv. SSR*, Seriya Fiz. i Tekhn. Nauk, No. 4, 1965.

METHOD OF MEASURING HEAT CAPACITIES AND THERMAL EFFECTS BASED ON QUASI-STEADY-STATE HEATING REGIME

M. Sh. Yagfarov

The theory of quasi-steady-state temperature fields [1] provides the considerable promise of this regime for developing methods of determining thermal characteristics. One positive aspect of these methods is experimental rapidity, wide temperature range of measurements and the possibility of using automatic devices.

The present article describes a quasi-steady-state method designed to measure heat capacities and thermal effects with higher precision. The method is called the ternary thermal bridge.

The principles of single and binary thermal bridges for determining heat capacities and thermal conductivities were set forth by the present author in earlier studies [2-4]. The thermal bridge method is the name given to a method of measuring thermal flux given quasi-steady-state heating regime by concentrating it in a narrow section, a channel ("thermal bridge"). In the practice of measuring heat capacities and thermal effects, this is done by bringing together the test material directly with the heater by means of a metal rod. Concentration of the thermal flux substantially raises the experimental precision when measuring thermal values. In the double thermal bridge method use is made of the differential principle of measurement by comparing thermal fluxes in two similar thermal bridges, one of which brings together the test material and the heater, and the other is the reference. Air (that is, practically "null" heat capacity) usually serves as the reference material. The differential method of measurement makes it possible to easily take into account the proportion of the thermal flux arriving at the test material not through the "bridge" and substantially raises the sensitivity of the method. The double thermal bridge requires strict

symmetry in the measuring unit and careful compliance with linearity of heating.

The ternary thermal bridge method is less subject to the effect of these factors and is therefore more suitable for precision measurements, especially of small amounts of material. In this method thermal bridges are used to bring three identical symmetrically arranged vessels in contact with the heater. The test material is placed in one of these vessels, the second remains empty and serves as a reference, and material with known heat capacity is placed in the third, the so-called "control material." With such an arrangement possible disruptions of symmetry in putting the unit together appear only in the form of easily allowed-for systematic errors. Small deviations of heating from linearity also have practically no effect on results. Determination of heat capacities and thermal effects is carried out by measuring differences of temperature between vessels.

The second feature of the method boosting measurement precision is the absence in the setup of thermocouples in the ordinary sense of the word. As we know, measurement of temperature by thermocouples always involves certain, almost inevitable errors caused by the influx or outflux of heat along wires. Attempts at avoiding this effect by using thin wires or placing the largest possible number of such wires in the isothermal region near the point being measured have practically little value. In the method described, this problem is resolved by the fact that the unit itself constitutes a system of thermocouples. For this purpose the bridge is made up of thermocouple material (for example, copel). The thermal emf is induced between the bridge ends and the parts of the copper unit. Thus, the unit simultaneously performs the functions of heater and meter. As we can see from Figure 1, the block is connected directly to the instrument recording the thermal emf (to the pyrometer or the potentiometer) with the aid of three copper wires. The thermocouple arms in the meter-unit are three copper closed vessels. Thus, the test material lies within the thermocouple arm. This fact also considerably increases the precision of measurements, since the temperature is measured simultaneously over the entire specimen surface.

In addition to linear temperature rise, it is essential that the temperature in all parts of the unit housing at each moment in time be the same. To meet this condition of isothermicity, the housing of the unit, and also the vessels, must be made of material with a high coefficient of thermal conductivity. The most suitable for these purposes is copper. The copper is chrome-plated for measurements at high temperatures.

A diagram of the measuring unit is given in Figure 1. The housing of the unit is a copper cylinder, on one face of which three cylindrical recesses are provided. Copper vessels with lids, each of which is connected with the unit only through the bridge are placed in the recesses, symmetrically with respect to the sides. The distance between vessels and recess walls is desirably not less than 5-6 mm. In measuring the temperature rise in the unit, an ordinary thermocouple can be used, since here high precision of measurement is not required, or else yet another copper wire connected to the center of one of the bridges can be introduced. The heater spiral can be wound around the insulator directly at the unit. However, from the point of view of rapid cooling of the apparatus between experiments, it is desirable to use a separate furnace consisting of a cylinder with heater wound about it.

Derivation of the working formula is based on solution of the thermal conductivity equation [1]. In final form the working formula appears as follows:

$$C_p = \frac{c_n \cdot m_n}{m} \cdot \frac{l_1}{l_2} .$$

It is assumed that measuring instruments are brought up to identical sensitivity. As seen from the working formula, calibration of the instrument is not required.

The working formula for determination of thermal effects has the following form:

$$Q = \Delta t \left(mc \frac{S_1}{S_2} - m_n c_n \right)$$

We must dwell in more detail on the problem of measuring areas for endothermal and exothermal heat effects. As we know, measurement of the areas of peaks formed by differential recording during the period of an endothermal heat effect is employed in thermography for comparative evaluation of effect values, and also in several methods of quantitative thermography to determine the magnitude of heat effects. However, the limitation of peaks for obtaining a closed area here is to a considerable extent carried out in an arbitrary manner, which cannot but affect precision of results. The element of indeterminacy limiting peak areas is wholly absent in the method described. S_1 and S_2 represent areas enclosed between the zero line and the recording trace of the temperature difference in the time interval from the beginning to the end of the heat effect of an endothermal process period, and the sole condition in selecting the beginning and end of the effect is the requirement that the heat effect be wholly limited within the given interval of time. Consequently, there is no need to precisely select the beginning and end of the effect, which as we know is extremely difficult in several cases.

In thermography, establishing a correlation between heat effect and thermogram area for exothermal processes is even more difficult than for endothermal processes. Accordingly, the literature almost entirely lacks studies on this problem. In the ternary thermal bridge method, the area on the thermogram corresponding to the exothermal effect is also rigorously determined as in the case of the endothermal process. If the exothermal effect is small and the specimen temperature during the entire process does not exceed the etalon temperature, the peak on the thermogram corresponding to the thermal effect lies only on one side of the zero line. In this case, the area bounded between the zero line and the outer side of the peak in the interval from the onset to the conclusion of the effect is measured. If the exothermal effect is large enough and the specimen temperature exceeds the etalon temperature, the apex of the peak on the thermogram extends beyond the zero line. Then the area of this peak apex is read off from an area lying on the other side of the zero line, the value of which is determined as in the first case.

The error of thermal effect measurements in the method propounded is due mainly to errors of planimetry. Error in our studies on determining heat effects was of the order of 0.3-0.5 percent, and in heat capacity determinations -- 0.1-0.2 percent. We must note the high sensitivity of the method that allows us to conduct studies of material in very small quantities, down to as small as tenths of a milligram. The method is also convenient for the measurements at low temperatures. In this case, the unit must be in a tightly sealed vessel, in nitrogen atmosphere to obviate the effect of moisture on results.

Symbols

c_p = heat capacity of test material; c_k = heat capacity of control material; m = mass of test material; m_k = mass of control material; l_1 and l_2 = deviations of the measuring instrument, where l_1 is due to the difference of temperatures between the etalon vessel and the vessel in which the test material is placed, and l_2 = difference of temperatures between the etalon vessel and the vessel containing the control material; Q = measured heat effect; m and m_k = mass of test specimen and control material, respectively; c and c_k = heat capacity of test specimen and control material, corresponding to the heat effect temperature (or the mean temperature of the heat effect); S_1 and S_2 = areas on the thermogram when temperature is recorded in the coordinates of temperature versus time; $S_1 = \int_{\tau_1}^{\tau_2} \Delta t_1 d\tau$, $S_2 = \int_{\tau_1}^{\tau_2} \Delta t_2 d\tau$, where τ_1 and τ_2 = time of onset and conclusion of effects; Δt_1 = difference of temperatures between the etalon vessel and the vessel containing the test material; Δt_2 = difference of temperatures between the etalon vessel and the vessel in which the control material is placed; Δt = temperature rise in the unit in the time interval $\Delta\tau = \tau_2 - \tau_1$.

Cross section at A-A

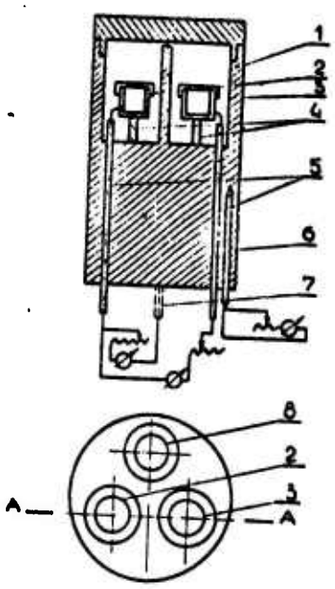

Figure 1. Diagram of measuring unit in the ternary thermal bridge method: 1, Unit housing; 2, Etalon vessel; 3, Vessel containing test material; 4, "Thermal bridges"; 5, 7, Copper wire leads; 6, Thermocouple used to measure temperature rise; 8, Vessel containing control material

References

1. Lykov, A. V., *Teoriya Teploprovodnosti,* [Theory of Thermal Conductivity], GITTL Press, Moscow, 1952.

2. Yagfarov, M. Sh., *IZv. Kazanskogo Fil. AN SSSR,* No. 6, 1961.

3. Agfarov, N. Sh., *Tezisy Dokl. 2-oy Mevhuz. Konf. po Metod. i pribor. Bor. dlya Teploiz. Ispyt,* Abstracts of Papers Presented at the Second Inter-institutional Conference on Methodology and Instruments for Heat-insulation Testing], Leningrad, p. 28, 1960.

4. Yagfarov, M. Sh., *Tezisy Dokl. 3-go Vsesoyuzn. Soveshch. po Termografii,* [Abstracts of Papers Presented at the Third All-Union Conference on Thermography], p. 44, 1962.